

rec'd with letter dtd 12/15/92



**United States
Department of
Agriculture**

Agricultural
Research
Service

Technical
Bulletin
Number 1655

Supercritical Flow Flumes for Measuring Sediment-Laden Flow

PURCHASED BY USDA
AGRICULTURAL RESEARCH SERVICE
FOR OFFICE USE ONLY

1028

9212230273 921215
PDR WASTE
WM-11 PDR



**United States
Department of
Agriculture**

Agricultural
Research
Service

Technical
Bulletin
Number 1655

Supercritical Flow Flumes for Measuring Sediment-Laden Flow

R. E. Smith, D. L. Chery, Jr., K. G. Renard,
and W. R. Gwinn

Acknowledgments

The authors wish to express their appreciation to the many people who helped develop these measuring flumes, only a few of whom can be mentioned here.

Special thanks to D. A. Woolhiser, Fort Collins, Colo., whose cooperation made possible the 1:5 outdoor hydraulic model tests leading to development of the control dikes and a confident rating of the flume's lower flows. Howard Larson with his staff of technicians at Tombstone, Ariz., for many years provided the much needed help and understanding in building and evaluating these flumes. Gary Smillie carried on calibration measurements at the Walnut Gulch watershed after the principal investigators left.

We thank D. G. DeCoursey, Oxford, Miss., F. W. Blaisdell, St. Anthony Falls, Minn., and J. W. Ruff, Fort Collins, Colo., for their many helpful suggestions in the preparation of this publication.

Abstract

Smith, R. E., D. L. Chery, Jr., K. G. Renard, and W. R. Gwinn. 1981. Supercritical flow flumes for measuring sediment-laden flow. U.S. Department of Agriculture Technical Bulletin No. 1655, 72 p., illus.

A general type of supercritical flow flume has been developed over many years of experience and testing in discharge measurements at the Walnut Gulch experimental watershed, Tombstone, Ariz. The design and experience with the original type flume, called the Walnut Gulch flume, is discussed and its features and application difficulties are described. Methods have been developed to analyze flows that exhibited lateral asymmetry in cross sectional profile, and porous dikes have been developed to considerably reduce asymmetry in the alluvial approach section to these flumes. Rating relations have been developed by both experimental and theoretical means. The experience with the Walnut Gulch flumes has led to an improved design of supercritical flume, called the Santa Rita flume. The Santa Rita flume design is presented in several sizes, along with a discussion of design requirements for stilling well intakes to minimize sediment inundation, record lag interpretation, and construction methods.

Keywords: Open channel, flow, flume, stilling well, sediment transport, measurement, supercritical, alluvial, sonar, pressure transducer, instrumentation, design, intake.

Trade names and the names of commercial companies are used in this publication solely to provide specific information. Mention of a trade name or manufacturer does not constitute a guarantee or warranty of the product by the U.S. Department of Agriculture nor an endorsement by the Department over other products not mentioned.

Contents

	Page
List of symbols	4
Introduction	5
Hydraulic classification of flumes	5
Hydrologic properties of ephemeral alluvial streams	5
Background and history	9
Hydraulic theory in supercritical flow measurement	12
Measurement sensitivities	12
Flow equations	13
Model similitude	14
Experimental development of Walnut Gulch flumes	15
Original model studies	15
Colorado State University 1:5 model rating of the floor section	16
Scaling of the 1:5 model data	17
Analysis of model ratings	18
Prototype evaluations	20
Velocity measurements at flume 63.002	20
Prototype data at flume 63.006	22
Field application and performance evaluation	26
Stabilization of approach channels	26
Experimental arrangement	26
Model results	27
Prototype trials	27
Field experience	28
Estimation of discharge in asymmetrical flows	29
Design modifications	29
The Santa Rita flume	31
Weir extension flume	32
Sensing water level in heavy sediment conditions	33
Design of stilling well intake for sediment conditions	34
Analysis of lag in stilling well records	34
Construction and siting of flumes	35
Summary	38
Literature cited	39
Appendix A: Computer program to determine measuring section depth (y_m) for any given discharge, q for a supercritical depth flume	40
Appendix B: Selected model ratings for discharges for Walnut Gulch flumes 1, 2, 3, 4, 6, 7, 8, 11, and 15 in prototype dimensions	44
Appendix C: Design dimensions of Santa Rita flumes for a range of flow capacities	56
Appendix D: Construction drawings for a 1.5-m ³ /s metal Santa Rita flume	68

List of Symbols

Symbol	Description	Units	Symbol	Description	Units
a	Exponent for R in velocity relation		s	Subscript indicating smoother case	
A	Cross-section area of flow	L^2	S_c	Natural channel slope	L
A	Length of flume entrance	L	S_f	Friction slope of flume	L
A_o	Orifice area	L^2	S_o	Bottom slope of flume	L
A_w	Surface area at recorded depth	L^2	t	Width of water surface in flume at measuring point when depth is h	L
b	Parameter in a discharge rating relation		t	Time	T
C	Friction coefficient, or design parameter for entrance shape of Santa Rita flume		T	Top width of free surface of a channel flow	L
C_D	Discharge coefficient		T	Length of throat of flume	L
C_S	Orifice coefficient		V	Velocity	L/T
C_W	Dimensioned weir or flume coefficient		\bar{V}	Average velocity	L/T
D	Hydraulic depth = A/T	L	V_o	Velocity through the orifice	L/T
Fr	Froude number		w	Dimensionless parameter representing relative value of Fr	
g	Gravitational acceleration	L/T^2	W	Top width of a flume throat	L
h	Measured flow depth	L	WF	Projected width of floor section of a flume	L
h_e	Eddy loss head	L	x	Distance along flume	L
h_f	Flow head in the flume	L	X	Horizontal coordinate positive in upstream direction	L
h_n	Notch depth	L	x_p	Distance from critical section to the measuring section	L
h_o	Head at the orifice exit	L	y	Flow depth	L
h_w	Stilling well depth	L	y_m	Flow depth at the measuring section of a supercritical flume	L
i	Distance increment number in solution in finite difference expression		Y	Vertical coordinate	L
j	Subscript of incremental flow velocity and cross section area		z	Horizontal coordinate normal to and measured from the center of the flume	L
K_e	Eddy loss coefficient		ZF	Horizontal dimension per one unit vertical dimension in the side slope of a flume floor	
L	Scale ratio, or length from beginning of throat section of a flume to the measuring section		ZW	Horizontal dimension per one unit vertical dimension in the side slope of a flume wall	
L_w	Width of weir	L	α	Open channel velocity distribution energy coefficient	
m	Subscript indicating model		Δh	Head difference across the orifice	L
n	Manning roughness coefficient		Δt	Time step	T
p	Subscript indicating prototype		σ	Measurement sensitivity	T/L^2
q_o	Flow through an orifice	L^3/T			
Q	Flow discharge	L^3/T			
R	Hydraulic radius	L			
r	Subscript indicating rougher case				
r_c	Scaling ratio for roughness				

Supercritical Flow Flumes for Measuring Sediment-Laden Flow

By R. E. Smith, D. L. Chery, Jr., K. G. Renard,
and W. R. Gwinn¹

Introduction

This publication describes a general type of flume particularly suited for measuring discharge in streams with high velocities and high sediment concentrations. This kind of flow is common in many areas where runoff results from high-intensity rainstorms and the channels have a steep gradient (0.5 to 2.0 percent) and alluvial bed. This situation is common in the American West and Southwest, northern Mexico, certain areas of Australia, North Africa, the Middle East, and arid areas of Asia. Often, the regional ground water level lies considerably below the channel surface and, consequently, there is no base flow.

The laboratory and field experience involved in developing and evaluating the original flume, called the Walnut Gulch flume, is described here. In addition, we present an improved supercritical flume design that grew out of this experience and several typical designs covering a wide range of flows.

Hydraulic Classification of Flumes

To measure water discharge in an open channel, we apply our knowledge of the distribution of the energy of flowing water. For accurate measurements, we also need a location where hydraulic control exists. Hydraulic control occurs when a local flow condition exists such that the relation between discharge and depth is reasonably independent of changes in upstream or downstream conditions.

Flowing water has both potential and kinetic energy. When the total energy for a given discharge is minimum, critical flow is said to occur. Velocities greater than critical flow velocity, and therefore having a higher proportion of kinetic energy, define supercritical flow. Conversely, velocity lower than critical occurs in subcritical flow. Most discharge measuring structures in open channel flow depend on the fact that a contraction can cause subcritical flow to accelerate through critical flow. This constitutes a form of hydraulic control, and the known relation between kinetic and potential energy is then used to derive a presumed invariant relationship between flowing water depth and discharge. This relationship is the structure's rating.

Most open channel flow is subcritical, whether in canals or natural streams, with velocities well below critical, and flumes are usually designed to measure depth upstream of a contraction where critical flow is caused to occur.

High natural velocities and sediment concentrations in many locations prohibit the use of ordinary subcritical flow (often referred to as critical depth) flumes because these flumes require such low approach velocities that sediment is deposited. The deposited sediment causes a shift in the rating or a loss of hydraulic control.

The flumes described in this report have been developed to provide flow measurement for conditions of heavy sediment load where ordinary flumes do not perform satisfactorily. Such adverse conditions often coincide with situations of critical hydrologic interest. This may be the case when ephemeral flow represents a scarce water resource or when flash floods in otherwise dry channels are potentially damaging to local agriculture.

Hydrologic Properties of Ephemeral Alluvial Streams

The supercritical flumes discussed in this publication have application in a wide variety of hydrologic conditions, but measurement of ephemeral flows is a major one. Therefore, a summary of the peculiar hydraulic problems of this type of hydrology is presented. Ephemeral streamflow in alluvial channels usually originates in the uplands where slopes are relatively steep. Streamflow velocities are therefore typically high.

Closely related to the occasional flow and steepness of slope is a typically high sediment load. Were these streams to flow more or less continuously, erosion processes would quickly develop a meandering, mild slope stream with the finer material flushed from the basin. Ephemeral flows are characterized by an imbalance between sediment load and carrying capacity, and often carry a large volume of sediment. Under these circumstances, the sedimentation processes are almost never in equilibrium and are either eroding or depositing sediment at any point along the stream. Ephemeral flow implies rapidly changing discharge so that the interrelated hydraulic processes of flow, bed forms, and sediment concentration are truly dynamic.

In channel networks, other factors complicate these dynamics. The movement and spatial variability of runoff-producing storms, as well as topography, cause surface runoff to enter the channel network at different times at different places. The convergence of these time-displaced hydrographs determines the pattern of flow at any given point along the channel. The sediment load in the water entering an ephemeral stream at any point affects the amount of alluvial materials picked up from the channel bed. If the sediment load of water entering

¹Research hydraulic engineers, Agricultural Research Service, U.S. Department of Agriculture: Smith is at the Engineering Research Center in Fort Collins, Colo.; Chery was formerly with the Southeast Watershed Research Program in Athens, Ga.; Renard is at the Southwest Rangeland Watershed Research Center in Tucson, Ariz.; and Gwinn is at the Water Conservation Structures Laboratory in Stillwater, Okla.

the channel is high, the channel may aggrade locally; however, if the sediment load is low, the channel can degrade extensively, depending on the armoring action of bed materials.

The effect of the local flow history on (a) the nature of the alluvial material at the beginning of any flow event and (b) the channel shape complicates the interrelation between flow and sediment. A larger, longer flow event will leave the channel in a different condition than would a series of smaller flows; it will leave different materials at the surface and will shape a different longitudinal and lateral channel configuration.

Problems of measuring the discharge in ephemeral streams are derived primarily from (a) the high velocities, (b) the sediment-carrying capacity of high velocities, and (c) temporal variations of the streambed shape and local flow direction, resulting from the ephemeral nature of the watershed.

Accurate flow measurement requires a flume that causes repeatable hydraulic conditions defining a unique predesigned relation between the flow depth and the discharge at some measuring point (or points). This means that the flume must exercise hydraulic control for a large range of upstream and downstream conditions. Most importantly, where there are heavy sediment loads, flumes cannot provide hydraulic control by reducing the velocity because the sediment load will likely deposit in the flume throat and hydraulic control will be lost. Flumes for these conditions must be designed with some understanding of the dynamic nature of the alluvial bed, the sediment load, and hydraulic parameters.

Failure to account for large sediment loads, for example, has caused severe measurement problems on very small watersheds in New Mexico and Arizona where weirs were installed to

measure flow. Sediment quickly filled the upstream ponds and depositional bars covered some weirs, destroying the control and severely reducing their effectiveness as measuring structures. This condition is illustrated in figure 1. This is a small watershed measuring station near Safford, Ariz. A weir causes hydraulic control by reducing the upstream kinetic energy to a negligible value, creating a pond of tranquil flow. The head measurement at a point above the weir is then an indication of the total specific energy involved (that is, there is no appreciable velocity head). The severe deceleration of flowing water makes a weir a very effective sediment trap, and, therefore, inappropriate where sediment load is high.

Many watershed research locations in the United States have used broadcrested *V*-notch weirs (developed by the Soil Conservation Service) to measure runoff, and found that continuous maintenance is required to remove sediment deposited in the pond above the weir. Figure 1 illustrates the type of wide deposition bar typical of stable conditions at these weirs.

The broad-crested *V*-notch weir may be used in channels that do not form a true tranquil pond above the weir. Rating data for these weirs are presented in *USDA Agriculture Handbook 224 (USDA 1979)*,² including corrections for upstream velocity at the measuring point. This correction is valid for a limited range of velocities and assumes the weir notch elevation to be above the channel bottom elevation.

²The year in *italic*, when it follows the author's name, refers to *Literature Cited*, p. 39.



FIGURE 1.—*V*-notch concrete weir filled with bed-load near Stafford, Ariz.

BN-48648

Recent field studies at the Walnut Gulch watershed and laboratory experiments by Ruff et al. (1977) at the Hydraulics Laboratory at Colorado State University have quantified the effects of the deposition on the rating of the weir. Sometimes, the structure no longer acts as a weir but rather loses total control of the low to moderate flows.

An experiment that demonstrated this was performed in the 1.22-m (4-ft) wide tilting flume at the USDA Water Conservation Laboratory, Tempe, Ariz. The 3:1 weir at Walnut Gulch location 63.113 was hydraulically modeled at a 1:5 scale. The prototype upstream bed had aggraded to near preinstallation grade of some 2 to 3 percent, with aggraded material just upstream of the weir some 3 cm (0.10 ft) higher than the weir notch. At all but a limited range of flow, the weir acted more as a free overfall than as a hydraulic control. Figure 2 is a photograph of the model test after one experiment. Figure 3 is a photograph of the prototype weir. Model deposition patterns were similar to those observed in the field.

Work by Ruff et al. (1977) and field measurements at an experimental tandem-flume location (supercritical flume immediately below a sediment-filled weir) are shown in figures 4 and 5 to illustrate the effect of sediment deposition on weir ratings. The standard ratings used in the comparisons of figures 4 and 5 include the velocity correction in USDA Agriculture Handbook 224 (U.S. Department of Agriculture 1979) tables, based on the flow cross section area at the measuring point. In each of these cases, upstream channel slope was sufficiently mild to retain weir control at higher water levels where the narrowing effect of the V-notch could slow the flow and exert control. This was not the case, however, for the weir in figure 3 (Walnut Gulch Weir No. 63.113) where the upstream grade was so steep and the channel so narrow that essentially all control was lost. Obviously, the weir is not a suitable measuring device for these conditions.

Another structure that has more potential than a weir for measuring sediment-laden flow in small channel applications is the venturi flume, designed for higher but still mild flow conditions. Although this flume has application where sediment sizes and concentrations are relatively low, when used in ephemeral streams of southeast Arizona where considerable sediment moves as bedload, it failed to pass the sediment carried by the flow (fig. 6). In this example, sediment was deposited through the flume, including the throat where supercritical flow was designed to occur. In one experiment, turbulence-generating vanes were added in the approach section walls, but this still failed to prevent bottom sedimentation in the flume.

Such field observation clearly indicates the need for measuring flumes that will maintain a velocity sufficient to transport the sediment entrained in the flow.



FIGURE 2.—Photograph looking downstream at 1:5 model of Weir 63.113 at Walnut Gulch, after large simulated flow event. The weir exercises no control for lower flows as a result of alluvial filling.

BN-48649



FIGURE 3.—Weir location 63.113 at Walnut Gulch, near Tombstone, Ariz. The channel bed above the weir has achieved a new aggraded stable condition. BN-48650

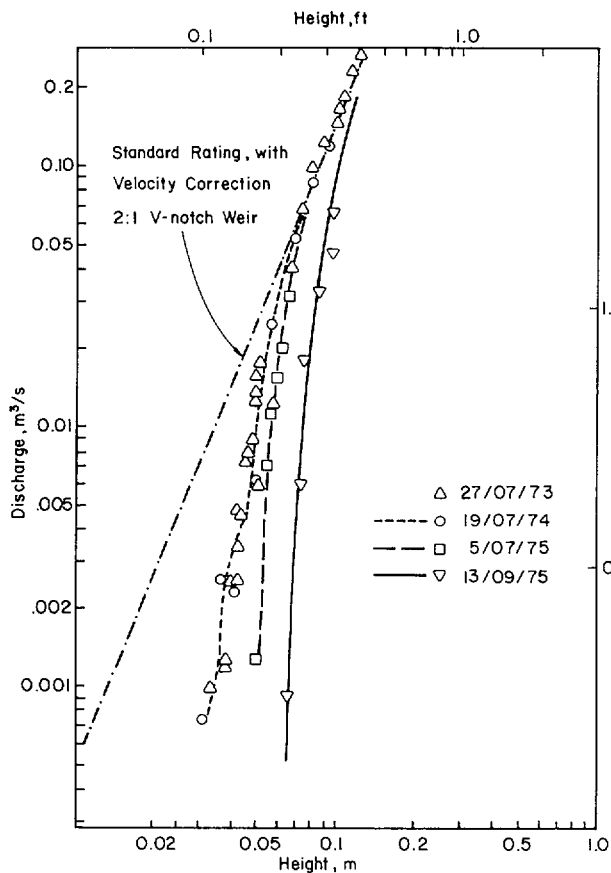


FIGURE 4.—Measured rating of an alluvial filled 2:1 V-notch weir, Walnut Gulch Location 63.102. Only at depths greater than 0.4 to 0.6 m (1.5 to 2 feet) does the weir exert control.

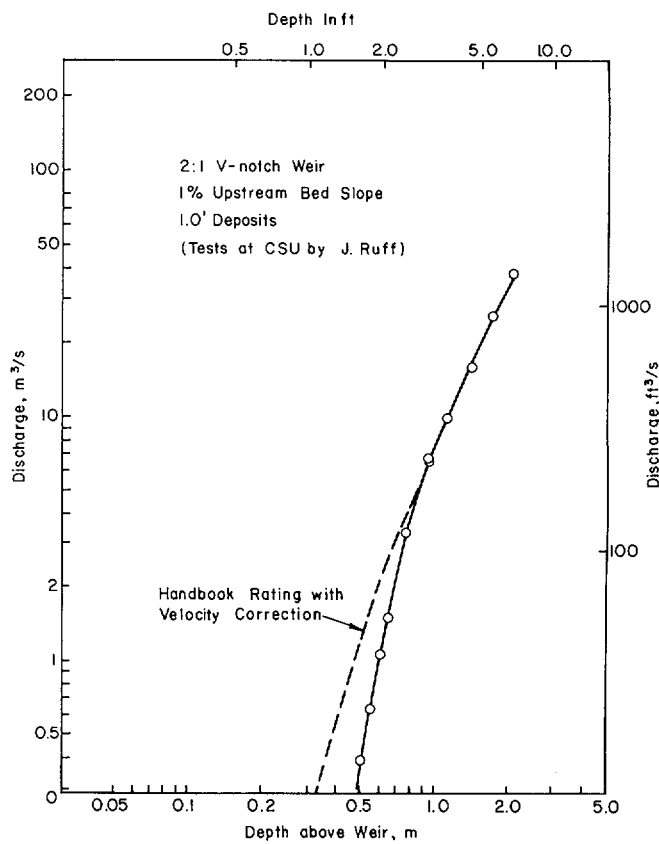


FIGURE 5.—Laboratory model simulation of the rating of a 2:1 V-notch weir with 0.3 m (1.0 foot) of upstream deposit depth (data from Ruff *et al.*, 1977).

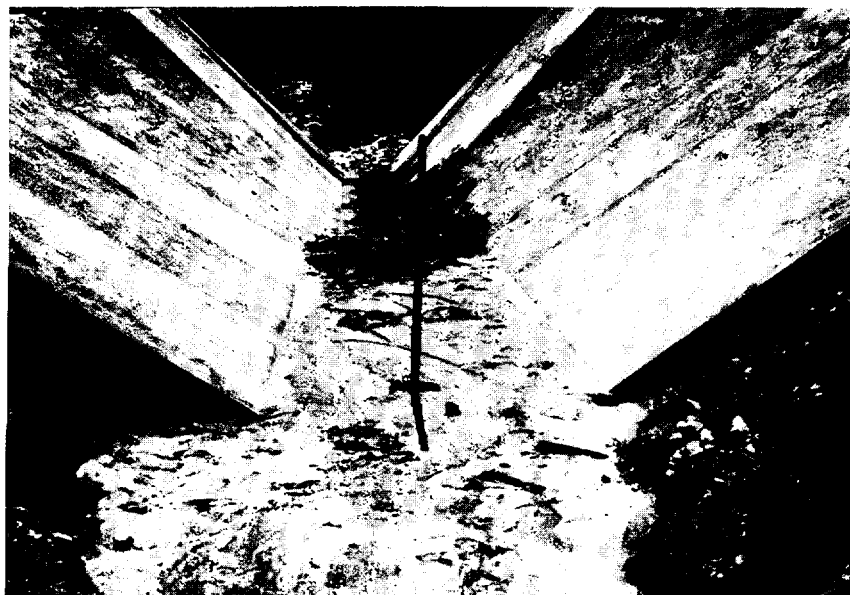


FIGURE 6.—Sediment deposited in a venturi flume after a summer storm flow at Walnut Gulch watershed, Arizona.

BN-48651

Figure 8 shows the structure at the Walnut Gulch outlet shortly after its completion. Later that summer, the structure failed as shown in figure 9. The failure occurred because it was (1) structurally inadequate to carry the weight of water involved, (2) hydrologically too small, and (3) hydraulically inadequate with resulting downstream scour undermining the concrete.

By the end of 1954, the only original structure left intact was the flume on the 2.3-km² (0.88-mi²) watershed. It had been seriously overtopped, however, and was replaced in 1967. The flume at the 22.3-km² (8.61-mi²) watershed, called subwater-

shed 5, has been extensively undermined and damaged below the critical section. A new supercritical flume was built downstream in 1966.

A structure similar to those described above at Walnut Gulch was built at the outlet of a 73.5-km² (67-mi²) watershed at Alamogordo Creek. This structure remains intact today, although extensive repairs have been required to prevent the hydraulic jump at the lower edge of the flume from undermining the structure. Sheet piling and large boulders have been anchored below the flume to protect against undercutting.



FIGURE 8.—Critical flow flume originally installed for flow measurement at the Walnut Gulch Watershed outlet, 1954. BN-48652



FIGURE 9.—The first structure for Watershed 1 was seriously damaged by the first large flows of the first season of use, 1954. The sidewalls and floor were badly undermined and inundated as shown here, and were completely washed out by the end of the season. BN-48653

As a result of these early failures, a series of hydraulic model investigations began in 1957 at the ARS Stillwater Hydraulic Laboratory, Stillwater, Okla. From these tests evolved the measuring device known today as the Walnut Gulch supercritical flume (Gwinn 1964), with the largest of 11 such structures on Walnut Gulch having a peak measuring capacity of over 623 m³/s (22,000 ft³/s) (fig. 10).

The design of this flume came from a study of earlier supercritical flumes, especially the San Dimas flume (Wilm et al. 1938), which had a supercritical throat with vertical sides, and the trapezoidal flume of Robinson (1961), discussed above. It was felt necessary to (a) contract the flow, (b) pass it through a throat section at supercritical velocity, and (c) measure the depth within this throat where hydrostatic pressure exists. The cross-sectional shape was chosen as a compromise, considering (a) the need to pass large floods, (b) the efficiency in matching flume shape to channel shape, and (c) the desire to measure low, moderate, and high flows.

Figure 11 shows the design geometry of a typical Walnut Gulch flume. The flume has a 4.57-m (15-ft) curved entrance approach to a 6.10-m- (20-ft) long straight section having a shallow V-shaped floor and sidewalls with one-to-one slope.

The curved entrance approach has a cylindroid surface (coordinate origin shown in fig. 12) defined by the equation:

$$y = 0.03x + \frac{z - 0.09842x^2}{0.0287x^2 + 1}$$

where:

x = horizontal coordinate positive in the upstream direction, in meters

y = vertical coordinate, in meters

z = horizontal coordinate normal to and measured from the centerline of the flume, in meters

or

$$y = 0.03x + \frac{z - 0.03x^2}{0.00267x^2 + 1}$$

where x , y , and z are in feet.

An isometric view of this surface is shown in figure 12. The floor of the flume has a slope of 0.03 in the downstream direction parallel to the centerline to insure movement of sediment through the flume. This is the same slope used in the San Dimas flume (Wilm et al. 1938).

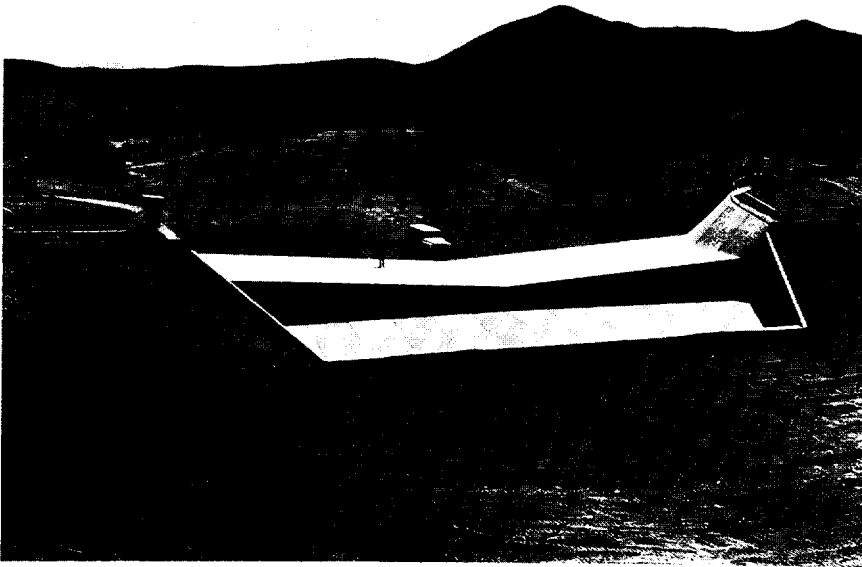


FIGURE 10.—The finished structure at the outlet of Walnut Gulch is considerably larger than the earlier one shown in figure 9 (4-21-64). BN-48654

Hydraulic Theory in Supercritical Flow Measurement

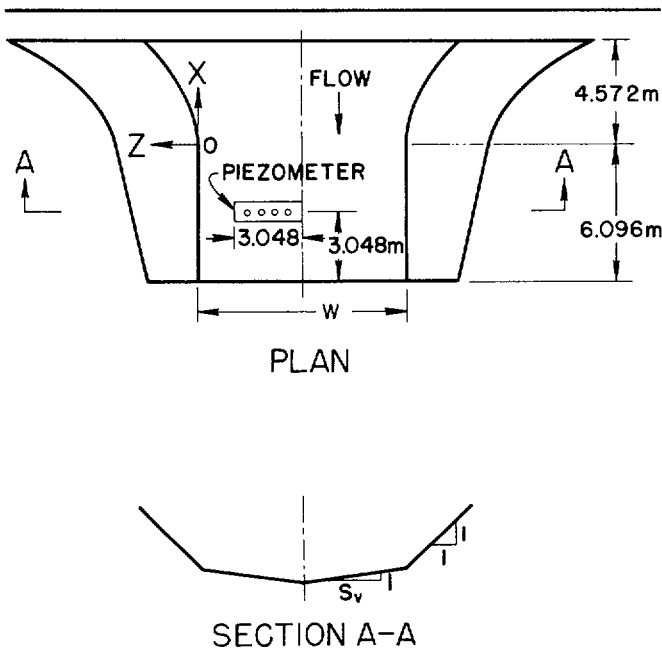


FIGURE 11.—Walnut Gulch supercritical measuring flume.

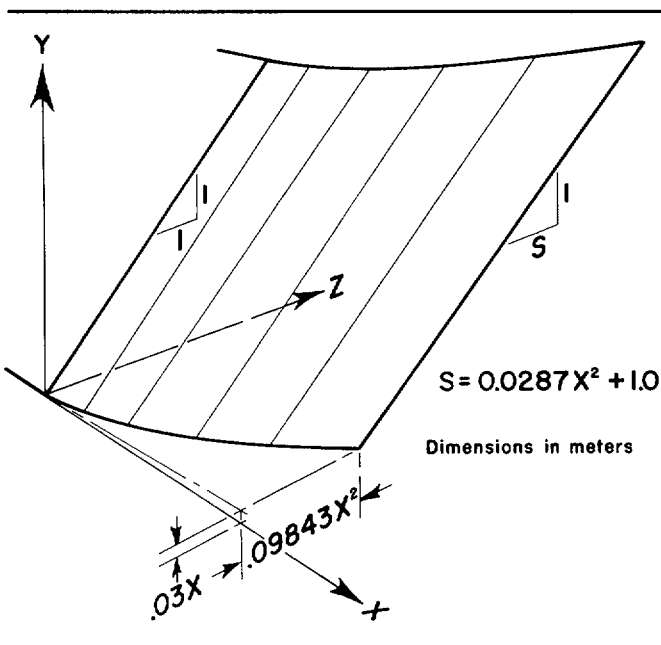


FIGURE 12.—Approach cylindroid surface, Walnut Gulch flume.

Before discussing the experimental development and field performance of this flume, it is useful to understand some of the hydraulic theory that deals with the measurements of flow and the development of a flume's rating by use of hydraulic models. In the following section, we present a brief explanation of the measurement sensitivity that may be reduced in order to pass heavily sediment-laden flows. We also discuss the hydraulic theory of flow through a supercritical flume and the theory that governs the similitude of model and prototype. Both mathematical and hydraulic models have played an important role in the development and analysis of this type of flume.

When natural stream velocities are sufficiently high, common flumes, which depend on measuring head upstream of a critical flow control section, are not suitable for reasons discussed above. In this case, we may still use a critical flow control section, but we measure depth below the critical section as the flow is accelerating in the supercritical region. The insurance that no deposition will take place in the flume itself is obtained at the cost of some sensitivity.

Measurement Sensitivities

Measurement sensitivity σ may be defined for our purpose here as:

$$\sigma(Q) = \frac{dh}{dQ} \quad (1)$$

where Q is discharge, and h is measured depth. Thus, equation 1 states that sensitivity is a measure of the relative change in depth with a unit change in discharge. Typically, for a weir or flume that forces the flow to pass through a critical depth section and measures a rating depth, h , above or below critical depth, the discharge is:

$$Q = C_w h^b$$

in which b is a parameter; or

$$h = \left[\frac{Q}{C_w} \right]^{1/b}$$

where C_w is a dimensioned weir or flume coefficient that includes the effect of flow area geometry. Sensitivity is thus

$$\sigma(Q) = \frac{dh}{dQ} = \frac{C_w^{-1/b}}{b} Q^{\frac{1-b}{b}} \quad (2)$$

Although velocities are widely different, both flumes and weirs have a value for b of 1.5, if width is constant. The value of b may be greater than 2 if width varies with depth.

Sensitivity for a particular discharge is then a function of C_w and b , and since flumes with high velocities have large C_w , they exhibit a lower sensitivity than measuring devices with low velocity and small C_w .

Flow Equations

Since almost all flumes or weirs use a critical flow section as a control for measurement, critical, subcritical, and often supercritical flow are experienced. All three forms of flow are defined in reference to the Froude number, Fr;

$$Fr = \frac{V}{\sqrt{gD}} \quad (3)$$

where V is velocity,
 g is gravitational acceleration, and
 D is hydraulic depth, defined as the cross section area of the flow, A , divided by the width of the free surface, T .

Weirs use a free overfall where critical flow, $Fr = 1$, occurs near the brink, downstream from the measuring point. Parshall or venturi flumes have transition sections that force flow through critical to supercritical flow for a short distance and then resume subcritical flow at or before the flume exit.

Supercritical flow flumes force flow through a critical section **above** the depth measuring point; depth is measured in the throat where flow is accelerating to normal depth for the supercritical slope within the flume throat.

Flow in this section is described by the same steady non-uniform flow equations that apply to other flumes. These are:

$$\frac{\partial Q}{\partial x} = 0 \quad (4a)$$

$$\frac{V}{g} \frac{\partial V}{\partial x} + \frac{\partial y}{\partial x} = S_o - S_f \quad (4b)$$

in which Q = discharge = AV
 A = cross section area = $A(y)$
 y = depth
 x = distance along flume
 V = velocity
 g = gravitational acceleration
 S_o = bottom slope of flume
 S_f = friction slope of flume.

S_f is calculated from the friction relation defining uniform flow. For the Chezy or Manning relationship,

$$V = CR^a S_f^{1/2} \quad (5)$$

in which R is hydraulic radius and C is the friction coefficient. For the Chezy roughness relation, $a = 1/2$. If a Manning relation is used, $a = 2/3$, and $C = \frac{1.49}{n}$, (English units) where n is the Manning roughness coefficient. Solving equation 5 for S_f , we have

$$S_f = \frac{V^2}{C^2} R^{-2a} \quad (6)$$

To calculate flow depth at any point within the flume, equation 4 is employed, starting with the critical depth section as a boundary condition. The transition region is divided into arbitrarily small increments, as illustrated in figure 13, and equation 4 is used in a finite difference expression. The equation thus becomes a Bernoulli equation for flow between the two sections i and $i + 1$:

$$y_i + \alpha \frac{V_i^2}{2g} = y_{i+1} + \alpha \frac{V_{i+1}^2}{2g} + h_e + \Delta x(\bar{S}_f - S_o), \quad (7a)$$

with

$$V_i A_i = V_{i+1} A_{i+1} \quad (7b)$$

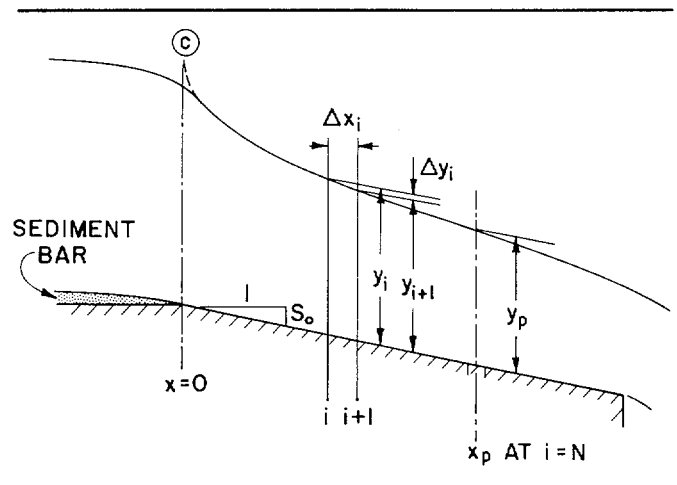


FIGURE 13.—Definition sketch of flow in supercritical transition.

Here α is the open channel energy coefficient (Chow 1959). \bar{S}_f is taken from equation 6 using a mean value of V and R in the length Δx . The eddy loss head (h_e) is defined by Chow (1959) as

$$h_e = K_e \alpha \left| \frac{V_i^2 - V_{i+1}^2}{2g} \right|$$

in which K_e is eddy loss coefficient. Chow (1959) gives typical upper limits of 0.1 and 0.2 for K_e in gradually converging and diverging reaches, respectively (English units). Section C (fig. 13) is about where critical depth occurs. Mathematically, this is a singular point, where the surface water slope is undefined. Practically, in alluvial channels with moving beds, the channel bed material will often form a region of transition of bottom slope from natural channel slope, S_c , to the imposed flume slope, S_o , where $S_c < S_o$.

In applying equation 7 to a specific flume, we use the actual geometry at each section to define:

$$R = R(x,y) \quad (8)$$

$$A = A(x,y). \quad (9)$$

Computationally, the distance from the critical section to the measuring section, x_p , is divided into $N-1$ increments. Equations 7, 8, and 9 are solved between successive sections $i = 1$ through $i = N$.

The boundary condition upstream at $i = 1$ (critical section) specifies that for a given Q , the Froude number is (nominally) 1.0, so that, by definition

$$V = \frac{Q}{A_i} = \left[\frac{gy_1}{\alpha_1} \right]^{1/2}. \quad (10)$$

Thus, y_1 and $A(Q, y_1)$ may be found from the geometry of the flume. Newton iteration is used to calculate y_{i+1} from equation 7 in sections 1 through $N-1$, and therefore to calculate y_p for any given discharge Q . A computer program developed for the simulation described herein is listed in Appendix A.

This numerical method provides a mathematical model for flow within a supercritical flume of any specified geometry. The same model will provide simulation of a subcritical flume, such as a venturi or Parshall flume, where depth is measured above a critical section, provided the numerical steps move upstream from the critical condition rather than downstream.

The analysis of the Walnut Gulch and similar supercritical flumes described below depend on both theoretical and experimental studies. Hydraulic models were an important part of the rating of the Walnut Gulch flumes. The transfer of model ratings to prototype ratings depends on proper use of hydraulic similitude, discussed below.

Model Similitude

Laws of similitude must be considered in using a hydraulic model to predict the rating of a larger flume. The most appropriate similitude criterion for open channel flow is the Froude number, which implies equality of the ratio of inertia to gravity forces for both model and prototype. Another important criterion is the Reynolds number, which implies equality of the ratios of inertia forces to viscous or friction forces in model and prototype. Both criteria cannot be met simultaneously, but for fully turbulent open channel flow with a high Reynolds number, the friction changes little with the Reynolds number. Therefore, the Froude number is commonly the governing similitude criterion.

When model scales in the horizontal and vertical are the same, the model is referred to as undistorted. When they are different, it is a distorted model. An undistorted scale model uses identical scale ratios in all three spatial dimensions, providing geometrical similarity. Using an undistorted model, with a scale ratio of L (using subscript p for prototype and m for model):

$$y_p = Ly_m \quad (11)$$

$$A_p = L^2 A_m \quad (12)$$

The Froude number is defined as

$$Fr = \frac{V}{\sqrt{gD}} \quad (13)$$

where D is hydraulic depth. Thus, if $Fr_m = Fr_p$,

$$\frac{V_m}{\sqrt{gD_m}} = \frac{V_p}{\sqrt{gD_p}}$$

or, from equation 11,

$$V_p = V_m \left(\frac{D_p}{D_m} \right)^{1/2} = V_m \sqrt{L} \quad (14)$$

where D_m and D_p are hydraulic depth of model and prototype, respectively. From equation 12,

$$Q_p = V_p A_p = Q_m L^{5/2} \quad (15)$$

Thus, equations 11 and 15 allow us to estimate a prototype rating from a hydraulic model rating.

Experimental Development of Walnut Gulch Flumes

Original Model Studies

The initial supercritical flume design was studied in the laboratory using a 1:32 scale model of a flume whose geometry was as shown in figure 11, with floor width of 9.14 m (30 ft), as in Walnut Gulch flume No. 3 (63.003). Piezometers flush with the surface were located in the downstream half of the straight section, both in the V-shaped floor and sides of the flume. The purpose of these measurements was to determine the best location to measure the head. Results of some of these measurements are shown in figure 14. Station 10+75 was the outlet end of the flume. The pressure on the floor at the measuring section of the flume was found to be approximately hydrostatic when the depth of the flow is less than the

distance to the downstream edge of the flume. The midpoint of the narrow, straight portion of the flume was selected as the best point to measure the head. For Walnut Gulch flume No. 3, the total width (4.57 m; 15 ft) of one side of the floor was used to measure the head and acted as the intake to the stilling well. For larger flumes, the length of the intake was limited to 3.05 m (10 ft) as shown in figure 11. The development of the flumes and model techniques used in these studies were reported by Gwinn (1964, 1970). The various flume dimensions were chosen solely to match existing channel geometry and reflect a compromise between desire for contraction and need for peak flow capacity. A summary of the flume dimensions and scales used in the model studies is given in table 1.

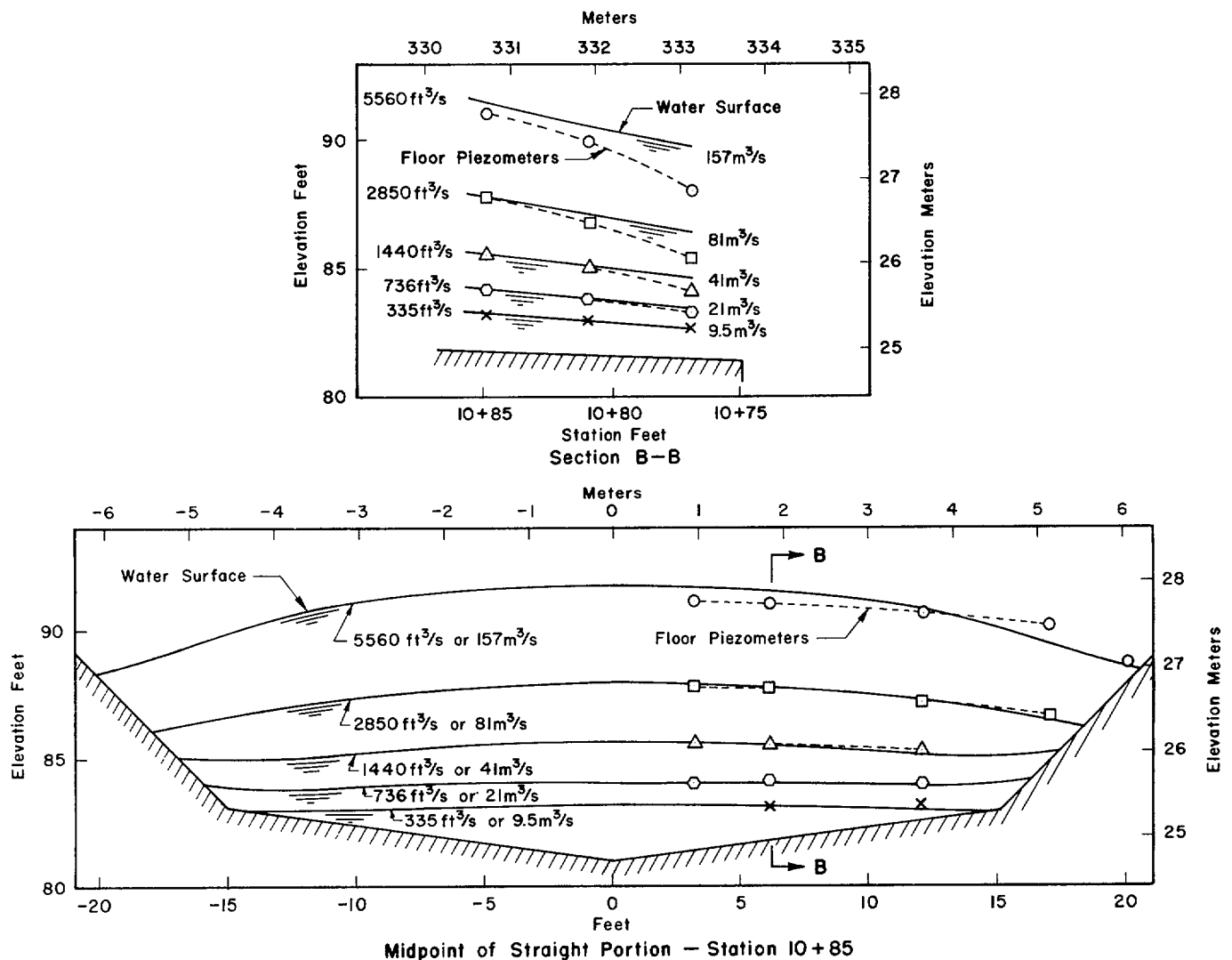


FIGURE 14.—Water surface profiles and floor piezometer measurements for the initial design of Walnut Gulch Flume No. 3.

TABLE 1.—Summary of laboratory-calibrated Walnut Gulch flumes

Flume No.	Floor cross slope (S_p)	Depth at sidewall intersection		Flume width		Maximum discharge		Model length scale
		Meters	Feet	Meters	Feet	M^3/s	ft^3/s	
1	15	1.22	4	36.58	120	740	26,000	1:40
2	15	.61	2	24.38	80	560	19,700	1:40, 1:20
2	15	.90	2.95	24.96	81.9	560	19,700	1:20
3	7.5	.61	2	9.14	30	170	6,000	1:32
4	10	.08	.25	1.52	5	34	1,200	1:30
6	10	1.07	3.50	21.33	70	470	16,500	1:30
7	10	0.61	2	12.19	40	244	8,600	1:30
8	10	.61	2	12.19	40	244	8,600	1:30
11	10	.46	1.50	9.14	30	170	6,000	1:30
15	10	.61	2	12.19	40	235	8,300	1:30

¹Original floor, combination slope 1 on 5 for 3 m (10 ft) and horizontal for 9.14 m (30 ft), (fig. 15).

²Revised floor, combination slope 1 on 5 for 0.503 m (1.65 ft) and 1 on 15 for 11.98 m (39.3 ft).

Prototype ratings were originally obtained from the small model studies by a scaling that used a discharge coefficient, C_d . Model results were used to obtain a value of C_d in the expression

$$Q_m = C_D \frac{t_m}{2} \sqrt{2g} h_m^{1.5} \quad (16)$$

in which t is width of water surface at the measuring point when depth is h . C_D is dimensionless and is assumed to apply, therefore, to a prototype scale relationship for Q_p , using equation 16 where $h_p = Lh_m$ and $t_p = Lt_m$. C_D includes a distortion factor for flows above the sidewall-floor intersection, since $\frac{t}{2} h_m$ represents area for floor region geometry only. Model scale L , in these cases, is from 20 to 40, as in table 1. Model roughness was assumed properly scaled in comparison with prototype roughness, and no correction was applied. Selected data from these model ratings in prototype dimensions are given in Appendix B. A more complete discussion of the model results has been given by Gwinn (1970).

Colorado State University 1:5 Model Rating of the Floor Section

The small scale model studies at the Water Conservation Structure Laboratories in Stillwater, Okla., were unable to accurately evaluate low flow ratings. Subsequent knowledge of the distribution of flow depths indicated that this was an

important range of flow in the ephemeral type of hydrologic regime of the southwestern U.S. watersheds. Figure 15 shows the sample distribution of flume flow depths for flumes 1 and 6 (code numbers 63.001 and 63.006, respectively), indicating some 96 to 93 percent peak flow depths, respectively, occur in the floor region. The floor region of these flumes refers to that portion of the flume cross section below the intersection of the bottom V-shaped region and the 1:1 sidewalls. To better define low flow ratings, a larger scale 1:5 model study was initiated in a 6-m (20-ft) flume at the Colorado State University Engineering Research Center. The model consisted entirely of the flume floor section of the Walnut Gulch flumes with a sandbed approach. It had a cross-channel slope of 1:10 with a longitudinal slope of 3 percent. It was constructed of epoxy-coated plywood with an estimated Manning roughness of 0.011. Figure 16 shows the flume and sandbed approach.

Discharge rates were measured downstream from the model by a well-calibrated knife edge rectangular weir. Water was supplied by a pump from a lake below the flume. Upstream bed topography was simulated by sand placed and maintained at approximately the 1-percent slope of the natural channel. The model scale was not distorted. Head was measured by manometer at several points across the measuring section, located 7.62 m (25 ft) (in prototype dimensions) below the entrance edge of the floor.

Figure 17 summarizes results of the tests over a wide range of flows encompassing the capacity of the floor section.

Scaling of the 1:5 Model Data

Equation 15 neglects differences in friction coefficient C between model and prototype. More rigorously, equations 14 and 15 are independent of friction and friction law at a critical flow control where $Fr = 1$ in both model and prototype. If friction is dissimilar between model and prototype and flow is at normal depth as described by equation 5, scaling following the Froude number criterion depends upon which hydraulic friction relation is taken to apply (Murphy 1950, Chapter 8). The Chezy friction law satisfies the Froude number criterion if the velocities are scaled by the geometric scale ratio, $L^{1/2}$, (equation 14) multiplied by the ratio of roughness coefficients, C . The Manning friction law requires geometric scale ratio for velocity to be multiplied by $\frac{C_p}{C_m} L^{1/6}$. For example, equation 14, for differing surface roughness, C_m and C_p , for Chezy's law becomes

$$V_p = V_m \frac{C_p}{C_m} \sqrt{L} \quad (\text{normal flow}) \quad (17)$$

and, for Manning's law, becomes

$$V_p = V_m \frac{C_p}{C_m} L^{1/6} \sqrt{L} \quad (\text{normal flow}) \quad (18)$$

in which case, C is $\frac{1.49}{n}$, $n = \text{Manning's } n$.

The hydraulic conditions of this model study introduce a special problem in model scaling. The flume floor surfaces were significantly different. For the model, it was polished epoxy coating; for the prototype, it is finished concrete. Also, the flow is not critical at the measuring point. Therefore, roughness and geometric scaling are necessary. Moreover, flow conditions at the measuring point for which scaling is necessary are between critical flow, $Fr = 1$ (independent of roughness), and supercritical normal flow. Thus, scaling will lie somewhere between that required for critical flow and that required for normal flow, where roughness must be scaled as in equations 17 or 18.

The scaling procedure used here employs the numerical model (equations 7a and b for flow through the flume) to characterize scaling for the different roughness in the flume throat. In this region, flow is neither normal nor critical. We rewrite equations 17 and 18 as

$$V_p = V_m r_c \sqrt{L} \quad (19)$$

in which r_c is the scaling ratio for roughness. As noted above, $r_c = 1$ at critical depth, and is defined by equations 17 or 18 for normal depth.

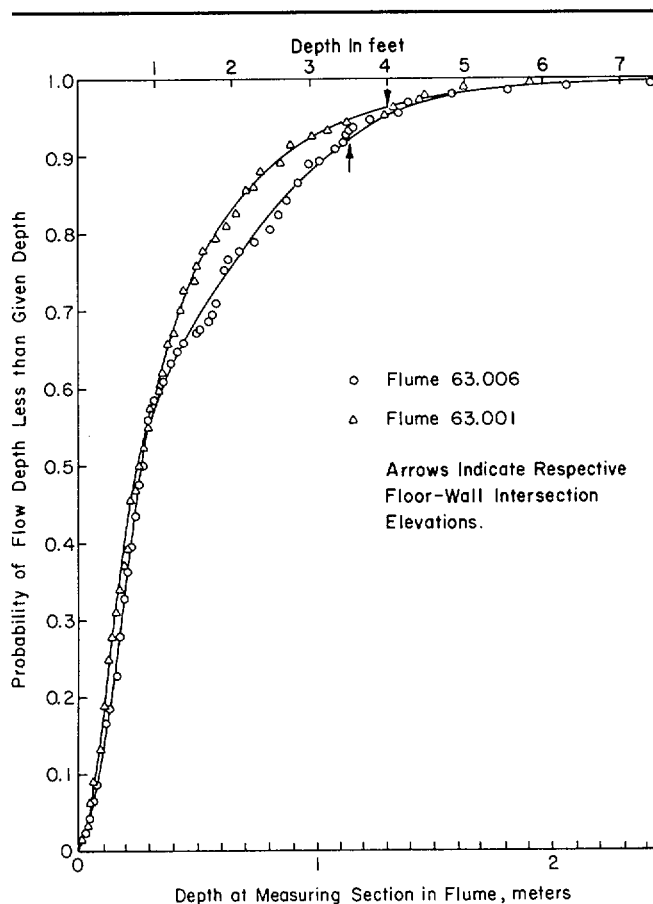


FIGURE 15.—Sample distribution of flow depths for flumes 63.001 and 63.006 at Walnut Gulch. Floor-wall intersection occurs at 1.07 m (3.5 ft) for flume 63.003, and at 1.22 m (4.0 ft) for flume 63.001.



FIGURE 16.—1:5 scale model of floor section of the Walnut Gulch supercritical flume, looking downstream along the sand approach. BN-48655

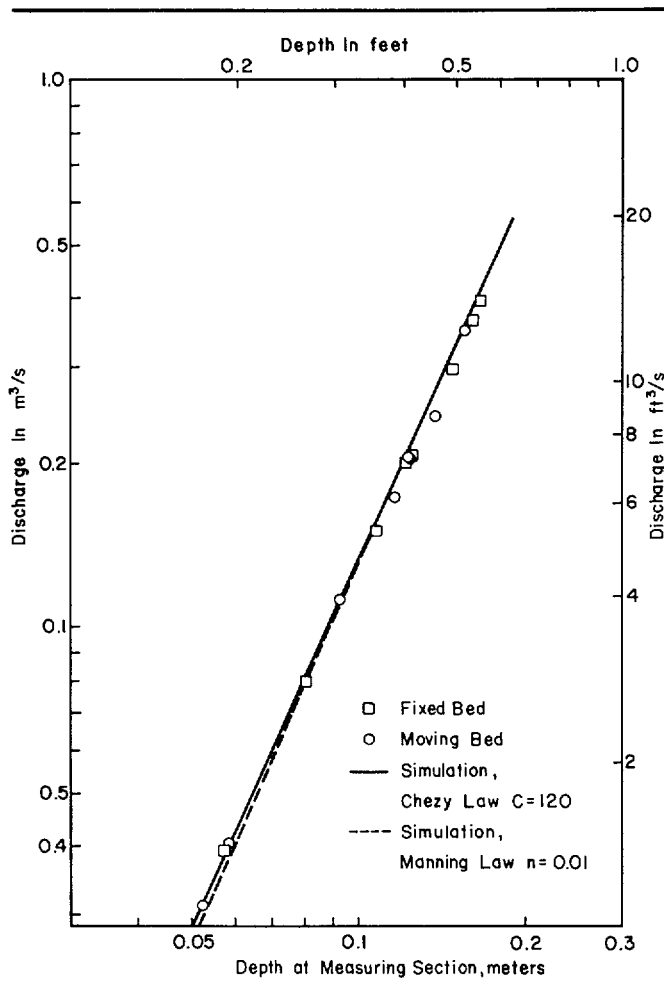


FIGURE 17.—Plot of experimental 1:5 model rating from experiments at Colorado State University and from computer simulation.

The following procedure was developed to evaluate r_c for the transition flow in the supercritical throat. If we assume flumes are identical except for roughness, with the same discharge in each flume, by the Chezy law,

$$C_r h_r^{2.5} = C_s h_s^{2.5}$$

where subscripts r and s refer to the rougher and smoother case, respectively. Scaling ratio, r_c , due to the Chezy roughness alone, is found as

$$r_c = \frac{C_r}{C_s} = \left(\frac{h_s}{h_r} \right)^{2.5} \quad (20a)$$

since the prototype is rougher than the model in this case. For the Manning roughness law, similarly,

$$r_c = \frac{C_r}{C_s} = \left(\frac{h_s}{h_r} \right)^{2.67} \quad (20b)$$

The Froude number at normal depth in supercritical flow, Fr_n , is always greater than one, and the Froude number at the measuring point $X = X_p$ (fig. 13), Fr_p , is always less than Fr_n . Expressed in equation form,

$$Fr_n > Fr_p > 1.$$

We define a dimensionless parameter, w , to represent the relative value of Fr_p , within its limits. Let

$$w = \frac{Fr_p - 1}{Fr_n - 1} \quad (21)$$

so that $1 > w > 0$, with $w = 1$ at normal flow and $w = 0$ at the critical section.

Simulations were performed over the range of model discharges 0.0003 to 0.57 m³/s (0.01 to 20 ft³/s) for a ratio of roughness coefficients of 1.2 (Chezy $C = 113$ and 134 or Manning's $n = 0.013$ to 0.011). The relation between r_c and the parameter w is found from this numerical simulation, and the results are expressed graphically as shown in figure 18. This graphical relation is then used to find r_c given w for a particular model test whose relative roughness parameters have the same ratio. Here, w is for the model from which scaling is to be done. The results in this figure should not be taken as general, even though both variables are dimensionless. For example, w at $x = 1$ m in the smoother case is not the same as w for $x = 1$ m in the rougher case. It does provide a more accurate estimate of prototype scale rating for conditions in the supercritical drawdown region.

Analysis of Model Ratings

Scaled values are computed in table 2 and plotted in figure 19 along with scaled results from the 1:30 model test at Stillwater and the computed rating from equations 7a and b. Within the respective ranges of applicability of the two model studies, rating relations for the supercritical flumes from the Stillwater and Colorado State University model tests are in excellent agreement.

Figure 19 also shows the computer simulation for the same conditions, indicating the ability to simulate ratings by using the mathematical model. Either the Manning or Chezy friction relation may be used for higher flows, and sufficient data at the very lowest flows are not available to discriminate categorically between the two relationships.

TABLE 2.—Scaling of Colorado State University flume model results

Q_m		h_m		F_{pm}	w_s	r_c^1	Q_p^2		h_p^2	
<i>Fixed bed</i>										
M^3/s	(Cfs)	Centimeters	Feet				M^3/s	ft^3/s	Meters	Feet
0.0374	1.32	5.85	0.192	2.28	0.242	0.973	2.03	71.8	0.29	0.96
.0402	1.42	5.97	.196	2.28	.242	.973	2.19	77.2	.30	.98
.079	2.79	8.23	.27	2.01	.19	.981	4.33	153.0	.41	1.35
.150	5.30	10.97	.36	1.86	.16	.985	8.27	292.	.55	1.80
.199	7.01	12.47	.409	1.79	.15	.986	10.93	386.	.625	2.05
.2033	7.18	12.5	.41	1.79	.15	.986	11.21	396.	.625	2.05
.244	8.61	13.9	.457	1.69	.13	.989	13.48	476.	.695	2.28
.297	10.49	15.0	.493	1.69	.13	.989	16.42	580.	.750	2.46
.364	12.87	16.4	.538	1.65	.12	.990	20.16	712.	.820	2.69
.395	13.96	17.0	.558	1.64	.12	.990	21.89	773.	.85	2.79
<i>Moving bed (upstream)</i>										
.031	1.09	5.33	.175	2.32	.25	.972	1.68	59.2	.265	.87
.111	3.92	9.45	.310	2.0	.19	.981	6.09	215.	.47	1.55
.174	6.15	11.89	.390	1.77	.15	.986	9.60	339.	.59	1.95
.205	7.25	12.74	.418	1.75	.14	.987	11.3	400.	.637	2.09
.244	8.62	14.05	.461	1.63	.12	.990	13.5	477.	.700	2.30
.349	12.32	15.8	.52	1.72	.13	.989	19.3	681.	.792	2.60

¹For all data, $Q_p(m^3/s) = 30.83 h_p^{2.2}$, h_p in meters, with $r^2 = 0.9993$, or $Q_p(ft^3/s) = 79.75 h_p^{2.2}$, h_p in feet.

²From figure 13 with w_s from model Froude numbers.

The computer model may also be used to demonstrate the sensitivity of rating at the control section to changes in the actual location of the critical flow section. The hypothesis is that in many streams steep slopes may cause critical flow to occur above the specified section, and the Froude number at the presumed critical flow point may be somewhat larger than 1.0. Table 3 shows computer simulation results, indicating that small changes in Froude number at the flume entrance do not have a large effect on the rating relationship, especially at lower flows.

Using the best fit regression line given below table 2, one may evaluate relative sensitivity of these flumes. For example, one may compare sensitivity of a typical supercritical flume of 1:10 cross-channel floor slope, at approximately 30 m^3/s , with that of a weir of the same approximate width, L_w . The weir rating is $Q = 3.3 L_w h^{1.5}$, approximately. One may apply equation 2 and find that the supercritical flume is only some 40 percent less sensitive than the weir.

TABLE 3.—Effect of upstream Froude number on flume rating simulation data for 21.34-m-(70-ft) wide flume

Discharge (m^3/s)	Froude number at $x = 0$			
	1.0	1.1	1.2	1.4
	-----Depth, m-----			
0.057 -----	0.0578	0.0578	0.0577	0.0577
0.28 -----	.1175	.1175	.1173	.1168
2.8 -----	.3289	.3284	.3273	.3236
28 -----	.9096	.9068	.9007	.8818

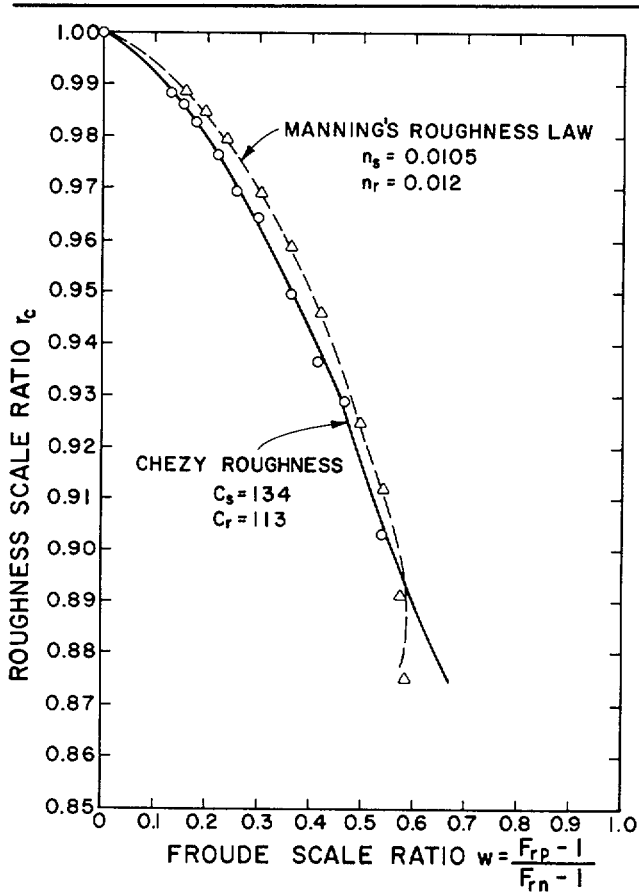


FIGURE 18.—Graphical procedure developed from computer simulation to estimate roughness scaling for transition flow.

Prototype Evaluations

Velocity measurements for evaluation of prototype rating for the Walnut Gulch flumes are difficult if not impractical using ordinary stream current metering methods. Flow discharges at any point and, for that matter channel cross sections, change quite rapidly during the flows in this hydrologic regime. Moreover, flows are ephemeral and unpredictable, velocities are often above most current meter ranges, and the amount of sediment and other suspended matter make using current meters impractical in most cases. The limited amount of prototype verification information is presented below. This includes one special measurement in the early flume history and a major ongoing instrumentation effort at another flume. Field performance of the Walnut Gulch flumes was briefly summarized by Smith and Chery (1974).

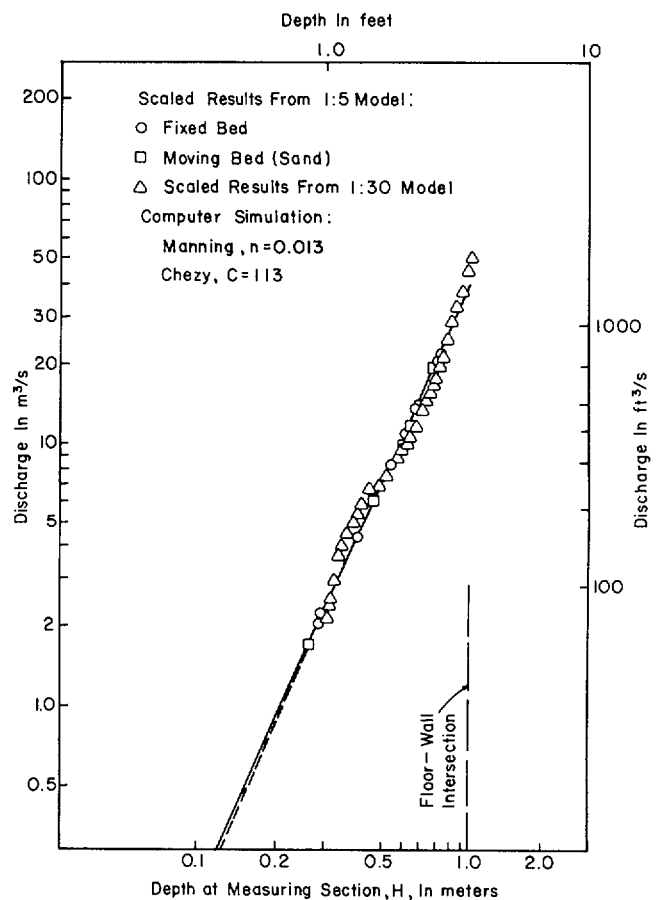


FIGURE 19.—Prototype rating for flume 63.006 developed from 1:5 model tests, scaled as in equation 19. Also shown are scaled results from the 1:30 model tests at Stillwater, Okla.

Velocity Measurements at Flume 63.002

When Walnut Gulch flume No. 2 (code number 63.002) was built, a railroad adjacent to the measuring site restricted the flume geometry and overall head loss available for use by the measurement structure. Thus, the geometry at the cross section was made to include a floor geometry with no cross slope, but it did include a 0.61-m- (2-ft) deep \times 6.1-m- (20-ft) wide notch (fig. 20) to provide additional sensitivity for measuring the base flow, which often occurs at this station.

On July 31, 1961, current meter measurements were taken in the "notch" of this flume using a Price current meter. The measurements were made from a rigid temporary bridge, which was positioned across the notched section of the flume near the flume entrance. Although the velocities at this point were high, flow depths were not changing rapidly enough to affect the measurements, and debris did not collect on the

meter. Thus, we have considerable confidence in the accuracy of these discharge measurements, although a few measured velocities required extrapolation of the meter calibration curve.

The results of the measurements, shown in figure 20, appear to agree with the laboratory-determined values from the model studies. The slight departure of the measured data from the small model rating and the bias in comparison with the computer model may be partly associated with the need to extrapolate the current meter calibration for this measure-

ment. Perhaps more important in evaluating these results is the apparent movement of the critical flow section to several feet upstream from the flume entrance. This movement of control was likely the result of the streambed narrowing in response to the flume notch. The general agreement among the three estimated ratings, however, added confidence to the scaled (1:30) model rating at higher discharges. At lower flow depths, water viscosity was a potential problem in the small scale model.

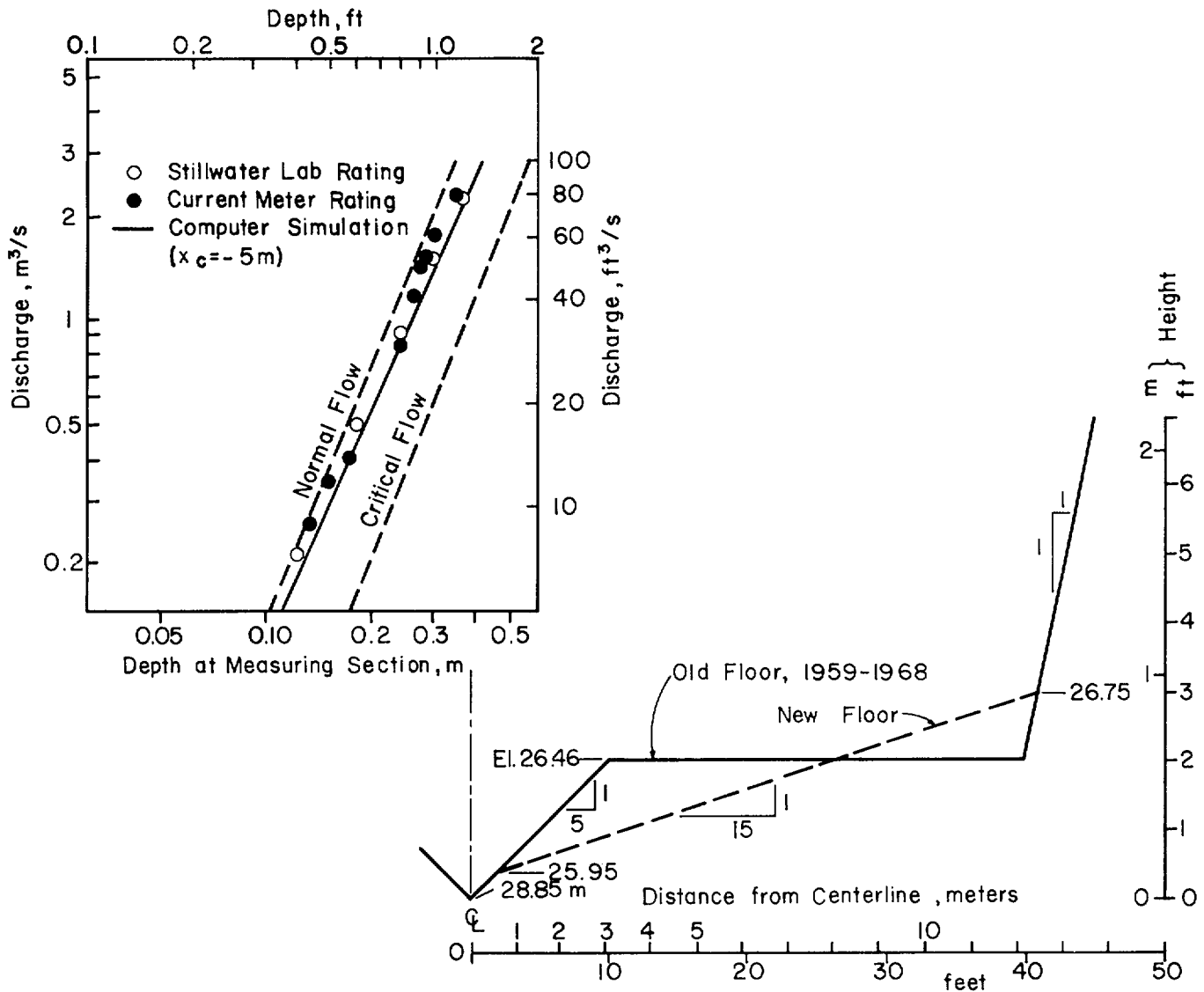


FIGURE 20.—Sketch of early cross-section at flume 63.002, and plot of current meter results obtained in 1961. Numerical model comparison indicates strongly that critical flow was occurring some distance above the flume during this test.

After the railroad was abandoned in 1970, the flat cross-sloped floor was replaced with the sloping floor shown in figure 20. The new floor affords greater sensitivity at depths exceeding 0.6 m (2 ft) than was possible with the shallow flow over the flat floor.

Prototype Data at Flume 63.006

In response to the need for prototype information on hydraulics of the Walnut Gulch flumes, a special study of flume 6 (station 63.006) was initiated in June 1973. An instrumentation footbridge 1.2 m (4 ft) wide and 30.5 m (100 ft) long was installed across this flume at approximately the measuring section, so that sampling across the flow would be possible. A movable carriage was mounted on the bridge to allow sampling at selected locations in both x and y dimensions. The instrument carriage and bridge are illustrated in figure 21.

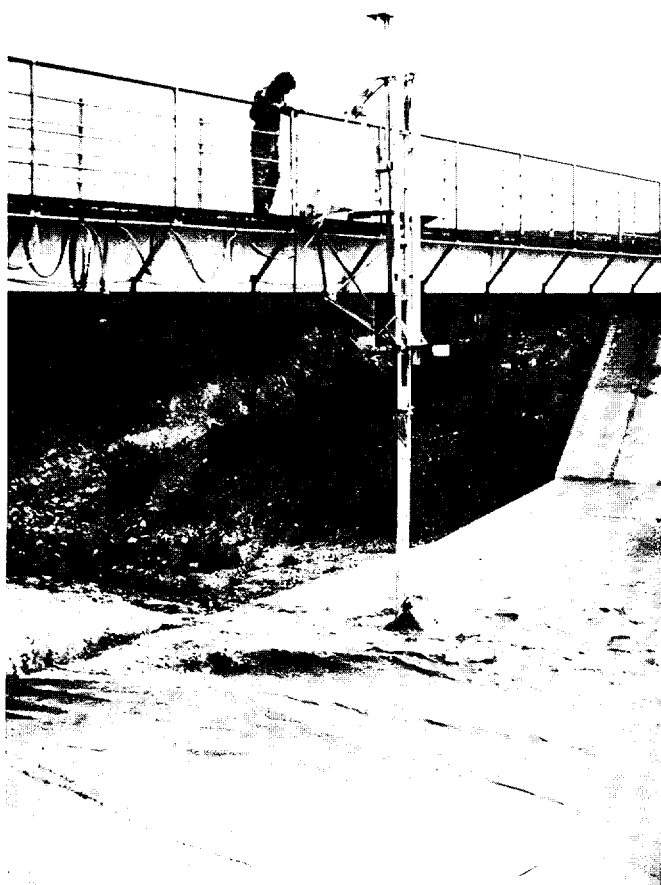


FIGURE 21.—Instrument carriage and velocity meter probe in use at flume 63.006, August 10, 1976. BN-48656

A streamlined electromagnetic velocity meter was mounted at the bottom of a vertical, movable probe, at a 45° incline to pass trash without damage or interference with meter readings. The meter has range capability that matches the high velocities in the flume throat. Depth of flow is recorded by using two sonar depth gages, one fixed at the center of the flume and a second moving with the sampling carriage. Potentiometers automatically record the x and y positions of the velocity probe. All hydraulic data are recorded digitally for automatic processing.

Measurements were made during 15 flow events in 1974-77 with varying degrees of success. From these measurements, four scans from four events, shown in figures 22 through 25, were selected as valid representations of the range of flow depths observed to date. These measured flows ranged in average depth from 0.38 m (1.25 ft) to 0.89 m (2.92 ft) with discharges of about 1.81 to 29.3 m³/s (64 to 1,036 ft³/s).

Velocity contours were estimated from the point measurements of the velocity probe. At each point, at least two samples of velocity were recorded. After the data were obtained, it was observed that after moving the probe the first measurement was usually low because of the time constant of the instrument response. Thus, the low first values were disregarded. Of all the cross sections, only scan No. 12 on September 4, 1975, has two points in which there is considerable confidence. Both were obtained by placing the probe in one position for several minutes, just before the scan and then just after the scan. The average velocity for both points was 0.25 m³/s (8.8 ft³/s) (fig. 23).

The area between each contour was measured and multiplied by its representative velocity to determine the discharge and calculate the velocity distribution (energy) coefficient, α . This coefficient was calculated by the following relation:

$$\alpha = \frac{\sum_j V_j^3 \Delta a_j}{\bar{V}^3 A} \quad (22)$$

where v_j = point velocity between contours;
 \bar{V} = average velocity
 a_j = incremental cross section area, contour j
 A = total cross section area.

The discharges calculated by these computations are plotted at both the centerline depth and the mean depth in figure 26. The line on this plot is the flume rating from 1:5 model tests. Also shown in symbols is the laboratory rating prepared from the early 1:30 scale model tests. For a given depth, less than 1 m (3 ft), the measured discharge is less than the rating relation indicates. This difference decreases as the depth increases until the measured values agree with the laboratory ratings at about 1 m (3 ft).

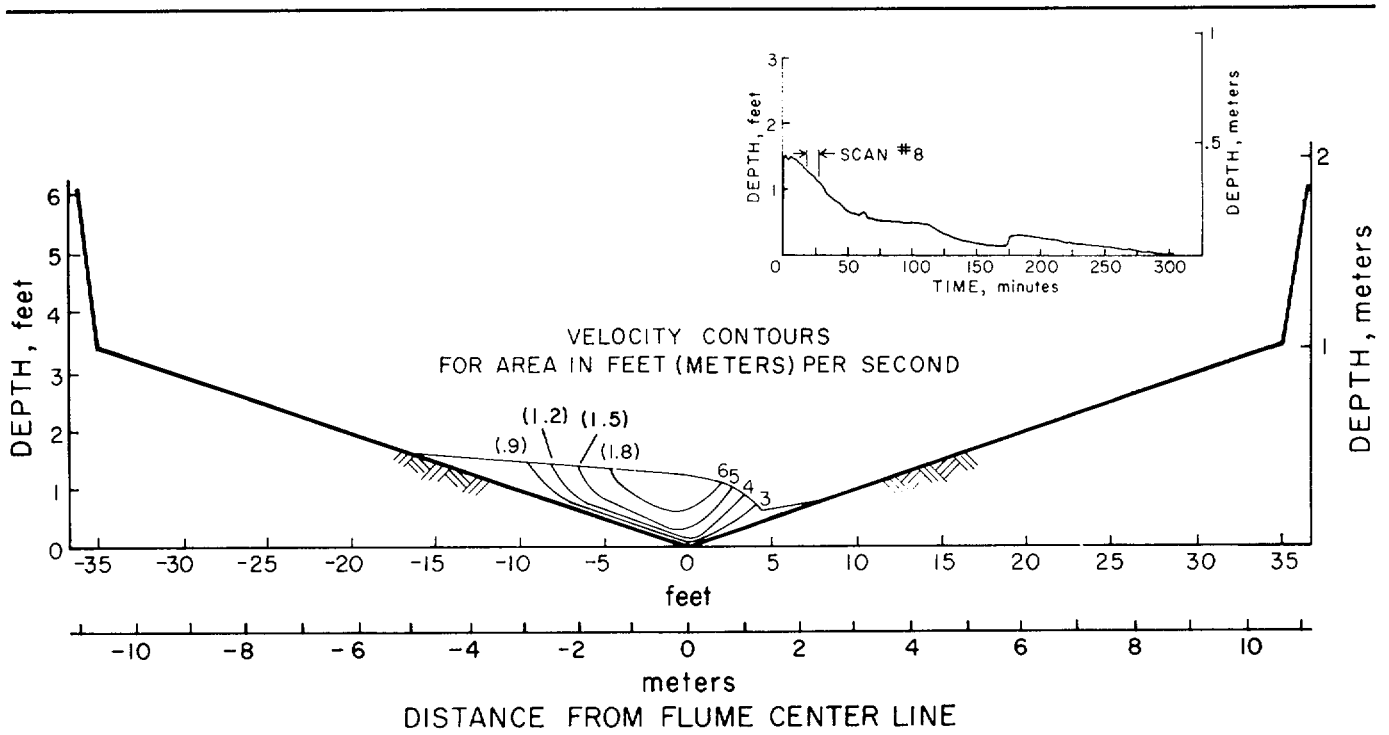


FIGURE 22.—Flume 63.006, flow profile and velocity contours for flow of September 6, 1974, scan No. 8.

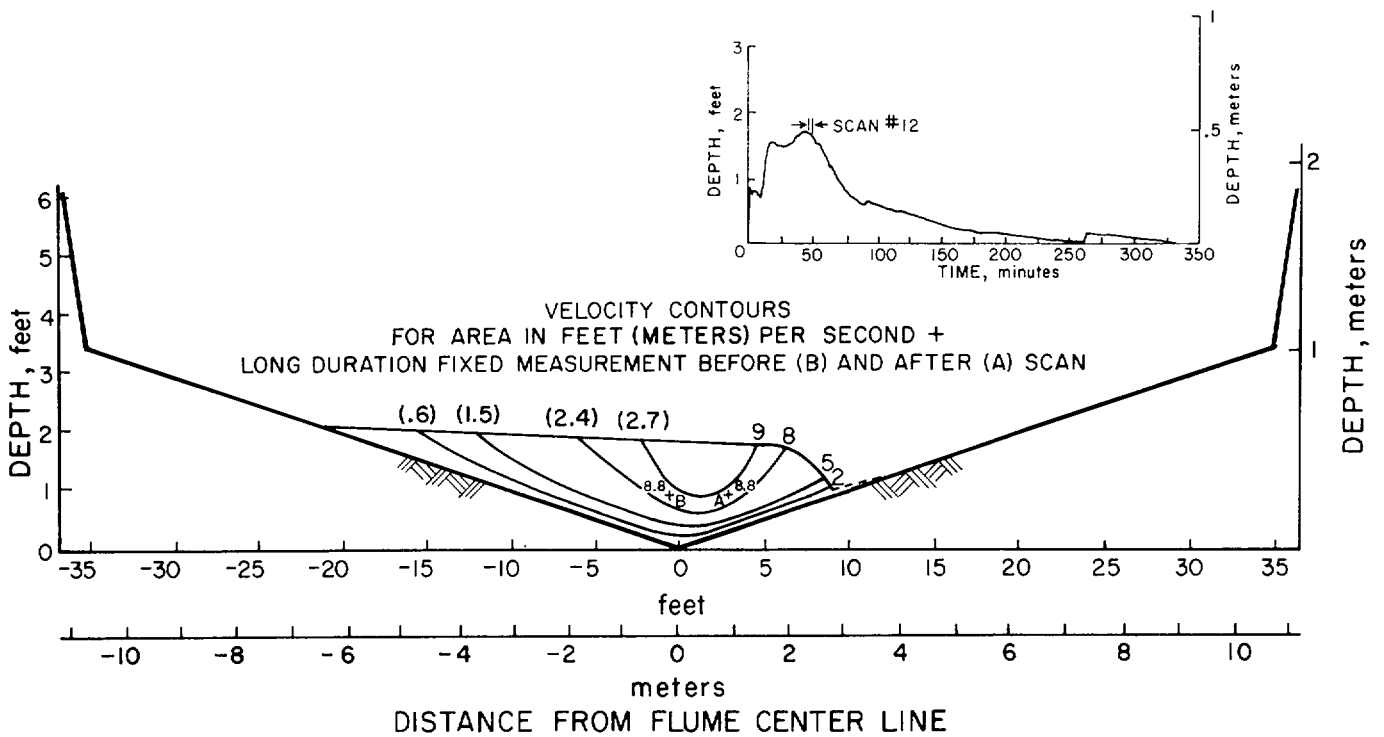


FIGURE 23.—Flume 63.006, flow profile and velocity contours for flow of September 5, 1975, scan No. 12.

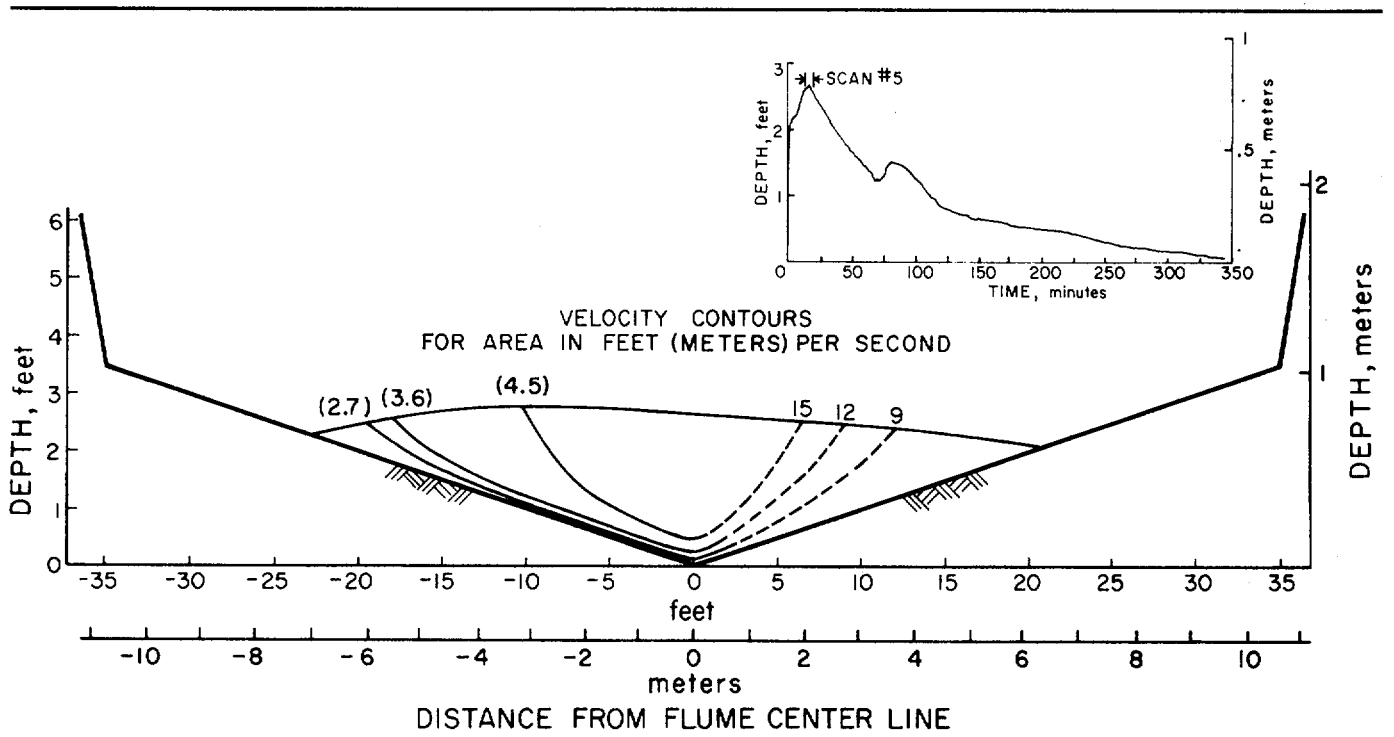


FIGURE 24.—Flume 63.006, flow profile and velocity contours for flow of July 22, 1975, scan No. 5.

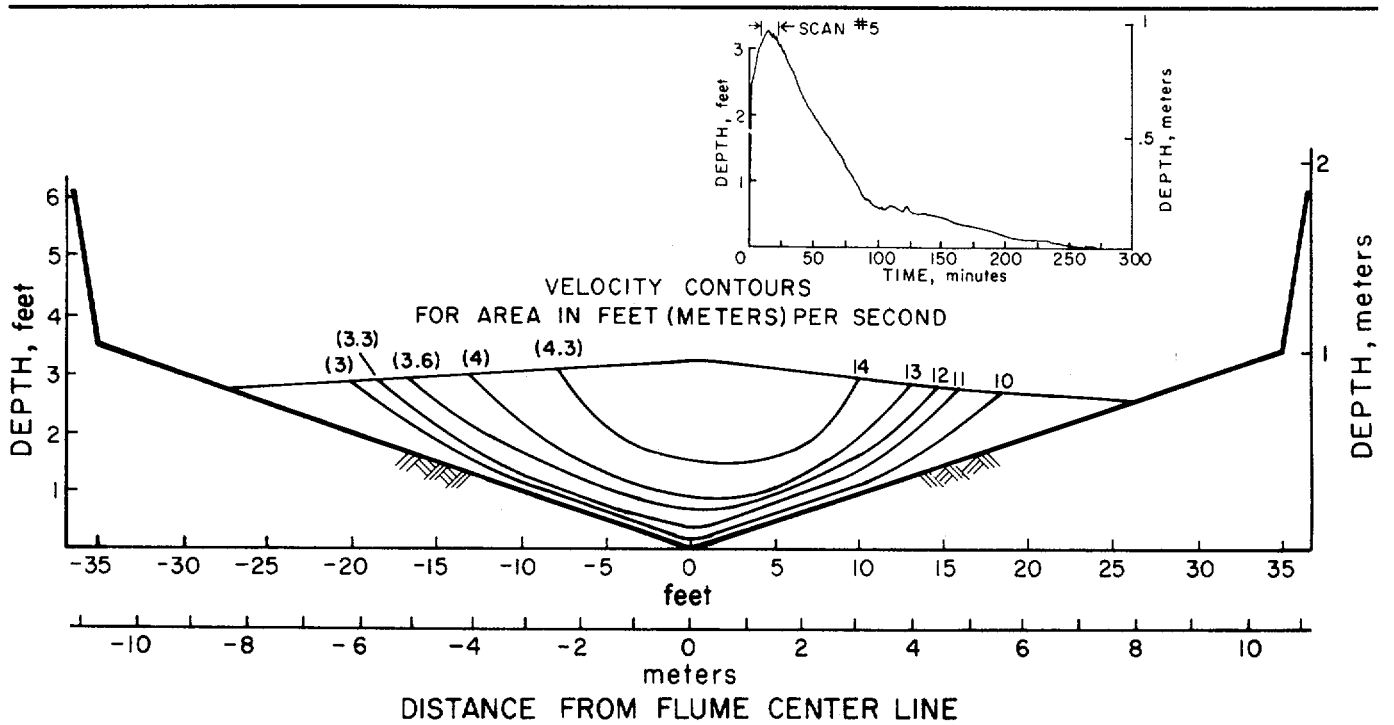


FIGURE 25.—Flume 63.006, flow profile and velocity contours for flow of September 2, 1974, scan No. 5.

These departures from the rated discharge are believed to be a result of the flow entering the flume at an angle and having an asymmetrical cross section at the measuring point of the flume. The profiles in figures 22 through 24 show the various surface configurations of this asymmetrical flow. Flow depths must exceed about 1 m (3 ft) at this location before the flow will align itself enough that the flume geometry will control the flow in the measuring section, and produce a nearly symmetrical cross section, as is seen in figure 25.

The high-water traces on the flume floor, resulting from a medium depth flow of 0.46 and 0.61 m (1.5 to 2 ft) entering the flume at an angle, are shown in figure 27. This shows clearly that the path of the flow riding up on the left side of the flume and then turning back toward the centerline causes a standing wave to form about halfway through the flume and to extend to the outlet of the flume. This wave causes the stepped profile at the measuring section seen in the cross section plots of figures 22 and 23. Photograph of a small wave occurring in the flow of August 10, 1976, is shown in figure 21.

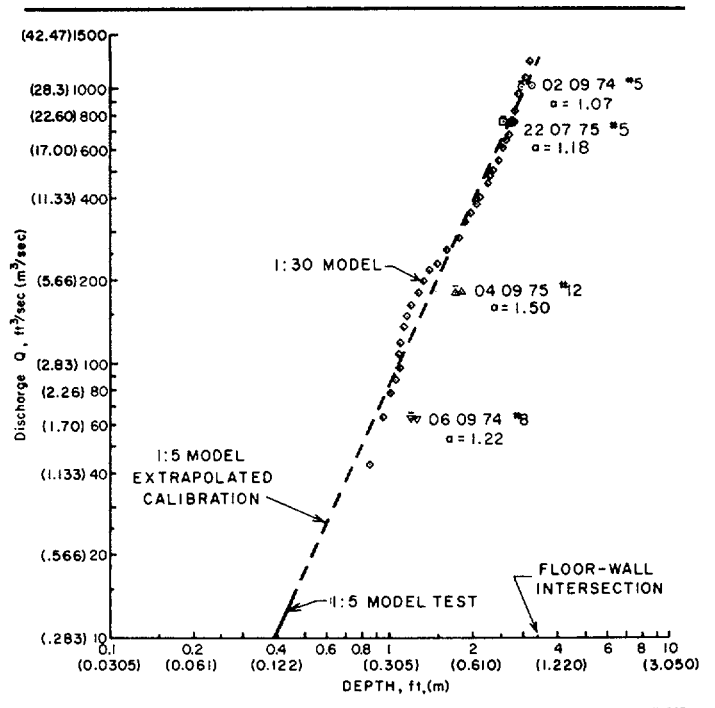


FIGURE 26.—Laboratory rating relation for flume 63.006 compared with measured values.

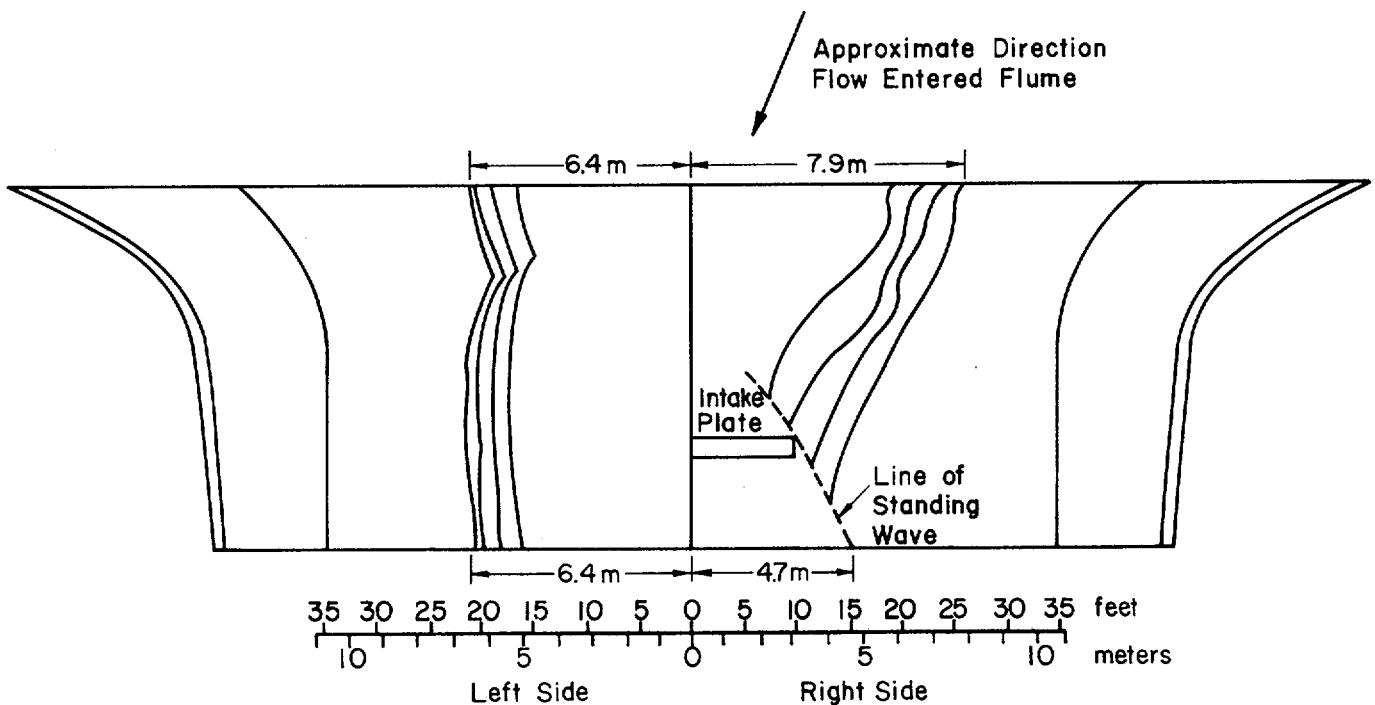


FIGURE 27.—High water traces for flow of August 17, 1976.

Field Application and Performance Evaluation

Stabilization of Approach Channels

Compounding the alluvial flow measurement problems outlined above, which led to the development of the Walnut Gulch flume, is the instability of thalweg location in the ephemeral flows of wide alluvial channels such as Walnut Gulch. Extremely asymmetrical entrance conditions have been observed in these flumes many times (Smith and Chery 1974). Figure 28 is a dramatic illustration of the asymmetry of the alluvial bar formed during flow through flume No. 63.007. Not only are flow centroids off center, but also mean flow direction at the flume entrance is often at a significant angle to the centerline direction of the flume. Methods to correct this misalignment had been generally unsatisfactory up to the time of modeling the flume floor at Colorado State University in 1971.

Experimental arrangement.—The 6.1-m (20-ft) wide outdoor flume at Colorado State University used for the 1:5 model rating of the floor section was also used to conduct tests on methods to stabilize the alluvial approach channel conditions. Views of the experimental arrangement are shown in figure 11. Sand was placed to a 60-cm (2-ft) depth for 15 m (50 ft) upstream from the 1:5 scale model of the flume floor section. The sand was chosen to closely model the mean grain size of sand found at Walnut Gulch; however, rocks and large gravel were not present, although slope and general bed shape were duplicated. Water was introduced into the sand approach severely off center to test the adequacy of a number of possible arrangements of dikes and fences for moving flow to a centered, aligned position. Sand was introduced at the upstream end of the alluvial section to maintain a bedload without



FIGURE 28.—View of flume 63.007 looking upstream, showing the large alluvial bar at the flume entrance which indicates a strongly asymmetrical entrance condition.

BN-48657

appreciable net scour. Figure 29 shows how the model duplicated standing waves common at flume 6 (and others), and affords a view of the asymmetry of the bedload.



FIGURE 29.—Standing wave produced in the measuring section of the 1:5 model at Colorado State University. The pattern of asymmetrical flow produced by flow entering the flume floor from the upper right is reflected in the pattern of bed load, which is easily seen through the relatively clear water.

BN-48658

Model results.—The first series of tests used 0.64-cm (1/4-inch) mesh hardware cloth “fences” or porous dikes placed in the alluvium with their tops at the desired bed elevation, assuming the bed steepens as measured, with a transition from the 1-percent natural slope flat bed to the 3-percent slope 1:10 floor of the flume. These fences were placed in equally spaced pairs at a 45° horizontal angle to the centerline, with each pair allowing a 5-m (15-ft) (prototype) open space in the channel center.

These fences or porous dikes did help to center the flow, but the control was inefficient. A centered bar developed, and the thalweg that developed during recession was to one side of this bar. Also, a slight wave formed on either side within the flume probably due to the contraction around the center bar. The fences proved inadequate to control the sand elevation without more positive control of the water.

The next series of tests used metal sheets acting as low, impervious dikes. In contrast to the porous sand dikes, these were placed to model a 0.3-m (1-ft) extension above expected minimum bed elevation, and the dike tops maintained a 1:10 cross-channel slope and a 1-percent upstream slope. These dikes provided positive control of the flow as would be expected; however, small scour areas formed at the center end of the dikes during recession, causing low flows to favor a position at one side of the open center section. Some scour behind these impervious dikes was also noted in every test.

The last series of tests used porous dikes (0.64-cm) (1/4-inch) (hardware cloth) on the same pattern as the impermeable dikes tested previously. These dikes are distinguished from the fences previously described in that they are higher and act to direct the flow rather than attempt to stabilize the sand bar location alone. This arrangement appeared to be a satisfactory method of control, with a minimum amount of scour and no appreciable asymmetry at the flume entrance, as illustrated in figure 30.

Prototype trials.—Existing Walnut Gulch flume No. 3, code No. 63.003, 12.2 m (40 ft) wide, was used as a prototype test site, and porous dikes constructed of surplus aircraft landing mat were installed early in the summer of 1971. One previously installed dike pair was incorporated into the arrangement as the upstream pair. The resulting pattern consisted of two pairs of dikes, at approximately a 45° angle to the centerline, with a 4.9-m (16-ft) center opening and the upstream pair of dikes at approximately a 30° angle to the centerline. Figure 31 shows the condition of the alluvium and dikes after a large flow at this site soon after dike installation. Several conclusions from this first prototype test were:

- a) Scour at the higher flows requires strong supports to prevent possible overturning of the dikes. Also, the dikes may accelerate scour and undermine the supports.
- b) Trash in the flow makes it imperative that the mesh openings be larger than 2.5 cm (1 inch) and the fences be aligned no more than 30° to centerline.
- c) Sand replaced around the fences after installation must be carefully compacted.

Field Experience

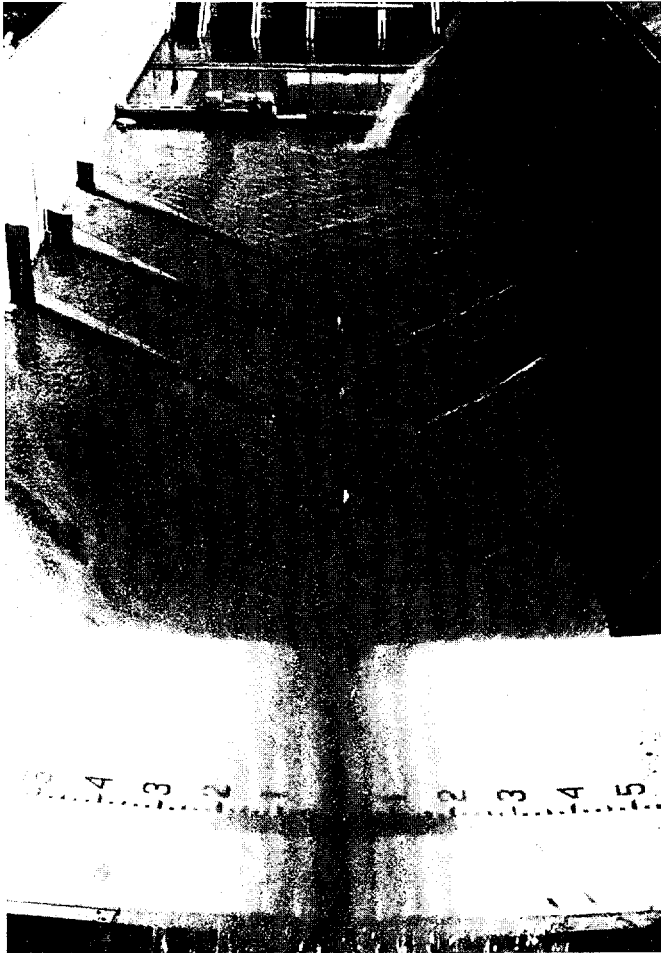


FIGURE 30.—The 1:5 model was used to develop the porous control dikes shown here. The porous dikes are effective in preventing asymmetry upstream of the flume entrance. BN-48659



FIGURE 31.—Prototype control dikes at flume 63.003 after large storm flow in early dike evaluation at Walnut Gulch Watershed. BN-48660

Porous flow control dikes at an angle of 30° to the flow have been placed above all but the smallest (site 63.004) Walnut Gulch flumes. As a result, maximum observed flow asymmetry has been limited to approximately 10 percent occurring at the widest flume (63.001). Figure 32 shows the controlled alluvial channel above flume 63.011. Flume 63.006 was left uncontrolled to obtain additional data on hydraulic conditions in asymmetrical flow into the flume. Control dikes will be installed there when experimentation is completed.

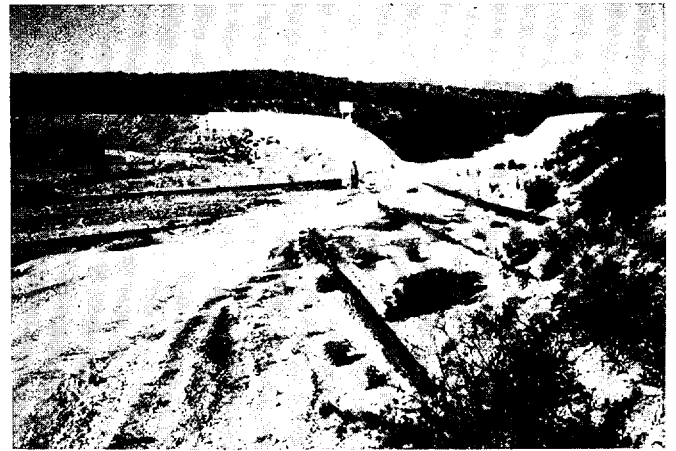


FIGURE 32.—Control dikes in place above flume 63.011, Walnut Gulch Watershed. BN-48661

Flows to date have shown little or no tendency to undercut or modify the dikes' performance. Exceptions have occurred at flume 63.001 where incoming flows were severely off center (an additional dike was installed), and at flume 63.002 where considerable damage occurred to some portions of the dikes and large holes were scoured downstream of the dikes after the large (1.5-m, or 5-ft peak depth) flow of July 17, 1975. Periodically, debris needs to be cleaned from dike openings to prevent excessive hydraulic roughness at the dike locations. Upstream dikes, which have the largest hydraulic forces acting upon them, must be anchored against overturning because the larger flows cause the bed to become fluid to a greater depth, thus maximizing the hydraulic overturning pressure.

Estimation of Discharge in Asymmetrical Flows

Since many years of early records at Walnut Gulch include flows with asymmetries ranging in extent from mild to severe, a method was devised to estimate discharge from such biased depth readings, based on the Colorado State University model tests. The operating assumption is that the area of flow at the measuring point for an asymmetrical cross section is roughly equal to the area for the discharge flowing symmetrically.

Figure 33 indicates that the assumption of conservation of area under asymmetry is apparently reasonable, based on the model test results at Colorado State University. Flow depths across the flow for asymmetrical flow conditions in the model were taken by a series of manometers during tests that imitated asymmetrical entrance into the flume.

For many flows at Walnut Gulch, there were observer notes giving elevations of each edge of the flow at the measuring point, in addition to the stilling well record of the mean depth over the stilling well intake plate. From this information and the study of typical asymmetrical cross section shapes from the model tests (fig. 34), the cross section areas were estimated from records and observer notes. The equivalent uniform flow depth may then be calculated from this area, and the rating is then calculated for that depth at that particular flume.

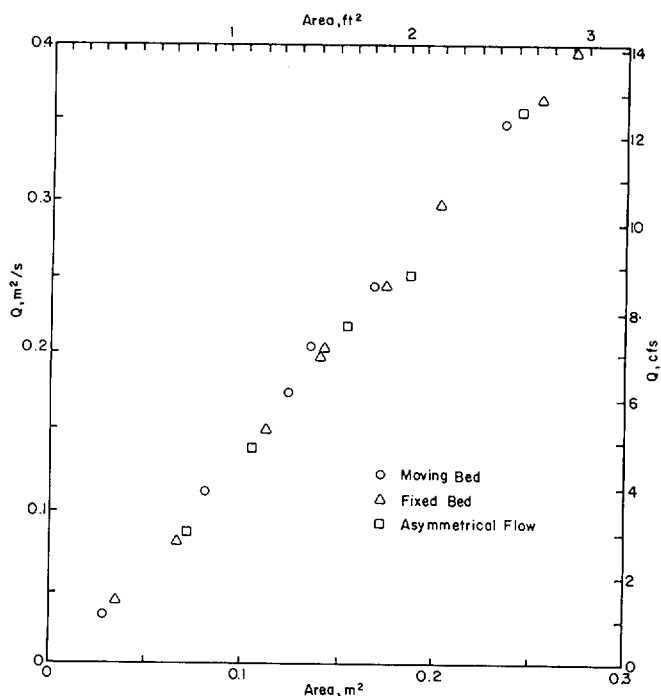


FIGURE 33.—Discharge-area relations; symmetrical and asymmetrical conditions.

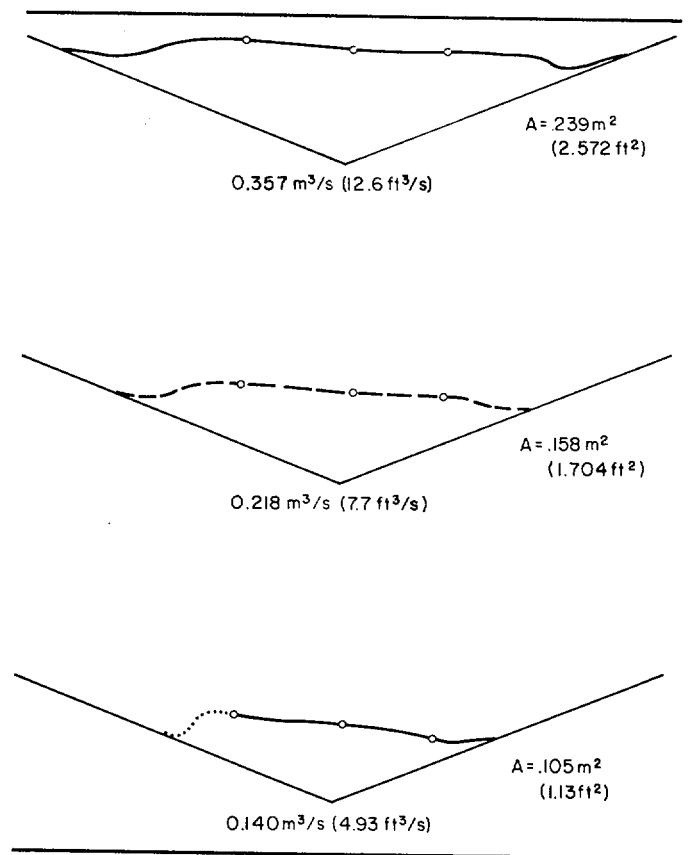


FIGURE 34.—Cross-section shapes at measuring section in Colorado State University 1:5 model flume. (Drawings not to scale.)

Design Modifications

Use and observation of the Walnut Gulch flumes to date have indicated some modifications and design limits for better performance.

The original effort in designing and testing these flumes emphasized their ability to pass and measure the peak flows of large floods. Indeed, the experience in 1954 with the first flumes used in the Walnut Gulch watershed was with a series of unusually large and, in some cases, disastrous flash floods. As a result, flows that were confined to the portion of the flume below the 1:1 sidewalls, called the floor region, were not given much consideration. Experience since 1954, as illustrated in figure 10, has revealed that flow depth distribution places the overwhelming majority of flows in the floor region of most of the flumes. Mean flume depth could be increased by a narrowing of flume geometry, which would force a significant contraction from the channel shape. This might, however, increase low-flow upstream control problems discussed above, and would require more attention to entrance transition conditions.

As originally designed, the Walnut Gulch flumes exhibit the characteristic of a shifting location of critical section as flow depth increases above the floor-wall intersection. At some flow depth above the intersection, control is expected to pass from the floor slope to the wall contraction. The depth at which this occurs depends on the particular flume geometry, as well as local upstream conditions. Unfortunately, the large width-to-length ratios of the larger Walnut Gulch flumes make wall control poor, unless flow depths are well above floor-wall intersection height. At the great widths and velocity of flows, with the relatively shallow depths encountered, contraction at the walls cannot change conditions at the center of the flume within the relatively short flow length of the flume.

Only a small number of flows have occurred that were deep enough to submerge the 1:1 flume sidewall, and no observations or measurements have been obtained to indicate precisely when and if control is exerted on the flow by the side-wall contractions. Figure 35, for example, taken at flume 6, seems to indicate that the drawdown at the curved wall is local and does not appear to be affecting flow in the flume center. "Humped" water surface cross sections, such as shown in figure 14, plus similar ones noted in field observation may reflect this condition.

Curved wall contractions or other flow redirection at higher flows and approach velocities typically generate surface waves (Wilm et al. 1938), which would affect flow within a supercritical flume; however, model tests and field observations indicate that channel conditions at higher flows usually produce relatively lower velocities at the channel sides. In fact, large standing waves, indicative of local supercritical flow conditions, are often observed in the channel thalweg. Under these conditions, a flume should not contract the natural channel width excessively, since it could generate waves affecting the flume measurement.

These observations indicate that the wall contraction (curved) region should be located to produce the critical flow control section at the same place that the sloping floor (throat) of the flume begins, so that the control section location will not change at increasing discharge. These observations also indicate careful judgment be exercised in extent of contraction used, with consideration given to length-to-width ratio of flumes. For very wide channels, it seems reasonable not to expect control from wall contractions.

These considerations were incorporated in the design of the Santa Rita flume, developed primarily for somewhat smaller capacity channels, which are described in the following chapter.



FIGURE 35.—Photograph of flow at night through Walnut Gulch Flume 63.006 (date unknown). BN-48662

The Santa Rita Flume

The previously described difficulties with weirs and venturi flumes and favorable experience with the Walnut Gulch supercritical flume in measuring sediment-laden flow prompted the development of an improved design for a supercritical flow flume. This flume was intended for use in small channel flow measurement, generally less than $4 \text{ m}^3/\text{s}$ ($100 \text{ ft}^3/\text{s}$); however, there seems to be no reason for limiting the size of the flume as long as certain proportions are maintained. The basic features and geometry of this flume are shown in figure 36. The name, Santa Rita, comes from the experimental area, south of Tucson, where the flume was first extensively used.

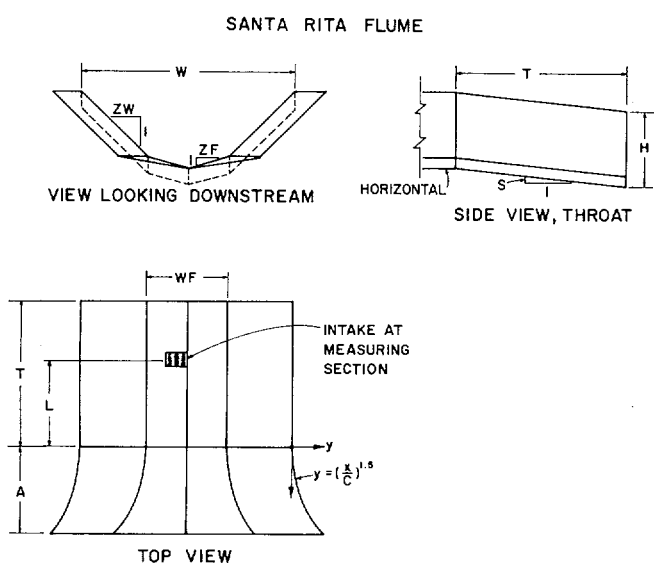


FIGURE 36.—Generalized design features of the Santa Rita supercritical flume.

The flume design incorporates two improvements over the original Walnut Gulch flume. The slope of the floor breaks at the entrance to the throat defined by the walls, rather than at the entrance to the curved approach. No movement of the measuring section should occur, therefore, for flows over the entire measurable range. Also, curvature of the approach wall has been reduced somewhat to decrease the tendency of waves to develop in the throat when flow direction changes too rapidly at the entrance walls for high entrance velocities. The length of the throat of such a flume is arbitrary, although the designs illustrated here are intended to insure that the supercritical drawdown profile is well developed upstream from the measuring section for the largest flow expected. Another important design consideration is that the distance below the measuring point to the flume exit be longer than the deepest flow expected. This is necessary to prevent modification of the hydrostatic pressure distribution at the measuring section

by the downstream overfall. As a rule of thumb, the measuring section should be at approximately two maximum depths downstream of the critical section, and the flume exit should be at least one and one-half depths beyond the measuring section.

One flume was rated at full scale in the 2.44-m (8-ft) wide tilting recirculating flume at the Engineering Research Center, Colorado State University. The data are shown in figure 37, along with computer simulation using both Manning's and Chezy's roughness relationships.

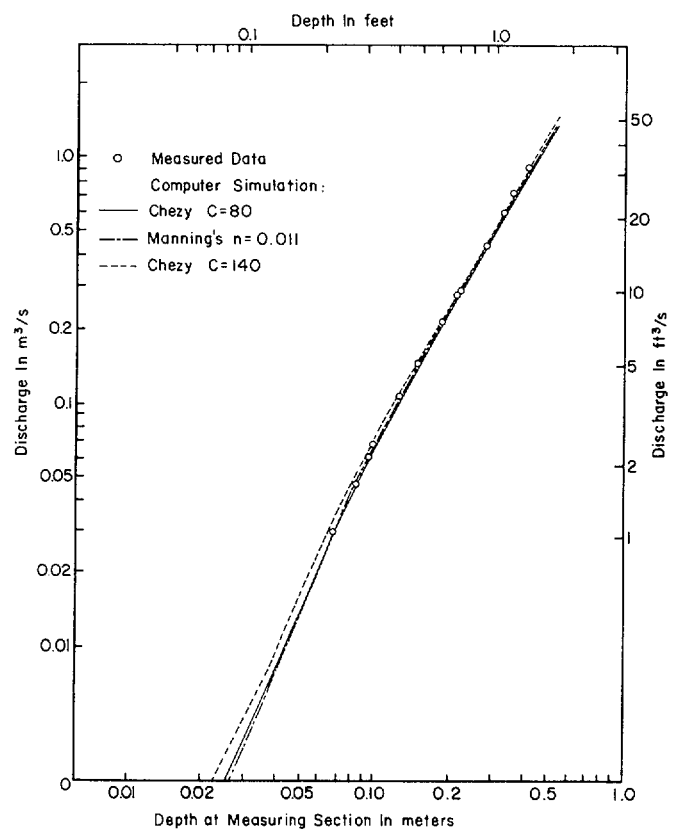


FIGURE 37.—Rating by hydraulic tests and by computer simulation for a $2.1 \text{ m}^3/\text{s}$ ($75 \text{ ft}^3/\text{s}$) Santa Rita flume.

Dimensions and ratings for several sizes of the Santa Rita flume are presented in Appendix C in both English and metric dimensions. The ratings assume that the Santa Rita flumes with capacity smaller than $5 \text{ m}^3/\text{s}$ ($100 \text{ ft}^3/\text{s}$) are made of metal, and all others are assumed made of concrete. Our experience suggests that after construction, a single rating point should be taken during low flow by volumetric measurement of discharge at the downstream overfall. At low flows, if flow at the measuring point is nearly at normal depth, the

rating gives a value of roughness for use in the computer rating. Then, a more accurate rating can be simulated. Small errors in estimation of flume roughness do not significantly affect higher flow ratings.

Some judgment is appropriate in designing the length and expansion of the approach. This depends on the width and slope of the stream channel at the site. Suggested approach curvatures and lengths are shown. Since the approach floor has no longitudinal slope, the alluvium will form a bar on the approach floor, which will taper out before the critical section where flow accelerates. This has been observed to occur at all installations to date.

The first such flume was made of concrete, using gunite and metal screeds to control the finished shape; however, most of the other early flumes were made of steel, constructed in the shop to be moved to the measurement site. Appendix D shows typical fabrication plans for a metal Santa Rita flume.

If $ZF \rightarrow \infty$ (fig. 36) or the floor section is flat, the Santa Rita flume becomes trapezoidal, recalling the early design of Robinson (1961). In this version, the stilling well intake is located in the sloping wall adjacent to the floor intersection. This design, while sacrificing some lower flow sensitivity (depending on the floor width), has the advantage of a stilling well intake that traps far less sediment than the flumes with a V-shaped floor, where much of bedload flows directly over the intake slots. The trapezoidal shape, with $ZF \rightarrow \infty$, cannot be simulated by the computer program in appendix A without minor modifications.

A method for handling the high exit velocities needs to be devised. A rock-lined (preferably cement-mortared) depression in the bed, into which the flume can discharge, has worked well at one location. In other sites in the Santa Rita range, the channel is sufficiently rocky that artificial downstream protection has not been required. Natural pools developed and apparently became stabilized, providing an energy dissipation pool during flow periods. Several large Santa Rita flumes are presently (1979) being installed in a watershed in Mississippi. These are located in erodible sand material; therefore, downstream scour protection is being designed by model testing.

In general, channels where sediment and stream velocities require supercritical flumes have relatively steep channel slopes and do not have tailwater inundation problems. After flume installation, a transition period of upstream bed accretion and limited downstream degradation should be expected. The original Walnut Gulch flumes were installed nearly a meter above the channel bottom; however, from experience gained since installation, this now seems unnecessary. Considerable upstream accretion has taken place at each flume over a period of several years, and the drop to streambed at the downstream edge of the flume is now a potential safety hazard.

Weir Extension Flume

One method developed to reclaim measurement stations where weirs are being inundated with bedload sediment is construction of a supercritical V-shape or triangular flume just below the weir. The former weir becomes the upstream cutoff wall for the flume, as shown in figure 38. As in the Santa Rita flume, the length of the measuring section should lie at least one and one-half depths upstream of the flume exit to reduce the effects of the free overfall on the pressure distribution at the measuring section.

Appendix C includes dimensions and rating table for two sample triangular flumes. Local entrance flow conditions will determine whether it is necessary to construct approach walls for a site where a weir is being converted.

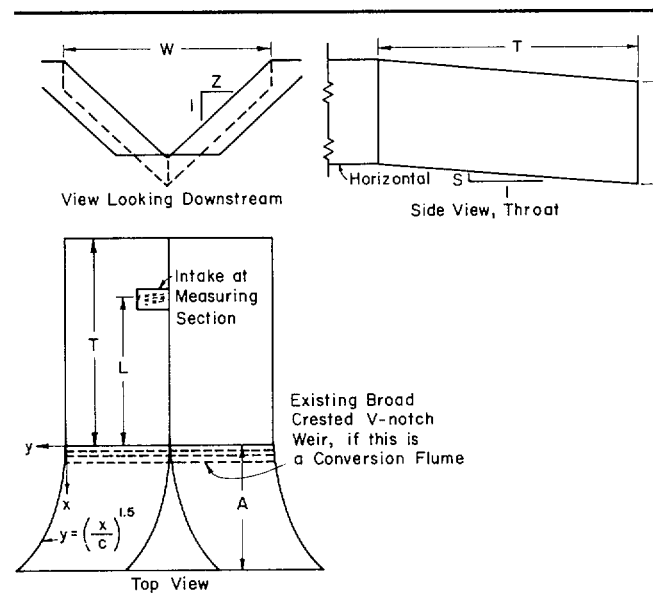


FIGURE 38.—A supercritical flume design which uses an existing V-notch weir for an upstream cutoff wall.

Sensing Water Level in Heavy Sediment Conditions

Problems arise in sensing water level in a supercritical flume, not due to the velocity of the flow, but due to the nature of the flow. These are (a) rapid rise in flow depths, (b) high sediment loads, and (c) long periods of no flow. These conditions can occur also in subcritical flow flumes.

The first and third conditions constitute a hydraulic problem in stilling well design; for each event, the stilling well must first be filled from water flowing through the flume before flow depths can be recorded. Times to peak flow of only a few minutes are not uncommon even for flows of more than 100 m³/s, and the recorded level will lag the flume level by as much as several minutes. Large sediment traps need to be provided under the intake in the flume to deal with the high sediment loads. Records obtained from the stilling wells originally constructed in the Walnut Gulch flumes are affected by all of the above conditions. Flows are often obscured by sand deposition in the stilling well after only an hour or two of flow. Figure 39 shows the extent of sand accumulation in the original intakes. This typically must be removed after each flow event.

An ideal water-level sensor would operate without taking on any volume of water from the flow. The nitrogen bubble gage, with a servomanometer follower, has this feature; however, there are serious problems in locating a bubble orifice in the boundary layer of a high-velocity heavily sediment-laden flow such that it will (a) not disturb the flow so as to record a biased value of the local hydrostatic pressure, and (b) not allow sediment to enter and clog the gasline. It remains to be demonstrated how this can be accomplished for reliable operation in field situations. In order to sense low flows, the bubble outlet must be located at the center notch of a

V-shaped floor, where exposure to bedload sediment is most extensive. An experimental installation of a bubbler gage in a Santa Rita flume is presently (1979) being evaluated. The outlet tube for nitrogen is installed near the notch of the floor but at a slight upward angle. The resultant tube opening, cut flush with the flume floor, presents an elongated elliptical orifice to the floor.

Two electronic depth-sensing devices, a sonar and pressure transducer, have been used at flume 63.006 to measure stage. Both have the ideal characteristic of not taking any volume of water from the flow and, thus, have no intake and stilling well problems.

The sonar transducer functions by measuring the time that a high-frequency audible sound wave travels to a reflecting surface and returns to the transducer. Care must be used in positioning the transducer with respect to the flow surface, but, in general, the instrument has proved to be quite reliable and durable. It has given resolutions of stage sufficient to plot all the flow profiles illustrated in figures 17 through 20.

The pressure transducers used have had a measuring surface about 2 cm in diameter on which the strain is measured flush with the flume floor. These are commercially available models. Pressure transducers with small tubes leading to the measuring surface were not used because sediment could plug the tubes, and air could easily be trapped inside. These transducers measure the stage very accurately when functioning; however, the types used to date have not proved durable for the rigorous demands of stage measurement in the field conditions. Damage of the measuring surfaces occurred quite readily, and shifts in the zero calibration were a common



FIGURE 39.—Technicians removing sand from beneath the intake plate at Walnut Gulch Flume 6. Sand completely seals the intakes, often after a few hours of flow.

BN-48663

occurrence. With improved design of the mounting (later pressure transducers were mounted inside a small intake box to protect them) and associated electronics, a pressure transducer may prove to be most useful for fixed-position measurement of stages.

Design of Stilling Well Intake for Sediment Conditions

The most common water-level sensor is a float located in a stilling well. An optimum design would (a) take on a minimum volume of water (considering an initial dry or unfilled system), (b) respond quickly to water surface elevation changes, and (c) trap all sediment (other than wash load) prior to entering the stilling well. The first two requirements are compatible, but the large amount of sediment entering the intakes obviates the desired condition of minimum volume of water in the stilling well system. In addition, reduction of sediment entry by using a small surface area for intake slots reduces the dynamic response of the stilling well considerably. The effect of differences in fluid density between flow and stilling well on the recording accuracy has been discussed previously by Ree and Garton (1971).

Good water-level measurements in heavily sediment-laden flows are difficult to obtain because the lowest point, where intakes should be located, is also the point most exposed to the bedload movement. A reasonable compromise design would include the following:

1. A minimum diameter of stilling well, and, thus, a narrow but possibly deeper float, so that the float volume is large enough to overcome drag within the recorder mechanism.
2. A pipe connecting the intake with the stilling well that is as short as practical and of a diameter that balances head loss with minimization of volume. This pipe should also have no interior high points where air can be trapped.
3. As much volume for deposited sand storage below the intake slots as practicable. The expected flow duration, bedload, and intervals between servicing should be considered in sizing.
4. A slot area that allows water entry at a tolerable head loss for no more than the expected average rate of rise.

In addition, the intake should be constructed so as to allow convenient servicing and cleanout.

Figure 40 is a sketch of the generalized design being used for several supercritical flumes. Stilling wells are used that have a 15-cm (6-inch) or 20-cm (8-inch) diameter. This restricts the float size and may prevent use of some of the larger water-level recorders. The float counterweight may have to be located outside the stilling well.

Tapered slots are milled into the intake plate perpendicular to the flow, with larger slot width on the inside. This helps reduce lodging of particles in the slots during inflow. Provisions are made at each installation to facilitate sediment trap cleaning and flushing. Little sediment deposition in the stilling well bottom has been observed, but cleanout must be provided.

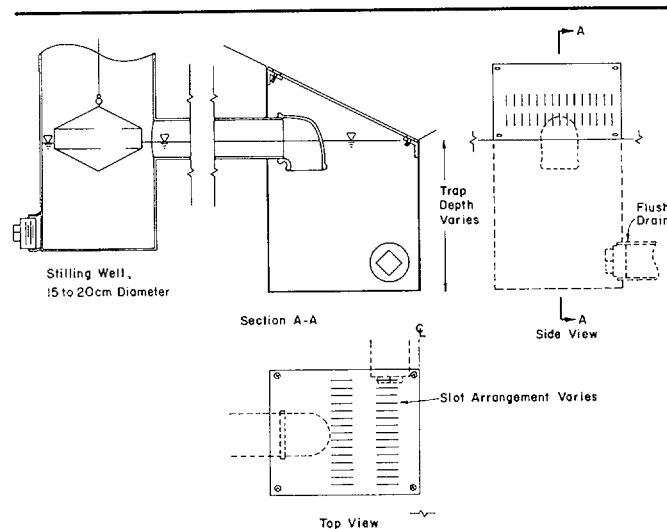


FIGURE 40.—Example design of stilling well entrance for trapping sediment during ephemeral flows.

Analysis of Lag in Stilling Well Records

Stilling well systems may exhibit considerable lag in the recorded depth as compared with actual flow depth in the flume when rapid rates of rise occur. This is caused by both the volume of the intake system that must be filled and the resistance to flow through the intake plate orifices. For example, the original Walnut Gulch intakes with 0.9-m-diameter stilling wells, 0.61-m × 3-m (2-ft × 10-ft) intake boxes, and large connecting tunnels, altogether comprise several cubic meters of water (and sediment) storage volume.

Flow records can easily be analyzed to estimate actual hydrograph rise, which may be necessary if intake slot area is restricted to prevent excessive sand influx. Consider the intake slot as a simple orifice. The equation for head loss through the orifice is written as:

$$\Delta h = h_f - h_o = \frac{1}{C_s^2} \frac{V_o^2}{2g} \quad (22)$$

where Δh is the head difference across the orifice
 h_f is the head in the flume, L ,
 h_o is the head at the orifice exit, L ,
 C_s is the orifice coefficient,
 V_o is the velocity through the orifice, L/T ,
 g is the gravitational acceleration, L/T^2 .

We can also write continuity equations as follows:

$$V_o A_o = q_o \quad (23)$$

$$q_o = A_w \frac{dh_w}{dt} \quad (24)$$

in which A_o is the orifice area, L^2 ,
 q_o is the flow through the orifice, L^2/T ,
 A_w is the surface area at recorded depth, L^2 ,
 h_w is the stilling well depth, L , and
 t is time.

Two cases may be distinguished. In the first case, the recorded depth h_w is less than the notch depth h_n , such that $h_o = h_n$ and equation 22 becomes

$$h_f - h_n = \frac{1}{2g} \left(\frac{V_o}{C_s} \right)^2 \quad (25)$$

Combining equations 23 and 24 into 25, and considering the change over time step Δt , we have

$$h_f(t) = h_n + \frac{1}{2g} \frac{A_w}{A_o} \frac{[h_w(t) - h_w(t - \Delta t)]^2}{C_s \Delta t} \quad (26)$$

In the second case, $h_w > h_n$ and $h_o = h_w$ so that

$$h_f(t) = \frac{h_w(t) + h_w(t + \Delta t)}{2} + \frac{1}{2g} \frac{A_w}{A_o} \frac{[h_w(t) - h_w(t - \Delta t)]^2}{C_s \Delta t} \quad (27)$$

Equations 26 and 27 are applied to the recorded sequence of flow depths of h_w divided into several Δt elements to calculate $h_f(t)$. A table of values for $A_w(h_w)$ describes the inlet system. One may also use equations 26 and 27 to solve for the entrance coefficient C_s if one or two observations of actual values of h_f and h_w are available. C_s may be estimated from hydraulic handbooks and is about 0.65.

Except in truly exceptional cases, lag correction for head loss through the intake plate and storage delay in the intake system is only necessary on the rising portion of a rapidly rising hydrograph, and thus will ordinarily be necessary only up to the point where $h_f \leq h_w$.

The position of a flume in a channel is important. Among the items to be considered are (1) channel width, (2) channel depth, (3) channel slope, (4) channel sinuosity, and (5) foundation material. Following selection of the drainage area desired, the site must be selected and the measuring device designed to fit the limitations of the stream site. For example, the flume cross sections at the entrance and at the measuring section must fit reasonably in the channel.

As previously discussed, some flow contraction is useful for control, but should be limited so that flow is not retarded to the extent that excessive ponding and deposition occur.

Geologic conditions at the measuring site are very important. The presence or absence of foundation material that can support the structure and its dynamic loads greatly affects the structural design and the costs. Where good foundation material is close to the channel surface, construction is relatively simple.

The presence of geologically resistant material also eliminates the need for scour protection downstream of the flume; thus, the scour pool can form in the resistant material without constructing an energy dissipator. At one location where the geologic material was insufficient to resist the anticipated scour, construction of an energy dissipator from reinforced concrete doubled the cost of the measuring station.

Finally, the presence of cohesive material at the measuring site enables the structure to intercept flow that might exist along the axis of the stream, below the surface of the channel alluvium. It is then possible to measure the total runoff or yield of the watershed with the exception of losses to deep ground water. Locations where flumes have been "keyed" into the bedrock assure minimum seepage under the structure.

When locating a flume, care must also be taken to avoid bends in the channel immediately upstream. In straight channel sections, the flow can be expected to enter the flume fairly symmetrically. Our experience suggests that the measuring station be located at least 10 flow widths downstream from channel bends.

Numerous construction techniques can be used for the flumes, depending upon the foundation, structural, and economic conditions prevailing. On small stations, it has been most satisfactory to construct the measuring device from sheet metal. In these instances, the flume was shop-assembled on a rigid rectangular wide-flange steel support frame, which was subsequently transported to the field site and positioned into the channel with a backhoe or small crane. The upstream end of the wide-flange support frame was then set on a concrete footing. The downstream support was made of large, threaded bolts anchored in concrete. The upstream footing serves as a cutoff, and the bolts in the downstream footing enable accurate leveling to obtain the desired slope. Small flumes such as this can also be made of reinforced concrete or gunite.

Concrete has proved to be an economical construction material on many streams because of the availability of suitable aggregate in the streambeds. The bed material often has a size distribution that is desirable for concrete aggregate and does not require screening and washing; thus, concrete costs can be low.

With the low costs of concrete construction, the larger measuring devices have been made exclusively of concrete in such a way as to minimize forming costs. The earliest stations consisted of concrete cells with support walls 3 m (9 ft) on centers and 30 cm (12 inches) thick rising from the bedrock to a point about 30 cm (12 inches) below finish grade. The honeycomb-type substructure cells were backfilled with the channel alluvium to provide additional structural support. The floor and walls were poured over the substructure cells. On some of the more recently constructed stations, upstream and downstream cutoff walls were connected by longitudinal and transverse walls to form a T-beam floor support. The openings were backfilled and compacted for additional support.

The earliest large measuring stations were made by pour forming the 1:1 sidewalls and the entrance parabolic sections. Control was obtained by stretching piano wire between extensions of the slope above and below the final grades. All layout control was made to ± 3 mm (± 0.01 ft) in the x-y-z planes. Forms were reused numerous times. The last few flumes were constructed by "shooting" gunite into place. Steel screeds were fixed at the finish plane slope, and the gunite concrete was then applied and struck off to the finish grades. This technique proved superior to ordinary forming methods.

On the floor sections, screeds were installed at the final grade, and the concrete pours were finished to the grade of the screeds. Control accuracy of ± 3 mm (± 0.01 ft) was maintained in the x-y-z planes.

A series of construction photographs for the large flume at the outlet of Walnut Gulch are shown in figures 41 to 43.

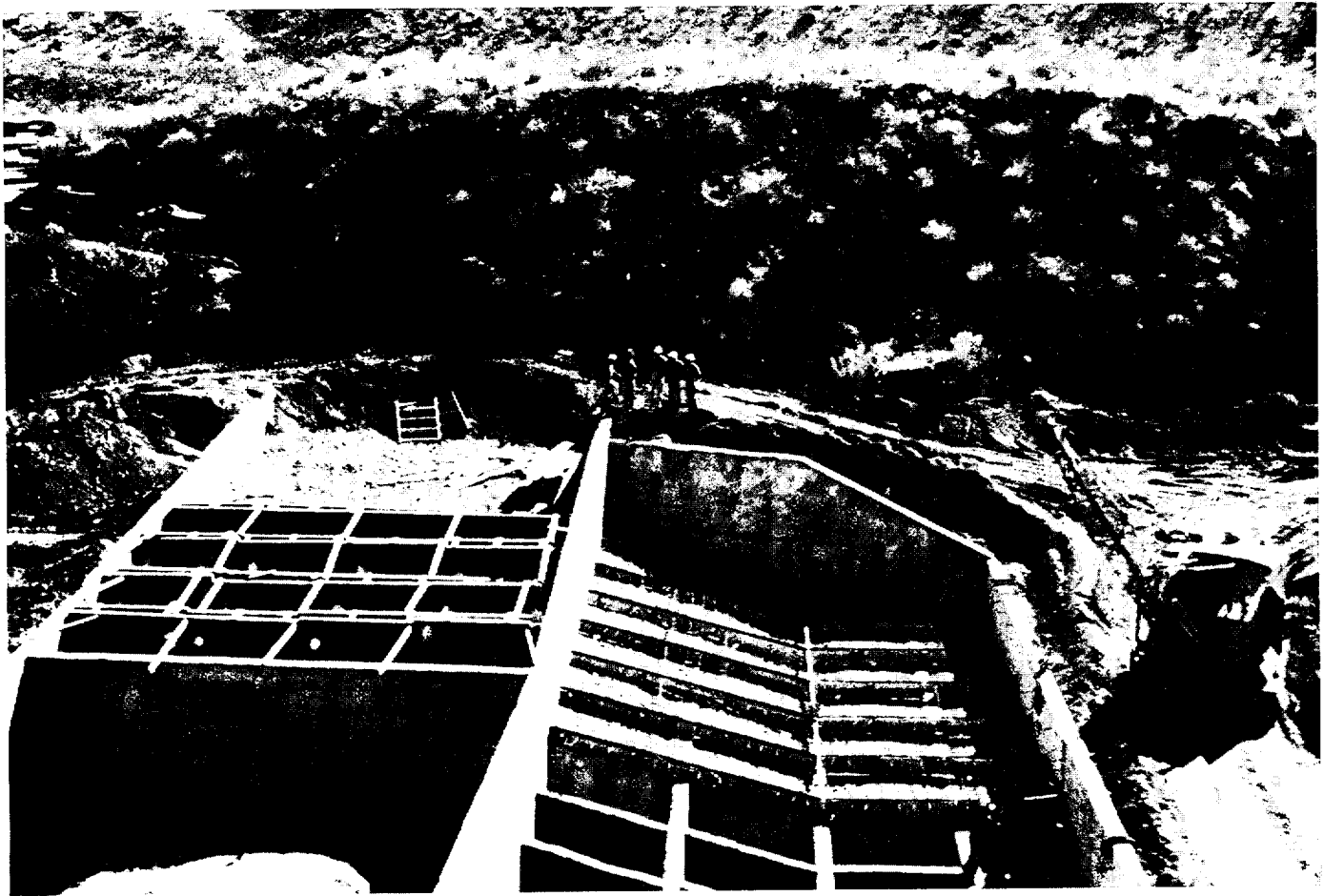


FIGURE 41.—Flume construction in early stages with form construction just beginning. BN-48664

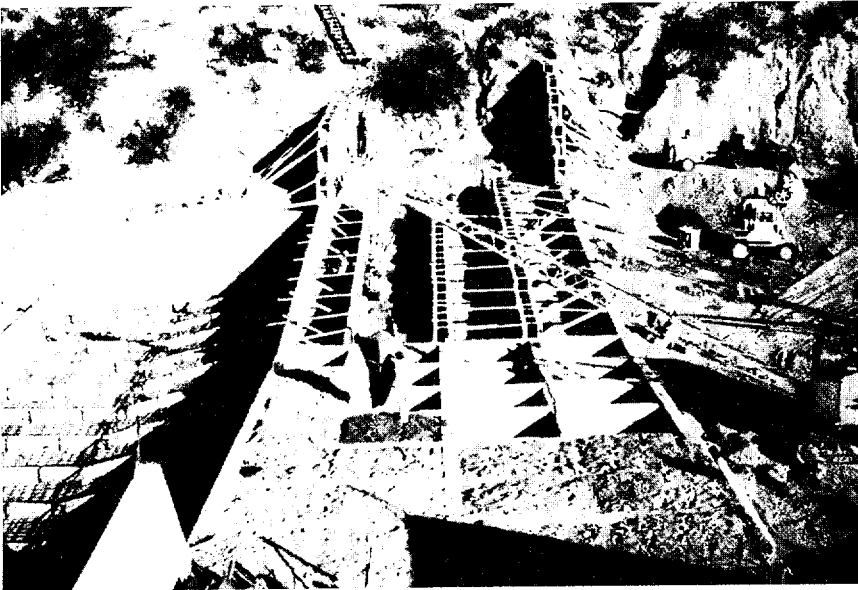


FIGURE 42.—Flume construction showing honeycomb floor support structure. Foreground honeycombs have been backfilled with gravel in preparation for floor pouring. BN-48665

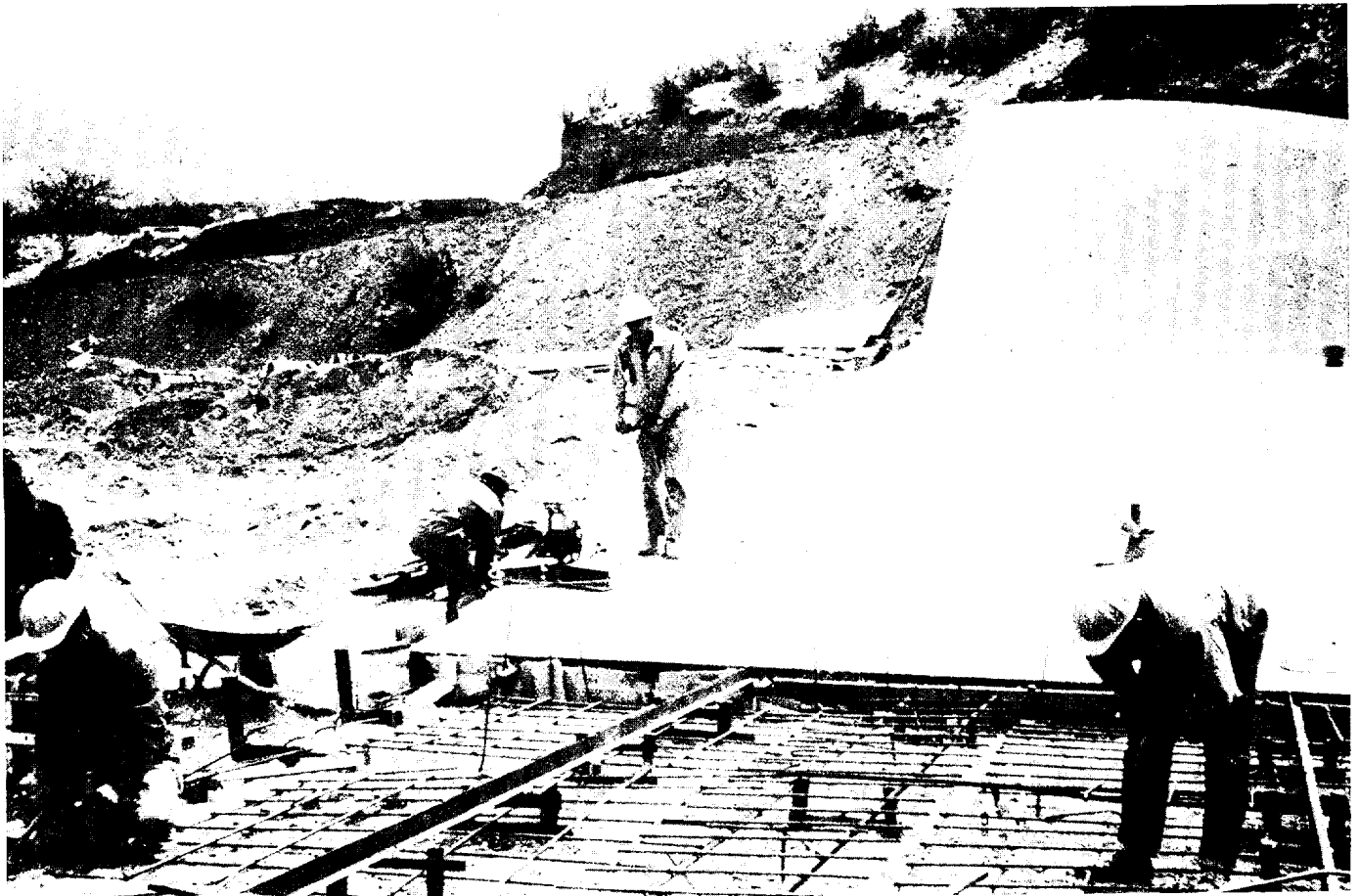


FIGURE 43.—Flume construction showing pouring of the floor area with screed controls in the foreground. BN-48666

Summary

No flume can be expected to solve hydraulic measurement problems for all conditions at any one site, much less to be ideal for a range of flow conditions at different locations. Nevertheless, for many heavily sediment-laden flows at high velocities, the flumes described in this bulletin have proved superior to presently available alternatives. For many conditions supercritical flow is necessary to transport the sediment load through any measuring device, and no other commonly used flume would be a suitable measuring facility.

Flumes made exceptionally wide to fit the geometry of channels require extra control measures, such as the porous control dikes in the approach channel described in this bulletin, to insure good flow control. Where the length of the flume is sufficiently greater than its width, extra control measures are not necessary. Ratings for several flume sizes are given in Appendix C.

Results of laboratory model and computer simulation experiments reported here indicate that Santa Rita flumes constructed with a wide variety of proportions may be rated with reasonable accuracy by computer simulation. The computer program is listed in Appendix A.

Extra care in design and maintenance is required to insure that the high sediment concentrations associated with high-velocity ephemeral flows do not interfere with measurement of depths by conventional float methods. Corrections for lag between the flume and stilling well water levels are necessary if the stage change is rapid. Use of bubble-type water level sensors may be a practical method, although present experience is insufficient to evaluate this technique as applied to the special conditions of high velocities and high sediment concentrations. Sonic transducers are useful devices for sensing sediment-laden water level where power is available, but require a permanent mounting above the flow.

Literature Cited

- (1) CHAMBERLAIN, A. R.
1957. PRELIMINARY MODEL TESTS OF A FLUME FOR MEASURING DISCHARGES OF STEEP EPHEMERAL STREAMS. Colorado State University, Civil Engineering Department, Report CER57ARC12, February 1957, 24 p.
- (2) CHOW, V. T.
1959. OPEN-CHANNEL HYDRAULICS. 680 p. McGraw-Hill Book. Co., New York.
- (3) GWINN, W. R.
1964. WALNUT GULCH SUPERCRITICAL MEASURING FLUME. Transactions of the American Society of Agricultural Engineers 10(3):197-199.
- (4) ———
1970. CALIBRATION OF WALNUT GULCH SUPERCRITICAL FLUMES. Proceedings of the American Society of Civil Engineers. 98(HY8):1681-1689.
- (5) MURPHY, GLENN
1950. SIMILITUDE IN ENGINEERING. 302 p. Ronald Press Co., New York.
- (6) REE, W. O.
1965. SWISS CHANNEL-TYPE GAGING STATIONS. U.S. Department of Agriculture, Agricultural Research Service, ARS 41-105, 10 p.
- (7) REE, W. O., and J. E. GARTON.
1971. EFFECT OF SUSPENDED SEDIMENT ON WATER SURFACE ELEVATION MEASUREMENT WITH FLOAT-OPERATED RECORDERS. Transactions of the American Society of Agricultural Engineers 14(3):503-504.
- (8) ROBINSON, A. R.
1961. STUDY OF THE BEAVER CREEK MEASURING FLUMES. Colorado State University, Civil Engineering Department, Report CER61ARR10, February 1961, 17 p.
- (9) RUFF, J. R., K. E. SAXTON, and CLEMENT DANG
1977. A DETAILED REPORT OF RATING BROAD-CRESTED V-NOTCH WEIRS WITH NARROW, SLOPING APPROACH CHANNELS AND SEDIMENT DEPOSITS. Colorado State University, Civil Engineering Department, Report CER76-77JFR-CD53, 348 p.
- (10) SMITH, R.E., and D. L. CHERY, JR.
1974. HYDRAULIC PERFORMANCE OF FLUMES FOR MEASUREMENT OF SEDIMENT LADEN FLASH FLOODS. Flash Floods Symposium, Proceedings of the Paris Symposium, International Association of Scientific Hydrology Publication No. 122, p. 17-22.
- (11) U.S. DEPARTMENT OF AGRICULTURE
1979. FIELD MANUAL FOR RESEARCH IN AGRICULTURAL HYDROLOGY. Agriculture Handbook No. 224, p. 75-104.
- (12) WILM, H. G., J. S. COTTON, and H. C. STOREY.
1938. MEASUREMENT OF DEBRIS-LADEN STREAM FLOW WITH CRITICAL-DEPTH FLUMES. Proceedings of the American Society of Civil Engineers Vol. 64, No. 8, Part 2. Transactions No. 103:1237-1278.

Appendix A

Computer program to determine measuring section depth (V_m) for any given discharge, q , for a supercritical depth flume.

```

PROGRAM STARITA (INPUT,OUTPUT,TAPE5=INPUT,TAPE6=OUTPUT)
DIMENSION H(11),X(11),A(11),W(11),E(11),R(11),SF(11),Z(11),
1 TITLE(4)
COMMON ZF,WF,I(Z,ZW)
2 READ(5,101) TITLE
3 WF = WIDTH OF FLOOR SECTION
4 ZF = LATERAL SLOPE OF FLOOR SECTION =COTAN OF ANGLE TO HORIZON
5 DX = ROUTING INTERVAL DISTANCE IN FT.
6 EPS = CONVERGENCE RELATIVE ERROR CRITERION
7 OPT = PRINT OPTION, PRINTS RESULTS AT EACH SECTION AND 0 IF .GT. 0.
8 FR = FROUDE NO. AT UPSTREAM SECTION
9 SZ = LONGITUDINAL FLOOR SLOPE = TAN OF ANGLE TO HORIZON
10 XMS = DISTANCE FROM UPSTREAM CONTROL SECTION TO MEASURING SECTION
11 UMAX,DLQ,ALPH,CRF,EK,EDDY,HMX,ZW
12 UMAX = MAX. DISCHARGE IN CFS FOR WHICH RATING IS DESIRED
13 DLQ IS STARTING MINIMUM VALUE OF DISCHARGE IN RATING
14 ALPH IS ENERGY COEFFICIENT FOR OPEN CHANNEL FLOW
15 CRF IS ROUGHNESS COEFFICIENT = 1.49/N FOR MANNING LAW IN FT.-SEC. SYSTEM
16 CRF = CHEZY C IN FT.-SEC. SYSTEM FOR ER=.5
17 METRIC MANNING CRF = 0.552*(ENGLISH CHEZY)
18 METRIC MANNING CRF = 1/MANNING N
19 ER IS ROUGHNESS LAW EXPONENT ON HYDRAULIC RADIUS, K.
20 EDDY IS EDDY LOSS COEFFICIENT
21 HMX = MAXIMUM DEPTH AT CONTROL TO HF CONSIDERED. MUST BE GT. DEPTH
22 CORRESPONDING TO QMAX
23 ZW = SLOPE OF FLOOR SIDEWALL = COTAN OF ANGLE TO HORIZON
24 READ(5,110) IPW,IMET
25 IMET = 0 FOR FT.-SEC. SYSTEM, IMET GT. 0. FOR MEIER - SEC. SYSTEM
26 IPW IS PARAM. FOR FLOOR AND WALL CONFIG.(=1) OR FLOOR ONLY(=0).
27 WRITE(6,102) TITLE
28 WRITE(6,103) TITLE
29 IF(11E1) 23,23,21
30 21 9 = 9.80665
31 UNITS = 3HMS
32 UNITS = 3HMS
33 WRITE(6,115)
34 50 TO 24
35 9 = 32.172
36 UNITS = 3HPT.
37 UNITS = 3MCF5
38 WRITE(6,116)
39 60 = 6*2.
40 WRITE(6,114) SZ,XMS
41 WRITE(6,104) ALPH,CRF,EDDY,ZF,WF,UMAX,DLQ,EPS,DX,FR,ER
42 IF(IPW.GT.0) WRITE(6,117) ZW
43 IFLAG = 0
44 XCR = 0.
45 CNM = 1./CRF/CRF
46 WCI = WF
47 HCI = 0.5*WCI/ZF
48 ACI = HCI*HCI*ZF
49 QTR = SQRT(ACI**3*G/ALPH/WCI)
50 WRITE(6,109) QTR,HC1
51 Q = DLQ
52 HM = (2.*ALPH/G*(Q/FR/ZF)**2)**0.2
53 CONTINUE
54 IF(Q.GT.QTR.AND.IPW.LI.1) 60 TO 150
55 CALL CKLOC(Q,QTR,ACI)
56 IF(XCI.GT.XCR) XCR = XCI
57 *** HH IS CRITICAL DEPTH AT XCR
58 ***** FIND FLOW CRITICAL DEPTH AT CONTROL XCR *****
59 IIZ = 1
60 IIRC = 0
61 IF(HM.LE.0.) HH = .001
62 IIRC = IIRC + 1

```

Computer program to determine measuring section depth (U_m)
for any given discharge, q , for a supercritical depth flume—Con.

```

10 IF(IIRC,1,1) GO TO 16
11 WRITE(6,1)9) HH
12 GO TO 200
13 IF(HH - HMA) 12,12,11
14 IF(HH - HMX) 15
15 IF(HH - HCI) 13,13,14
16 ZZ = ZF
17 GO TO 15
18 ZZ = ZW
19 CALL AREA(HH,XCR,AC,WC,HTR,RC,APH,RPH)
20 UHY = AC/WC
21 PC = UFR/SQRT(G/ALPH) - PC*SQRT(DHY)
22 PCP = UHY**1.5*Z7 - 1.5*SQRT(DHY)*APH
23 DC = PC/PCP
24 HH = HH - UC
25 IF(ABS(DC) - EPS) 18,10,10
26 A(I) = HH
27 CALL AREA(H(1),XCR,A(1),W(1),MTR,R(1),APH,RPH)
28 CC = 1./CRF/SQRT(SZ)
29 HS = 0.75*HH
30 ---- FINI NORMAL SUPERCRITICAL DEPTH, HS
31 IINC = 0
32 CALL AREA(HS,XCR,AS,WS,HI,RS,APH,RPH)
33 IINC = IINC + 1
34 IF(IINC - 20) 28,28,29
35 WRITE(6,1)2) Q
36 GO TO 100
37 FSP = AS*RS**ER - CC*Q
38 FSP = APH*RS**ER + AS*ER/RS**1.-ER)*RPH
39 IF(IINC.GE.10) WRITE(6,1)3) HS,FS,FSP
40 IEP = FS/FSP
41 HS = HS - IEP
42 IF(HS.GE.HM) HS = .9*HH
43 IF(HS.LE.0) HS = 0.1
44 IF(ABS(IEP) - EPS) 27,27,28
45 WRITE(6,1)4) XCR,UNITL,HS,UNITL,HS,UNITL,IIRC
46 FFIN = Q/AS/SQRT(G*.5*AS/WS/ALPH)
47 WRITE(6,1)8) FFIN
48 IICR = 0
49 V(1) = W/A(1)
50 Z(1) = 10. - SZ*XCR + H(1)
51 E(1) = Z(1) + ALPH*V(1)**2/GG
52 SF(1) = CNM*V(1)*V(1)/R(1)**(2.-ER)
53 DX1 = XCR/DX
54 DX1 = DX*(LHA + 1) - XCR
55 M = INT(XMS/DX) - LUX + 1
56 IF(DX1 - .1) 31,31,33
57 M = M - 1
58 DX1 = DX + DX1
59 X(1) = XCR
60 TS = XMS - XCP
61 DU 50 1 = 2*M
62 DIFF = 0
63 IF(1-2) 35,35,36
64 DX1 = DX1
65 GO TO 37
66 DX1 = DX
67 ---- ESTIMATE DEPTH AT NEXT SECTION
68 X(1) = X(J-1) + DX1
69 DS = X(1) - XCR
70 PR = 0.70 + 0.28*DS/TS
71 P = PR + (1. - PR)*(1. - DX1/DX)
72 H(I) = H(I-1)*P
73 IIER = 1
74 IIER=IITER+1

```

Computer program to determine measuring section depth (V_m)
for any given discharge, q , for a supercritical depth flume—Con.

```

99  IF(IJER - 20) 44,44,44,99
    WRITE(6,11) 0
90  GU TO 100
44  HIM = 1.001*H5
    H(1) = AMAX1(HIM,H(1))
    Z(1) = 10. - SZ*X(I) + H(1)
    CALL AREA(H(1),X(I),A(I),W(I),HTR,R(I),APH,RPH)
41  IF(IJER-10) 42,42,44
42  WRITE(6,105) X(I),H(I),UNITL,DIFF,IJER
43  V(I) = U/A(I)
    SF(I) = CNM*V(I)*V(I)/R(I)**(2.*ER)
    VP = -G*APH/A(I)/A(I)
    F(I) = Z(I) + ALPH*V(I)*V(I)/G
    F(I-1)**(2)/G - S*DX*(SF(I-1) + SF(I)) - EDDY*ALPH*(ABS(V(I))**2 - V
    F(I-1)**(2))/G - F(I)
    FP = -.5*CNM*DX*(2.*V(I)*VP/R(I)**(2.*ER) - V(I)*V(I)**2.*ER*RPH/R
    I(I)**(1)+2.*TR) - ALPH*(1. + EDDY)*V(I)*VP/G - 1.
    DIFF = F/FP
    H(I) = H(I) - DIFF
    IF(ABS(DIFF) - EPS) 480,40,40
61  XCR = XCR + 1.
    GU TO 100
480  IF(OPT)50,50,49
49  FRX = V(I)/SQRT(G*A(I)/W(I)/ALPH)
50  IF(I.LT.M) WRITE(6,105) X(I),H(I),UNITL,FRX,DIFF,IJER
    CONTINUE
100  WRITE(6,107) G,UNITU,H(M),UNITL,FRX
    QL = ALG10(Q) + 1.F-07
    IF(H)3,4,4
    J = INT(H)
    JCH = J-1
    GU TO 6
    JCH = INT(JCH)
    VMAN = B-FLOAT(JCH)
    DCU = 1.0
    IF(VMAN.LT.0.301) DCU = .2
    DG = DCG*10.0** (JCH)
    U = U + DG
    IF(U - GMAX) 9,9,7
    IF(UL-GMAX+.0001) H,150,150
    H
    GU TO 9
150  READ(5,110) ICON1
    IF(ICON1)200,200,1
200  CONTINUE
101  FORMAT(B11)
102  FORMAT(B11,1VX,H)S PROGRAM HYPOTHESES: RATING CURVE FOR W R GMIN
    IN FLUME BY DIRECT STEP COMPUTATION OF FLOW PROFILE;*9X;*ASSUMING
    TRANSITION OF CRITICAL SECTION FOR FLOW ABOVE FLOOR WALL INTERSECT
    JION*/10X*AS SPECIFIED BY SUBROUTINE CHLOC*/)
103  FORMAT(1H,2UX,H10/)
104  FORMAT(1H,5X,ALPHA = *F6.4*, ROUGHNESS = *F8.3*, EDDY LOSS RATIO
    U = *F6.4/10X* SIDE SLOPE OF FLOOR =1/*F4.1*, FLOOR WIDTH = *F5.2
    2.**, GMAX = *F10.3*, DELTA Q = *F6.3/10X*, CONVERGENCE CRITERION =
    41S*F8.5/20X*, HYDRAULIC EXPONENT = *F6.2/15X*, FNO. AT FLOOR COMIRUL
105  FORMAT(1H,4X,*A1 X = *F5.2*, H = *F8.5,A3*, FR = *F8.6*, DIFF = *F
    14.6*, AFTER *13,* ITERATIONS*)
106  FORMAT(DF10,U)
107  FORMAT(1H,5X,*FUK FLOW OF *F9.3,A3*, DEPTH AT MEASURING SECTION
    1 *F7.4,A3*, FK *F8.6)
108  FORMAT(1H0,20X,*A1 *F5.2,A3,* FROM STARI OF FLUME, CRITICAL DEPTH

```

Computer program to determine measuring section depth (y_m)
for any given discharge, q , for a supercritical depth flume—Con.

```

115 *F6.4,A3,* , NORMAL DEPTH IS *F6.4,A3,* , ITCR =*I5)
109 FORMAT(1H0,5X,*CALCULATED Q FOR TRANSITION FROM FLOOR TO WALL CONT
      IROL IS *F8.3,* , TRANSITION DEPTH IS *F8.4/)
110 FORMAT(2I5)
111 FORMAT(* PASSED TO NEXT Q WHEN ITER G.T. 20 AT Q =*F12.4)
112 FORMAT(* NORM DEPTH NOT FOUND AT 20 ITER FOR Q = *F12.2)
113 FORMAT(1H ,3(5X,F12.7))
114 FORMAT(1H ,10X*FLUME SLOPE IS *F7.5,* DIST. TO MEASURING SECTION
      IIS *F6.2)
115 FORMAT(/40H ALL DIMENSIONS IN METERS, Q IN M**3/SEC/)
116 FORMAT(/33H ALL DIMENSIONS IN FEET, Q IN CFS/)
117 FORMAT(22H WALL SIDE SLOPE IS 1/*F7.4)
118 FORMAT(* NORMAL FLOW FROUDE NO. =*F8.6)
119 FORMAT(50H CRITICAL DEPTH NOT CONVERGED AT 25 ITERS. TRIAL= ,F9.5)
      END
      SUBROUTINE CRLOC(Q,QTR,XCR)
      COMMON ZF,WF,ITZ,ZW
C ***** THIS VERSION APPLIES TO FLUMES WHICH HAVE FIXED CONTROL AT X = 0.
      XCR = 0.
      RETURN
      END
      SUBROUTINE AREA(H,X,A,W,HTR,R,APH,RPH)
      COMMON ZF,WF,ITZ,ZW
C ** THIS VERSION GOOD FOR FLUMES WITHOUT CRITICAL SECTION SHIFT (K3B)
      APH = 0.
      RPH = 0.
      W1 = WF
      ZW = SQRT(1. + ZF*ZF)
      HTR = WF*.5/ZF
C ---- HTR IS DEPTH OF FLOOR WALL INTERSECTION AT X
      IF (HTR - H) 30,20,20
20  A = H*H*ZF
      Y = 2.*H*ZF
      R = A/(2.*H*ZW)
      IF (ITZ) 29,29,21
21  APH = 2.*H*ZF
      RPH = ZF/ZW - A/(2.*H*H*ZW)
29  CONTINUE
      RETURN
30  A = HTR*HTR*ZF + (H-HTR)*(WT + (H-HTR)*ZW)
      Y = W1 + (H-HTR)*2.*ZW
      ZW = SQRT(1. + W1*ZW)
      R = A/(2.*HTR*ZW + (H-HTR)*ZW*2.)
      IF (ITZ) 31,31,31
31  HPM = H - HTR
      APH = W1 + 2.*HPM*ZW
      P = 2.*HTR*ZW + HPM*2.*ZW
      RPH = APH/P - A/P/P*2.*ZW
34  CONTINUE
      RETURN
      END

```

Appendix B

Selected model ratings of discharges for Walnut Gulch flumes 1, 2, 3, 4, 6, 7, 8, 11, and 15 in prototype dimensions.

WALNUT GULCH FLUME NO. LOCATED NEAR TOMBSTONE, ARIZONA
 EXP. NO. 1, FILLED APPROACH, DISCHARGE COEFFICIENTS FOR 1 TO 40 MODEL

TEST NO.	PROTOTYPE DISCHARGE (C.F.S.)	FLUME HEAD (FT.)	DISCHARGE C	CONTROL AREA (SQ. FT.)	UPSTREAM HYDRAULIC RADIUS (FT.)	APPROACH MANNING
1	19.04	10.37	1.12	1933	11.03	0.630
2	19.58	10.50	1.10	1927	11.34	0.620
3	19.68	10.43	1.10	1940	11.47	0.620
4	19.86	10.53	1.10	1979	11.49	0.645
5	19.84	10.53	1.10	1777	11.57	0.644
6	19.84	10.53	1.10	1777	11.57	0.644
7	19.84	10.53	1.10	1777	11.57	0.644
8	19.84	10.53	1.10	1777	11.57	0.644
9	19.84	10.53	1.10	1777	11.57	0.644
10	19.84	10.53	1.10	1777	11.57	0.644
11	19.84	10.53	1.10	1777	11.57	0.644
12	19.84	10.53	1.10	1777	11.57	0.644
13	19.84	10.53	1.10	1777	11.57	0.644
14	19.84	10.53	1.10	1777	11.57	0.644
15	19.84	10.53	1.10	1777	11.57	0.644
16	19.84	10.53	1.10	1777	11.57	0.644
17	19.84	10.53	1.10	1777	11.57	0.644
18	19.84	10.53	1.10	1777	11.57	0.644
19	19.84	10.53	1.10	1777	11.57	0.644
20	19.84	10.53	1.10	1777	11.57	0.644
21	19.84	10.53	1.10	1777	11.57	0.644
22	19.84	10.53	1.10	1777	11.57	0.644
23	19.84	10.53	1.10	1777	11.57	0.644
24	19.84	10.53	1.10	1777	11.57	0.644
25	19.84	10.53	1.10	1777	11.57	0.644
26	19.84	10.53	1.10	1777	11.57	0.644
27	19.84	10.53	1.10	1777	11.57	0.644
28	19.84	10.53	1.10	1777	11.57	0.644
29	19.84	10.53	1.10	1777	11.57	0.644
30	19.84	10.53	1.10	1777	11.57	0.644
31	19.84	10.53	1.10	1777	11.57	0.644
32	19.84	10.53	1.10	1777	11.57	0.644
33	19.84	10.53	1.10	1777	11.57	0.644
34	19.84	10.53	1.10	1777	11.57	0.644
35	19.84	10.53	1.10	1777	11.57	0.644
36	19.84	10.53	1.10	1777	11.57	0.644
37	19.84	10.53	1.10	1777	11.57	0.644
38	19.84	10.53	1.10	1777	11.57	0.644
39	19.84	10.53	1.10	1777	11.57	0.644
40	19.84	10.53	1.10	1777	11.57	0.644

Selected model ratings of discharges for Walnut Gulch flumes 1, 2,
3, 4, 6, 7, 8, 11, and 15 in prototype dimensions.—Con.

WALNUT GULCH FLUME NO. 2, LOCATED NEAR TOMBSTONE, ARIZONA, EXP. NO. 1
DISCHARGE COEFFICIENTS FOR 1 TO 20 MODEL, OLD FLOOR, SMOOTH CHANNEL

TEST NO.	PROTOTYPE DISCHARGE (C.F.S.)	FLUME HEAD (FT.)	DISCHARGE (SQ. FT.)	CONTROL AREA	HYDRAULIC RADIUS (FT.)	UPSTREAM APPROACH MANNING
1	2780	59	55	4940	2700	00
2	2220	44	8200	4853	2180	2185
3	2220	44	8200	4703	1835	2165
4	1750	44	8200	4320	1535	2175
5	1280	44	8200	4042	1280	2120
6	920	44	8200	3750	980	2060
7	620	44	8200	3450	740	2030
8	420	44	8200	3150	540	2000
9	260	44	8200	2850	390	2000
10	160	44	8200	2550	240	2000
11	100	44	8200	2250	190	2000
12	60	44	8200	1950	140	2000
13	40	44	8200	1650	110	2000
14	26	44	8200	1350	80	2000
15	16	44	8200	1050	60	2000
16	10	44	8200	750	40	2000
17	6	44	8200	450	20	2000
18	4	44	8200	300	10	2000
19	2.6	44	8200	150	5	2000
20	1.6	44	8200	75	2.5	2000
21	1.0	44	8200	45	1.5	2000
22	0.6	44	8200	30	1	2000
23	0.4	44	8200	15	0.5	2000
24	0.26	44	8200	7.5	0.25	2000
25	0.16	44	8200	3.75	0.125	2000
26	0.1	44	8200	2.25	0.075	2000
27	0.06	44	8200	1.35	0.045	2000
28	0.04	44	8200	0.9	0.03	2000
29	0.026	44	8200	0.45	0.015	2000
30	0.016	44	8200	0.225	0.0075	2000
31	0.01	44	8200	0.135	0.0045	2000
32	0.006	44	8200	0.075	0.00225	2000
33	0.004	44	8200	0.045	0.00135	2000
34	0.0026	44	8200	0.0225	0.000675	2000
35	0.0016	44	8200	0.0135	0.000405	2000
36	0.001	44	8200	0.0075	0.000225	2000
37	0.0006	44	8200	0.0045	0.000135	2000
38	0.0004	44	8200	0.00225	0.0000675	2000
39	0.00026	44	8200	0.00135	0.0000405	2000
40	0.00016	44	8200	0.00075	0.0000225	2000
41	0.0001	44	8200	0.00045	0.0000135	2000
42	0.00006	44	8200	0.000225	0.00000675	2000
43	0.00004	44	8200	0.000135	0.00000405	2000
44	0.000026	44	8200	0.000075	0.00000225	2000
45	0.000016	44	8200	0.000045	0.00000135	2000
46	0.00001	44	8200	0.0000225	0.000000675	2000
47	0.000006	44	8200	0.0000135	0.000000405	2000
48	0.000004	44	8200	0.0000075	0.000000225	2000
49	0.0000026	44	8200	0.0000045	0.000000135	2000
50	0.0000016	44	8200	0.00000225	0.0000000675	2000
51	0.000001	44	8200	0.00000135	0.0000000405	2000
52	0.0000006	44	8200	0.00000075	0.0000000225	2000
53	0.0000004	44	8200	0.00000045	0.0000000135	2000
54	0.00000026	44	8200	0.000000225	0.00000000675	2000
55	0.00000016	44	8200	0.000000135	0.00000000405	2000
56	0.0000001	44	8200	0.000000075	0.00000000225	2000
57	0.00000006	44	8200	0.000000045	0.00000000135	2000
58	0.00000004	44	8200	0.0000000225	0.000000000675	2000
59	0.000000026	44	8200	0.0000000135	0.000000000405	2000
60	0.000000016	44	8200	0.0000000075	0.000000000225	2000
61	0.00000001	44	8200	0.0000000045	0.000000000135	2000
62	0.000000006	44	8200	0.00000000225	0.0000000000675	2000
63	0.000000004	44	8200	0.00000000135	0.0000000000405	2000
64	0.0000000026	44	8200	0.00000000075	0.0000000000225	2000
65	0.0000000016	44	8200	0.00000000045	0.0000000000135	2000
66	0.000000001	44	8200	0.000000000225	0.00000000000675	2000
67	0.0000000006	44	8200	0.000000000135	0.00000000000405	2000
68	0.0000000004	44	8200	0.000000000075	0.00000000000225	2000
69	0.00000000026	44	8200	0.000000000045	0.00000000000135	2000
70	0.00000000016	44	8200	0.0000000000225	0.000000000000675	2000
71	0.0000000001	44	8200	0.0000000000135	0.000000000000405	2000
72	0.00000000006	44	8200	0.0000000000075	0.000000000000225	2000
73	0.00000000004	44	8200	0.0000000000045	0.000000000000135	2000
74	0.000000000026	44	8200	0.00000000000225	0.0000000000000675	2000
75	0.000000000016	44	8200	0.00000000000135	0.0000000000000405	2000
76	0.00000000001	44	8200	0.00000000000075	0.0000000000000225	2000
77	0.000000000006	44	8200	0.00000000000045	0.0000000000000135	2000
78	0.000000000004	44	8200	0.000000000000225	0.00000000000000675	2000
79	0.0000000000026	44	8200	0.000000000000135	0.00000000000000405	2000
80	0.0000000000016	44	8200	0.000000000000075	0.00000000000000225	2000
81	0.000000000001	44	8200	0.000000000000045	0.00000000000000135	2000
82	0.0000000000006	44	8200	0.0000000000000225	0.000000000000000675	2000
83	0.0000000000004	44	8200	0.0000000000000135	0.000000000000000405	2000
84	0.00000000000026	44	8200	0.0000000000000075	0.000000000000000225	2000
85	0.00000000000016	44	8200	0.0000000000000045	0.000000000000000135	2000
86	0.0000000000001	44	8200	0.00000000000000225	0.0000000000000000675	2000
87	0.00000000000006	44	8200	0.00000000000000135	0.0000000000000000405	2000
88	0.00000000000004	44	8200	0.00000000000000075	0.0000000000000000225	2000
89	0.000000000000026	44	8200	0.00000000000000045	0.0000000000000000135	2000
90	0.000000000000016	44	8200	0.000000000000000225	0.00000000000000000675	2000
91	0.00000000000001	44	8200	0.000000000000000135	0.00000000000000000405	2000
92	0.000000000000006	44	8200	0.000000000000000075	0.00000000000000000225	2000
93	0.000000000000004	44	8200	0.000000000000000045	0.00000000000000000135	2000
94	0.0000000000000026	44	8200	0.0000000000000000225	0.000000000000000000675	2000
95	0.0000000000000016	44	8200	0.0000000000000000135	0.000000000000000000405	2000
96	0.000000000000001	44	8200	0.0000000000000000075	0.000000000000000000225	2000
97	0.0000000000000006	44	8200	0.0000000000000000045	0.000000000000000000135	2000
98	0.0000000000000004	44	8200	0.00000000000000000225	0.0000000000000000000675	2000
99	0.00000000000000026	44	8200	0.00000000000000000135	0.0000000000000000000405	2000
100	0.00000000000000016	44	8200	0.00000000000000000075	0.0000000000000000000225	2000
101	0.0000000000000001	44	8200	0.00000000000000000045	0.0000000000000000000135	2000
102	0.00000000000000006	44	8200	0.000000000000000000225	0.00000000000000000000675	2000
103	0.00000000000000004	44	8200	0.000000000000000000135	0.00000000000000000000405	2000
104	0.000000000000000026	44	8200	0.000000000000000000075	0.00000000000000000000225	2000
105	0.000000000000000016	44	8200	0.000000000000000000045	0.00000000000000000000135	2000
106	0.00000000000000001	44	8200	0.0000000000000000000225	0.000000000000000000000675	2000
107	0.000000000000000006	44	8200	0.0000000000000000000135	0.000000000000000000000405	2000
108	0.000000000000000004	44	8200	0.0000000000000000000075	0.000000000000000000000225	2000
109	0.0000000000000000026	44	8200	0.0000000000000000000045	0.000000000000000000000135	2000
110	0.0000000000000000016	44	8200	0.00000000000000000000225	0.0000000000000000000000675	2000
111	0.000000000000000001	44	8200	0.00000000000000000000135	0.0000000000000000000000405	2000
112	0.0000000000000000006	44	8200	0.00000000000000000000075	0.0000000000000000000000225	2000
113	0.0000000000000000004	44	8200	0.00000000000000000000045	0.0000000000000000000000135	2000
114	0.00000000000000000026	44	8200	0.000000000000000000000225	0.00000000000000000000000675	2000
115	0.00000000000000000016	44	8200	0.000000000000000000000135	0.00000000000000000000000405	2000
116	0.0000000000000000001	44	8200	0.000000000000000000000075	0.00000000000000000000000225	2000
117	0.00000000000000000006	44	8200	0.000000000000000000000045	0.00000000000000000000000135	2000
118	0.00000000000000000004	44	8200	0.0000000000000000000000225	0.000000000000000000000000675	2000
119	0.000000000000000000026	44	8200	0.0000000000000000000000135	0.000000000000000000000000405	2000
120	0.000000000000000000016	44	8200	0.0000000000000000000000075	0.000000000000000000000000225	2000
121	0.00000000000000000001	44	8200	0.0000000000000000000000045	0.000000000000000000000000135	2000
122	0.000000000000000000006	44	8200	0.00000000000000000000000225	0.0000000000000000000000000675	2000
123	0.000000000000000000004	44	8200	0.00000000000000000000000135	0.0000000000000000000000000405	2000
124	0.0000000000000000000026	44	8200	0.00000000000000000000000075	0.0000000000000000000000000225	2000
125	0.0000000000000000000016	44	8200	0.00000000000000000000000045	0.0000000000000000000000000135	2000
126	0.000000000000000000001	44	8200	0.000000000000000000000000225	0.00000000000000000000000000675	2000
127	0.0000000000000000000006	44	8200	0.000000000000000000000000135	0.00000000000000000000000000405	2000
128	0.0000000000000000000004	44	8200	0.000000000000000000000000075	0.00000000000000000000000000225	2000
129	0.00000000000000000000026	44	8200	0.000000000000000000000000045	0.00000000000000000000000000135	2000
130						

Selected model ratings of discharges for Walnut Gulch flumes 1, 2, 3, 4, 6, 7, 8, 11, and 15 in prototype dimensions.—Con.

WALNUT GULCH FLUME NO. 3 LOCATED NEAR TOMBSTONE, ARIZONA		DISCHARGE COEFFICIENTS FOR 1 TO 32 MODEL		UPSTREAM APPROACH		
TEST NO.	PROTOTYPE DISCHARGE	FLUME HEAD	DISCHARGE	CONTROL AREA	HYDRAULIC RADIUS	MANNING N
(C.F.S.)	(FT.)	(SQ. FT.)	(FT.)	(SQ. FT.)	(FT.)	
1	7680	11.20	0.67	395.17	9.53	0.0373
2	7990	10.51	0.82	356.01	9.17	0.0373
3	6731	10.84	1.09	307.14	9.03	0.0333
4	4634	8.84	1.26	259.49	8.61	0.0333
5	4434	8.84	2.02	222.57	8.61	0.0333
6	4434	7.36	2.09	222.57	7.77	0.0340
7	4434	7.36	3.09	222.57	7.77	0.0340
8	3221	6.67	3.09	222.57	6.92	0.0335
9	4057	6.67	4.07	222.57	6.92	0.0335
10	4057	5.47	4.07	222.57	5.47	0.0289
11	2775	5.47	5.07	222.57	5.47	0.0289
12	1754	5.47	6.07	222.57	5.47	0.0289
13	1754	4.43	6.07	222.57	4.43	0.0223
14	1754	4.43	7.04	222.57	4.43	0.0223
15	1754	4.43	8.04	222.57	4.43	0.0223
16	7521	4.43	9.04	222.57	4.43	0.0223
17	7521	3.59	9.04	222.57	3.59	0.0223
18	7521	3.59	10.06	222.57	3.59	0.0223
19	4346	3.59	10.06	222.57	3.59	0.0223
20	4346	2.75	10.06	222.57	2.75	0.0223
21	4346	2.75	11.06	222.57	2.75	0.0223
22	4346	2.75	12.06	222.57	2.75	0.0223
23	4346	2.75	13.06	222.57	2.75	0.0223
24	4346	2.75	14.06	222.57	2.75	0.0223
25	4346	2.75	15.06	222.57	2.75	0.0223
26	4346	2.75	16.06	222.57	2.75	0.0223
27	4346	2.75	17.06	222.57	2.75	0.0223
28	4346	2.75	18.06	222.57	2.75	0.0223
29	4346	2.75	19.06	222.57	2.75	0.0223
30	4346	2.75	20.06	222.57	2.75	0.0223
31	4346	2.75	21.06	222.57	2.75	0.0223
32	4346	2.75	22.06	222.57	2.75	0.0223
33	4346	2.75	23.06	222.57	2.75	0.0223
34	4346	2.75	24.06	222.57	2.75	0.0223
35	4346	2.75	25.06	222.57	2.75	0.0223
36	4346	2.75	26.06	222.57	2.75	0.0223
37	4346	2.75	27.06	222.57	2.75	0.0223
38	4346	2.75	28.06	222.57	2.75	0.0223
39	4346	2.75	29.06	222.57	2.75	0.0223
40	4346	2.75	30.06	222.57	2.75	0.0223
41	4346	2.75	31.06	222.57	2.75	0.0223
42	4346	2.75	32.06	222.57	2.75	0.0223
43	4346	2.75	33.06	222.57	2.75	0.0223
44	4346	2.75	34.06	222.57	2.75	0.0223
45	4346	2.75	35.06	222.57	2.75	0.0223
46	4346	2.75	36.06	222.57	2.75	0.0223
47	4346	2.75	37.06	222.57	2.75	0.0223
48	4346	2.75	38.06	222.57	2.75	0.0223
49	4346	2.75	39.06	222.57	2.75	0.0223
50	4346	2.75	40.06	222.57	2.75	0.0223

Selected model ratings of discharges for Walnut Gulch flumes 1, 2, 3, 4, 6, 7, 8, 11, and 15 in prototype dimensions.—Con.

WALNUT GULCH FLUME NO. 4, LOCATED NEAR TOMBSTONE, ARIZONA
 EXP. NO. 1, UNFILLED APPROACH, DISCHARGE COEFFICIENTS FOR 1:30 MODEL

TEST PROTOTYPE FLUME DISCHARGE CONTROL AREA UPSTREAM APPROACH
 NO. DISCHARGE HEAD (C.F.S.) (FT.) (SQ. FT.) HYDRAULIC MANNING

TEST PROTOTYPE NO.	DISCHARGE (C.F.S.)	FLUME HEAD (FT.)	DISCHARGE (SQ. FT.)	CONTROL AREA (SQ. FT.)	UPSTREAM APPROACH HYDRAULIC MANNING
1	2287	9.76	1184	848	39
2	2084	9.36	1120	800	58
3	1901	8.94	1098	794	67
4	1651	8.49	1042	742	76
5	1586	8.35	1030	730	85
6	1274	7.74	870	670	116
7	1099	6.92	765	599	120
8	992	6.47	704	547	180
9	800	5.54	594	470	201
10	688	4.88	530	420	270
11	487	3.91	402	302	304
12	397	3.30	324	242	397
13	334	2.84	274	210	571
14	325	2.82	272	209	731
15	305	2.73	259	197	1051
16	272	2.52	230	185	1594
17	242	2.29	204	172	2094
18	220	2.11	189	162	2746
19	200	1.98	176	154	3511
20	186	1.86	166	148	4594
21	171	1.76	158	143	6111
22	158	1.68	151	139	7468
23	145	1.62	145	136	9461
24	135	1.57	140	134	11911
25	127	1.53	137	132	15429
26	120	1.50	134	131	19746
27	114	1.47	131	130	25111
28	109	1.45	129	129	31911
29	106	1.44	128	129	39468
30	100	1.42	126	128	49461
31	95	1.40	124	127	61911
32	90	1.38	122	126	75911
33	85	1.36	120	125	91911
34	80	1.34	118	124	10939
35	75	1.32	116	123	12971
36	70	1.30	114	122	15191
37	65	1.28	112	121	17542
38	60	1.26	110	120	20191
39	55	1.24	108	119	23094
40	50	1.22	106	118	26168
41	45	1.20	104	117	29461
42	40	1.18	102	116	33111
43	35	1.16	100	115	37168
44	30	1.14	98	114	41111
45	25	1.12	96	113	45168
46	20	1.10	94	112	49161
47	15	1.08	92	111	53111
48	10	1.06	90	110	57168
49	5	1.04	88	109	61111
50	0	1.02	86	108	65168

Selected model ratings of discharges for Walnut Gulch flumes 1, 2, 3, 4, 6, 7, 8, 11, and 15 in prototype dimensions.—Con.

EXP. NO. 2, PREDICTED FLOW NO. 4, LOCATED COEFFICIENTS FOR 1 TO 30 MODEL

TEST NO.	PROTOTYPE DISCHARGE (C.F.S.)	FLUME HEAD (FT.)	DISCHARGE C	CONTROL AREA (SQ. FT.)	UPSTREAM APPROACH HYDRAULIC MANNING
35	154	22	11	14	115
56	127	22	11	13	109
76	110	22	11	12	108
90	108	22	11	11	107
01	105	22	11	10	106
44	101	22	11	9	105
44	95	22	11	8	104
44	89	22	11	7	103
44	83	22	11	6	102
44	77	22	11	5	101
44	71	22	11	4	100
44	65	22	11	3	99
44	59	22	11	2	98
44	53	22	11	1	97
44	47	22	11	0	96
44	41	22	11	0	95
44	35	22	11	0	94
44	29	22	11	0	93
44	23	22	11	0	92
44	17	22	11	0	91
44	11	22	11	0	90
44	5	22	11	0	89
44	0	22	11	0	88
44	0	22	11	0	87
44	0	22	11	0	86
44	0	22	11	0	85
44	0	22	11	0	84
44	0	22	11	0	83
44	0	22	11	0	82
44	0	22	11	0	81
44	0	22	11	0	80
44	0	22	11	0	79
44	0	22	11	0	78
44	0	22	11	0	77
44	0	22	11	0	76
44	0	22	11	0	75
44	0	22	11	0	74
44	0	22	11	0	73
44	0	22	11	0	72
44	0	22	11	0	71
44	0	22	11	0	70
44	0	22	11	0	69
44	0	22	11	0	68
44	0	22	11	0	67
44	0	22	11	0	66
44	0	22	11	0	65
44	0	22	11	0	64
44	0	22	11	0	63
44	0	22	11	0	62
44	0	22	11	0	61
44	0	22	11	0	60
44	0	22	11	0	59
44	0	22	11	0	58
44	0	22	11	0	57
44	0	22	11	0	56
44	0	22	11	0	55
44	0	22	11	0	54
44	0	22	11	0	53
44	0	22	11	0	52
44	0	22	11	0	51
44	0	22	11	0	50
44	0	22	11	0	49
44	0	22	11	0	48
44	0	22	11	0	47
44	0	22	11	0	46
44	0	22	11	0	45
44	0	22	11	0	44
44	0	22	11	0	43
44	0	22	11	0	42
44	0	22	11	0	41
44	0	22	11	0	40
44	0	22	11	0	39
44	0	22	11	0	38
44	0	22	11	0	37
44	0	22	11	0	36
44	0	22	11	0	35
44	0	22	11	0	34
44	0	22	11	0	33
44	0	22	11	0	32
44	0	22	11	0	31
44	0	22	11	0	30
44	0	22	11	0	29
44	0	22	11	0	28
44	0	22	11	0	27
44	0	22	11	0	26
44	0	22	11	0	25
44	0	22	11	0	24
44	0	22	11	0	23
44	0	22	11	0	22
44	0	22	11	0	21
44	0	22	11	0	20
44	0	22	11	0	19
44	0	22	11	0	18
44	0	22	11	0	17
44	0	22	11	0	16
44	0	22	11	0	15
44	0	22	11	0	14
44	0	22	11	0	13
44	0	22	11	0	12
44	0	22	11	0	11
44	0	22	11	0	10
44	0	22	11	0	9
44	0	22	11	0	8
44	0	22	11	0	7
44	0	22	11	0	6
44	0	22	11	0	5
44	0	22	11	0	4
44	0	22	11	0	3
44	0	22	11	0	2
44	0	22	11	0	1
44	0	22	11	0	0

Selected model ratings of discharges for Walnut Gulch flumes 1, 2, 3, 4, 6, 7, 8, 11, and 15 in prototype dimensions.—Con.

WALNUT GULCH FLUME NO. 6 LOCATED NEAR TOMBSTONE, ARIZONA										
DISCHARGE COEFFICIENTS FOR 1 TO 30 MODEL										
TEST PROTOTYPE NO.	DISCHARGE	FLUME HEAD	DISCHARGE C	CONTROL AREA	UPSTREAM APPROACH HYDRAULIC RADIUS	MANNING	APPROACH	DISCHARGE	FLUME HEAD	DISCHARGE C
(C.F.S.)	(FT.)	(SQ. FT.)	(FT.)	(SQ. FT.)	(FT.)			(C.F.S.)	(FT.)	(C.F.S.)
13	90	33	0.67	74	9	0.0	0.0	3	81	0.67
14	43	38	0.67	74	0	0.0	0.0	2	70	0.67
14	45	40	0.68	77	0	0.0	0.0	3	65	0.68
14	47	41	0.67	72	0	0.0	0.0	3	64	0.67
14	48	43	0.69	75	0	0.0	0.0	3	66	0.69
14	49	44	0.71	77	0	0.0	0.0	3	67	0.71
15	01	33	0.73	74	0	0.0	0.0	3	69	0.73
15	02	33	0.76	73	0	0.0	0.0	3	72	0.76
15	03	33	0.78	73	0	0.0	0.0	3	78	0.78
15	04	33	0.84	70	0	0.0	0.0	3	84	0.84
15	05	33	0.90	67	0	0.0	0.0	3	90	0.90
15	06	33	0.94	65	0	0.0	0.0	3	94	0.94
15	07	33	0.97	63	0	0.0	0.0	3	97	0.97
15	08	33	0.99	62	0	0.0	0.0	3	99	0.99
16	00	42	0.99	60	0	0.0	0.0	3	99	0.99
16	01	42	0.99	59	0	0.0	0.0	3	99	0.99
16	02	42	0.99	58	0	0.0	0.0	3	99	0.99
16	03	42	0.99	57	0	0.0	0.0	3	99	0.99
16	04	42	0.99	56	0	0.0	0.0	3	99	0.99
16	05	42	0.99	55	0	0.0	0.0	3	99	0.99
16	06	42	0.99	54	0	0.0	0.0	3	99	0.99
16	07	42	0.99	53	0	0.0	0.0	3	99	0.99
16	08	42	0.99	52	0	0.0	0.0	3	99	0.99
16	09	42	0.99	51	0	0.0	0.0	3	99	0.99
16	10	42	0.99	50	0	0.0	0.0	3	99	0.99
17	01	44	0.99	49	0	0.0	0.0	3	99	0.99
17	02	44	0.99	48	0	0.0	0.0	3	99	0.99
17	03	44	0.99	47	0	0.0	0.0	3	99	0.99
17	04	44	0.99	46	0	0.0	0.0	3	99	0.99
17	05	44	0.99	45	0	0.0	0.0	3	99	0.99
17	06	44	0.99	44	0	0.0	0.0	3	99	0.99
17	07	44	0.99	43	0	0.0	0.0	3	99	0.99
17	08	44	0.99	42	0	0.0	0.0	3	99	0.99
17	09	44	0.99	41	0	0.0	0.0	3	99	0.99
17	10	44	0.99	40	0	0.0	0.0	3	99	0.99
17	11	44	0.99	39	0	0.0	0.0	3	99	0.99
17	12	44	0.99	38	0	0.0	0.0	3	99	0.99
17	13	44	0.99	37	0	0.0	0.0	3	99	0.99
17	14	44	0.99	36	0	0.0	0.0	3	99	0.99
17	15	44	0.99	35	0	0.0	0.0	3	99	0.99
17	16	44	0.99	34	0	0.0	0.0	3	99	0.99
17	17	44	0.99	33	0	0.0	0.0	3	99	0.99
17	18	44	0.99	32	0	0.0	0.0	3	99	0.99
17	19	44	0.99	31	0	0.0	0.0	3	99	0.99
17	20	44	0.99	30	0	0.0	0.0	3	99	0.99
17	21	44	0.99	29	0	0.0	0.0	3	99	0.99
17	22	44	0.99	28	0	0.0	0.0	3	99	0.99
17	23	44	0.99	27	0	0.0	0.0	3	99	0.99
17	24	44	0.99	26	0	0.0	0.0	3	99	0.99
17	25	44	0.99	25	0	0.0	0.0	3	99	0.99
17	26	44	0.99	24	0	0.0	0.0	3	99	0.99
17	27	44	0.99	23	0	0.0	0.0	3	99	0.99
17	28	44	0.99	22	0	0.0	0.0	3	99	0.99
17	29	44	0.99	21	0	0.0	0.0	3	99	0.99
17	30	44	0.99	20	0	0.0	0.0	3	99	0.99
17	31	44	0.99	19	0	0.0	0.0	3	99	0.99
17	32	44	0.99	18	0	0.0	0.0	3	99	0.99
17	33	44	0.99	17	0	0.0	0.0	3	99	0.99
17	34	44	0.99	16	0	0.0	0.0	3	99	0.99
17	35	44	0.99	15	0	0.0	0.0	3	99	0.99
17	36	44	0.99	14	0	0.0	0.0	3	99	0.99
17	37	44	0.99	13	0	0.0	0.0	3	99	0.99
17	38	44	0.99	12	0	0.0	0.0	3	99	0.99
17	39	44	0.99	11	0	0.0	0.0	3	99	0.99
17	40	44	0.99	10	0	0.0	0.0	3	99	0.99
17	41	44	0.99	9	0	0.0	0.0	3	99	0.99
17	42	44	0.99	8	0	0.0	0.0	3	99	0.99
17	43	44	0.99	7	0	0.0	0.0	3	99	0.99
17	44	44	0.99	6	0	0.0	0.0	3	99	0.99
17	45	44	0.99	5	0	0.0	0.0	3	99	0.99
17	46	44	0.99	4	0	0.0	0.0	3	99	0.99
17	47	44	0.99	3	0	0.0	0.0	3	99	0.99
17	48	44	0.99	2	0	0.0	0.0	3	99	0.99
17	49	44	0.99	1	0	0.0	0.0	3	99	0.99
17	50	44	0.99	0	0	0.0	0.0	3	99	0.99

Selected model ratings of discharges for Walnut Gulch flumes 1, 2, 3, 4, 6, 7, 8, 11, and 15 in prototype dimensions.—Cont.

WALNUT GULCH FLUME NO. 6 LOCATED NEAR TOMBSTONE, ARIZONA
DISCHARGE COEFFICIENTS FOR 1 TO 30 MODEL

TEST NO.	PROTOTYPE DISCHARGE (C.F.S.)	FLUME HEAD (FT.)	DISCHARGE	CONTROL AREA (SQ. FT.)	UPSTREAM APPROACH HYDRAULIC RADIUS (FT.)	MANNING N
22	10597	7.27	44	562.7	9.46	0.02
23	8828	5.05	11	425.3	7.42	0.02
24	9077	6.64	11	432.3	7.28	0.02
25	7371	5.57	11	332.1	6.41	0.02
26	4955	4.16	11	255.5	5.57	0.02
27	4084	3.88	11	210.6	5.18	0.02
28	4674	4.07	11	229.6	4.84	0.02
29	5206	4.52	11	263.9	4.79	0.02
30	2974	3.15	11	154.0	3.54	0.02
31	2929	3.28	11	163.9	3.70	0.02
32	2229	2.64	11	109.7	3.09	0.02
33	2229	2.64	11	109.7	3.09	0.02
34	2229	2.64	11	109.7	3.09	0.02
35	2229	2.64	11	109.7	3.09	0.02
36	2229	2.64	11	109.7	3.09	0.02
37	2229	2.64	11	109.7	3.09	0.02
38	2229	2.64	11	109.7	3.09	0.02
39	2229	2.64	11	109.7	3.09	0.02
40	2229	2.64	11	109.7	3.09	0.02
41	2229	2.64	11	109.7	3.09	0.02
42	2229	2.64	11	109.7	3.09	0.02
43	2229	2.64	11	109.7	3.09	0.02
44	2229	2.64	11	109.7	3.09	0.02
45	2229	2.64	11	109.7	3.09	0.02
46	2229	2.64	11	109.7	3.09	0.02
47	2229	2.64	11	109.7	3.09	0.02
48	2229	2.64	11	109.7	3.09	0.02
49	2229	2.64	11	109.7	3.09	0.02
50	2229	2.64	11	109.7	3.09	0.02
51	2229	2.64	11	109.7	3.09	0.02
52	2229	2.64	11	109.7	3.09	0.02
53	2229	2.64	11	109.7	3.09	0.02
54	2229	2.64	11	109.7	3.09	0.02
55	2229	2.64	11	109.7	3.09	0.02
56	2229	2.64	11	109.7	3.09	0.02
57	2229	2.64	11	109.7	3.09	0.02
58	2229	2.64	11	109.7	3.09	0.02
59	2229	2.64	11	109.7	3.09	0.02
60	2229	2.64	11	109.7	3.09	0.02

Selected model ratings of discharges for Walnut Gulch flumes 1, 2, 3, 4, 6, 7, 8, 11, and 15 in prototype dimensions.—Con.

EXP. NO. 4, WALNUT GULCH FLUME NO. 7, LOCATED NEAR TOMBSTONE, ARIZONA
 PREDICTED FILL; DISCHARGE COEFFICIENTS FOR 1 TO 30 MODEL

TEST NO.	PROTOTYPE DISCHARGE (C.F.S.)	FLUME HEAD (FT.)	DISCHARGE C	CONTROL AREA (SQ. FT.)	HYDRAULIC RADIUS (FT.)	UPSTREAM APPROACH MANNING
0	9080	11	1	495	9	0
1	8470	10	1	465	8	0
2	7800	10	1	444	8	0
3	6500	9	1	444	8	0
4	6050	9	1	444	8	0
5	5510	8	1	444	8	0
6	5100	8	1	444	8	0
7	4700	8	1	444	8	0
8	4300	7	1	444	8	0
9	3900	7	1	444	8	0
10	3500	7	1	444	8	0
11	3100	6	1	444	8	0
12	2700	6	1	444	8	0
13	2300	6	1	444	8	0
14	1900	5	1	444	8	0
15	1500	5	1	444	8	0
16	1100	4	1	444	8	0
17	700	4	1	444	8	0
18	300	3	1	444	8	0
19	100	2	1	444	8	0
20	100	2	1	444	8	0
21	100	2	1	444	8	0
22	100	2	1	444	8	0
23	100	2	1	444	8	0
24	100	2	1	444	8	0
25	100	2	1	444	8	0
26	100	2	1	444	8	0
27	100	2	1	444	8	0
28	100	2	1	444	8	0
29	100	2	1	444	8	0
30	100	2	1	444	8	0

Selected model ratings of discharges for Walnut Gulch flumes 1, 2, 3, 4, 6, 7, 8, 11, and 15 in prototype dimensions.—Con.

WALNUT GULCH FLUME NO. 8 LOCATED NEAR TOMBSTONE, ARIZONA
DISCHARGE COEFFICIENTS FOR 1 TO 30 MODEL

TEST NO.	PROTOTYPE DISCHARGE (C.F.S.)	FLUME HEAD (FT.)	DISCHARGE C	CONTROL AREA (SQ. FT.)	UPSTREAM HYDRAULIC RADIUS (FT.)	APPROACH MANNING N
1	17779	4.4	3300	14	76	0.021
2	17779	4.4	3300	14	76	0.021
3	17779	4.4	3300	14	76	0.021
4	17779	4.4	3300	14	76	0.021
5	17779	4.4	3300	14	76	0.021
6	17779	4.4	3300	14	76	0.021
7	17779	4.4	3300	14	76	0.021
8	17779	4.4	3300	14	76	0.021
9	17779	4.4	3300	14	76	0.021
10	17779	4.4	3300	14	76	0.021
11	17779	4.4	3300	14	76	0.021
12	17779	4.4	3300	14	76	0.021
13	17779	4.4	3300	14	76	0.021
14	17779	4.4	3300	14	76	0.021
15	17779	4.4	3300	14	76	0.021
16	17779	4.4	3300	14	76	0.021
17	17779	4.4	3300	14	76	0.021
18	17779	4.4	3300	14	76	0.021
19	17779	4.4	3300	14	76	0.021
20	17779	4.4	3300	14	76	0.021
21	17779	4.4	3300	14	76	0.021
22	17779	4.4	3300	14	76	0.021
23	17779	4.4	3300	14	76	0.021
24	17779	4.4	3300	14	76	0.021
25	17779	4.4	3300	14	76	0.021
26	17779	4.4	3300	14	76	0.021
27	17779	4.4	3300	14	76	0.021
28	17779	4.4	3300	14	76	0.021
29	17779	4.4	3300	14	76	0.021
30	17779	4.4	3300	14	76	0.021

Selected model ratings of discharges for Walnut Gulch flumes 1, 2, 3, 4, 6, 7, 8, 11, and 15 in prototype dimensions.—Con.

EXP. NO. 1, WALNUT GULCH FLUME NO. 11 LOCATED NEAR TOMBSTONE, ARIZONA
 FILLED APPROACH, DISCHARGE COEFFICIENTS FOR 1 TO 30 MODEL

TEST PROTOTYPE FLUME DISCHARGE CONTROL UPSTREAM APPROACH
 NO. DISCHARGE HEAD (C.F.S.) (SQ. FT.) HYDRAULIC RADIUS MANNING

TEST PROTOTYPE NO.	DISCHARGE HEAD (C.F.S.)	DISCHARGE (SQ. FT.)	CONTROL AREA (SQ. FT.)	UPSTREAM HYDRAULIC RADIUS (FT.)	APPROACH MANNING
1	59.48	1.00	44.57	7.26	0.01
2	32.64	0.02	43.22	6.91	0.04
3	36.99	0.06	43.10	6.65	0.05
4	33.63	0.12	42.87	6.52	0.05
5	30.63	0.23	42.68	6.42	0.05
6	27.79	0.35	42.53	6.34	0.05
7	24.87	0.47	42.40	6.29	0.05
8	22.67	0.58	42.30	6.25	0.05
9	20.51	0.68	42.23	6.22	0.05
10	18.90	0.77	42.18	6.20	0.05
11	17.51	0.85	42.15	6.19	0.05
12	16.24	0.91	42.13	6.18	0.05
13	15.08	0.97	42.12	6.18	0.05
14	14.02	1.02	42.11	6.17	0.05
15	13.05	1.06	42.11	6.17	0.05
16	12.20	1.09	42.11	6.17	0.05
17	11.44	1.11	42.11	6.17	0.05
18	10.76	1.11	42.11	6.17	0.05
19	10.15	1.11	42.11	6.17	0.05
20	9.60	1.11	42.11	6.17	0.05
21	9.10	1.11	42.11	6.17	0.05
22	8.64	1.11	42.11	6.17	0.05
23	8.22	1.11	42.11	6.17	0.05
24	7.83	1.11	42.11	6.17	0.05
25	7.46	1.11	42.11	6.17	0.05
26	7.11	1.11	42.11	6.17	0.05
27	6.78	1.11	42.11	6.17	0.05
28	6.46	1.11	42.11	6.17	0.05
29	6.16	1.11	42.11	6.17	0.05
30	5.87	1.11	42.11	6.17	0.05

Selected model ratings of discharges for Walnut Gulch flumes 1, 2,
3, 4, 6, 7, 8, 11, and 15 in prototype dimensions.—Con.

WALNUT GULCH FLUME NO. 15, LOCATED NEAR TOMBSTONE, ARIZONA
EXPERIMENT NO. 2, FILLED APPROACH COEFFICIENTS FOR 1 TO 30 MODEL

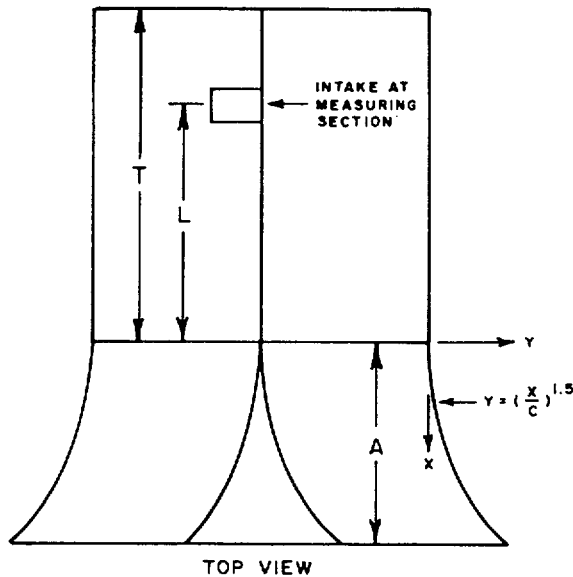
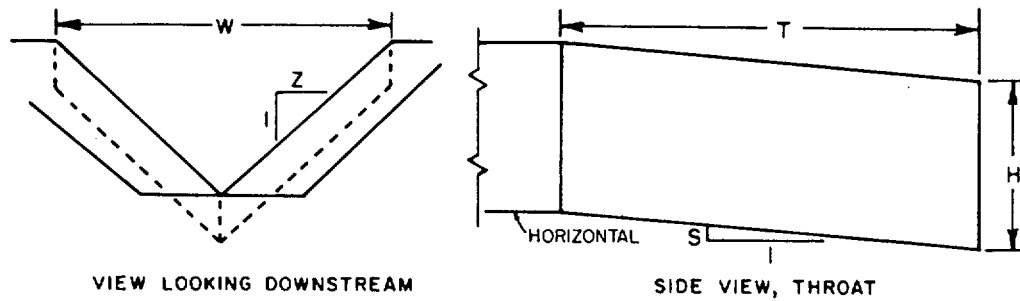
TEST NO.	PROTOTYPE DISCHARGE (C.F.S.)	FLUME HEAD (FT.)	DISCHARGE C	CONTROL AREA (SQ. FT.)	UPSTREAM HYDRAULIC RADIUS (FT.)	APPROACH MANNING N
50	10545	11.635	129	515	8.10	0.0629
51	7410	11.398	104	478	7.57	0.0635
52	7983	11.040	018	455	6.52	0.0652
53	7334	10.404	033	443	6.55	0.0668
54	6698	9.624	046	433	6.44	0.0689
55	6348	9.439	050	427	6.30	0.0697
56	5982	9.632	054	419	6.10	0.0694
57	5544	9.638	059	415	6.04	0.0684
58	5077	9.387	060	408	5.95	0.0661
59	4799	9.077	069	403	5.84	0.0660
60	4559	8.749	079	398	5.74	0.0654
61	4355	8.459	081	395	5.64	0.0651
62	4177	8.222	085	393	5.54	0.0649
63	4047	8.044	087	392	5.44	0.0646
64	3959	7.925	089	391	5.34	0.0644
65	3897	7.857	091	390	5.24	0.0642
66	3850	7.825	092	389	5.14	0.0640
67	3815	7.797	093	388	5.04	0.0638
68	3790	7.772	094	387	4.94	0.0636
69	3772	7.750	095	386	4.84	0.0634
70	3760	7.732	096	385	4.74	0.0632
71	3752	7.718	097	384	4.64	0.0630
72	3747	7.707	098	383	4.54	0.0628
73	3744	7.697	099	382	4.44	0.0626
74	3742	7.688	100	381	4.34	0.0624
75	3741	7.680	100	380	4.24	0.0622
76	3740	7.673	100	379	4.14	0.0620
77	3739	7.667	100	378	4.04	0.0618
78	3738	7.662	100	377	3.94	0.0616
79	3737	7.657	100	376	3.84	0.0614
80	3736	7.653	100	375	3.74	0.0612

Appendix C

Design dimensions of Santa Rita flumes for a range of flow capacities.

SANTA RITA FLUME - TRIANGULAR SECTION

DESIGN CAPACITY 0.5 m³/s



FLUME DIMENSIONS, METERS

L	2.0
T	2.7
H	0.5
W	2.0
S	0.03
Z	2.0
A	≥ 1.0
C	2.0

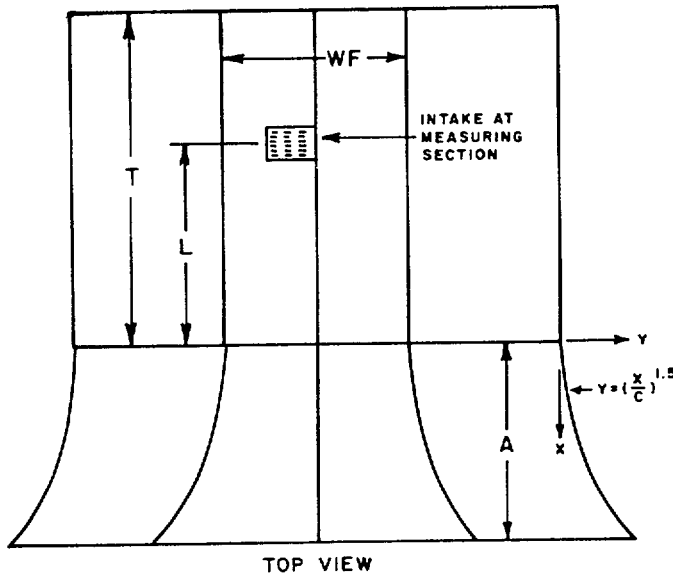
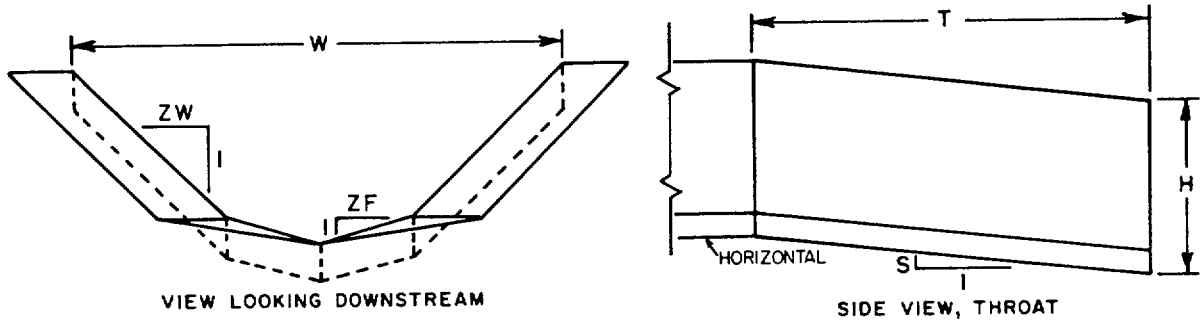
FLUME RATING

Q RANGE MULTIPLIER	HEAD IN METERS AT MEASURING SECTION					
	DISCHARGE, Q, RANGE IN m ³ /s					
	0.01	0.1	1.0	10	100	1000
1.0	0.063	0.176				
1.2	0.069	0.190				
1.4	0.074	0.203				
1.6	0.078	0.216				
1.8	0.082	0.227				
2.0	0.086	0.238				
3.0	0.103	0.284				
4.0	0.117	0.321				
5.0	0.129	0.354				
6.0	0.140					
7.0	0.150					
8.0	0.159					
9.0	0.168					

Design dimensions of Santa Rita flumes for a range of flow capacities—Con.

SANTA RITA FLUME

DESIGN CAPACITY 1.0 m³/s



FLUME DIMENSIONS, METERS

L	2.0	ZW	1.0
T	2.7	ZF	4.0
H	0.8625	S	0.03
W	2.0	A	≥ 1.0
WF	0.50	C	2.0

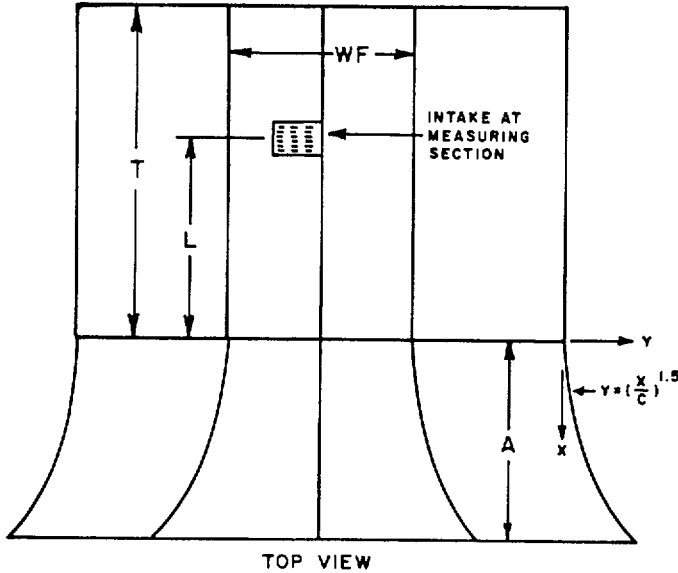
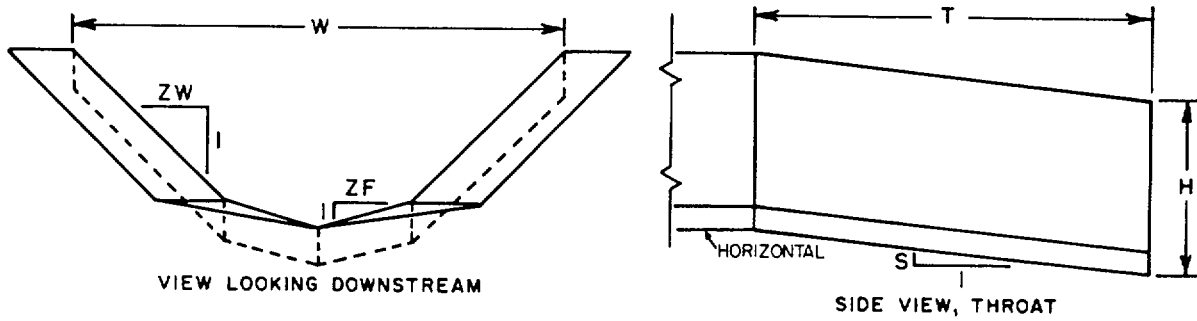
FLUME RATING

Q RANGE MULTIPLIER	HEAD IN METERS AT MEASURING SECTION					
	DISCHARGE, Q, RANGE IN m ³ /s					
	0.01	0.1	1.0	10	100	1000
1.0	0.046	0.139	0.493			
1.2	0.050	0.154				
1.4	0.053	0.168				
1.6	0.057	0.181				
1.8	0.059	0.193				
2.0	0.062	0.205				
3.0	0.075	0.257				
4.0	0.086	0.302				
5.0	0.096	0.341				
6.0	0.105	0.376				
7.0	0.114	0.409				
8.0	0.123	0.439				
9.0	0.131	0.467				

Design dimensions of Santa Rita flumes for a range of flow capacities—Con.

SANTA RITA FLUME

DESIGN CAPACITY 2.0 m³/s



FLUME DIMENSIONS, METERS

L	2.0	ZW	1.0
T	2.80	ZF	4.0
H	0.90	S	0.03
W	2.60	A	≥ 1.0
WF	1.0	C	2.0

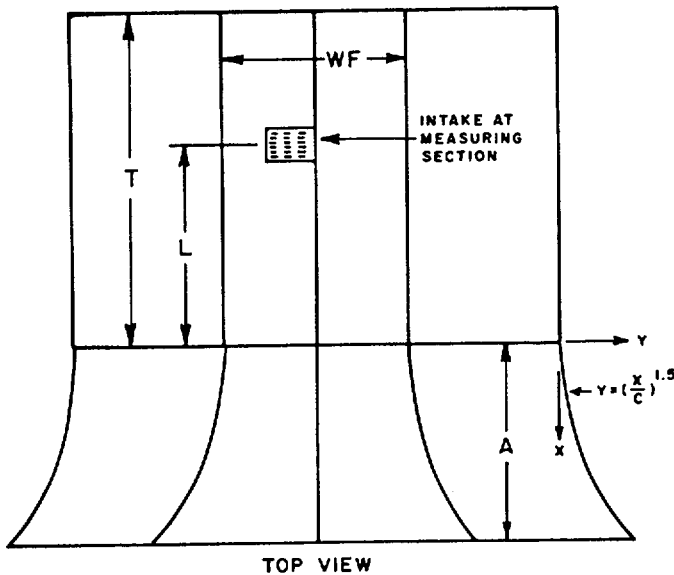
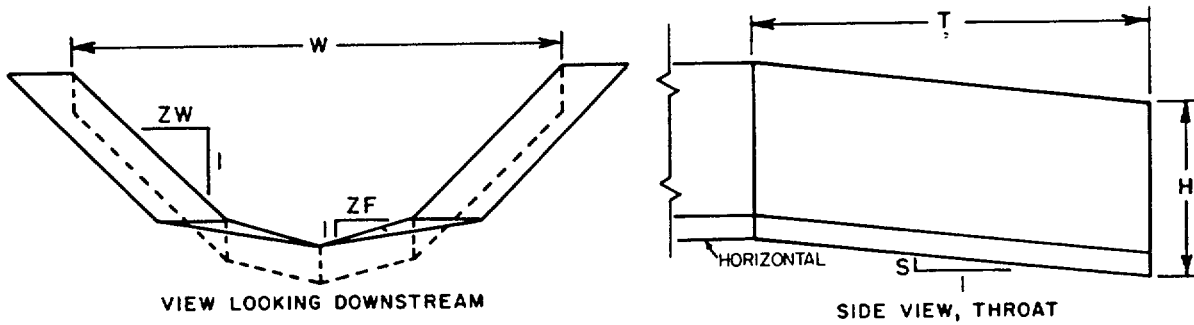
FLUME RATING

Q RANGE MULTIPLIER	HEAD IN METERS AT MEASURING SECTION					
	DISCHARGE, Q, RANGE IN m ³ /s					
	0.01	0.1	1.0	10	100	1000
1.0	0.046	0.127	0.411			
1.2	0.050	0.138	0.454			
1.4	0.054	0.147	0.494			
1.6	0.057	0.157	0.531			
1.8	0.060	0.168	0.567			
2.0	0.063	0.175	0.600			
3.0	0.075	0.214				
4.0	0.086	0.249				
5.0	0.095	0.281				
6.0	0.102	0.310				
7.0	0.110	0.338				
8.0	0.116	0.368				
9.0	0.122	0.388				

Design dimensions of Santa Rita flumes for a range of flow capacities—Con.

SANTA RITA FLUME

DESIGN CAPACITY 5.0 m³/s



FLUME DIMENSIONS, METERS

L	2.50	ZW	1.0
T	3.50	ZF	4.0
H	1.25	S	0.03
W	3.7	A	>1.50
WF	1.50	C	2.0

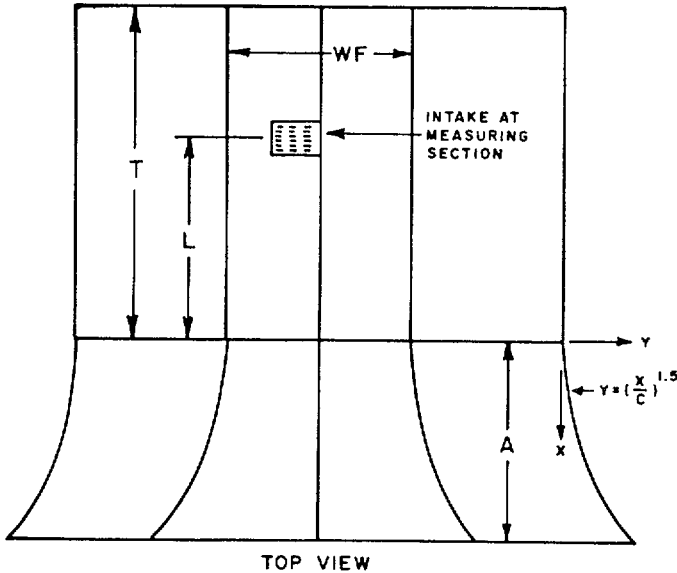
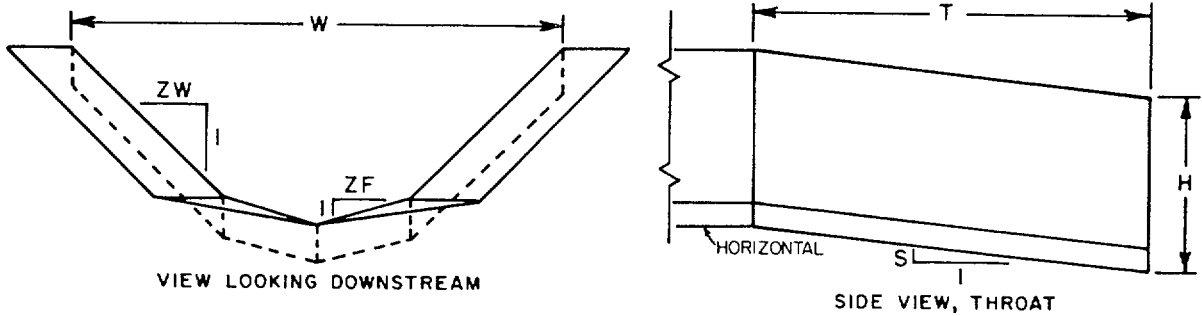
FLUME RATING

Q RANGE MULTIPLIER	HEAD IN METERS AT MEASURING SECTION					
	DISCHARGE, Q, RANGE IN m ³ /s					
	0.01	0.1	1.0	10	100	1000
1.0	0.045	0.125	0.359			
1.2	0.048	0.135	0.396			
1.4	0.052	0.145	0.430			
1.6	0.055	0.153	0.462			
1.8	0.058	0.161	0.493			
2.0	0.061	0.169	0.522			
3.0	0.073	0.200	0.651			
4.0	0.083	0.227	0.762			
5.0	0.092	0.253	0.860			
6.0	0.099	0.276				
7.0	0.106	0.298				
8.0	0.113	0.319				
9.0	0.119	0.340				

Design dimensions of Santa Rita flumes for a range of flow capacities—Con.

SANTA RITA FLUME

DESIGN CAPACITY 10 m³/s



FLUME DIMENSIONS, METERS

L	2.5	ZW	1.0
T	4.5	ZF	5.0
H	1.7	S	0.03
W	5.0	A	> 1.5
WF	2.0	C	2.0

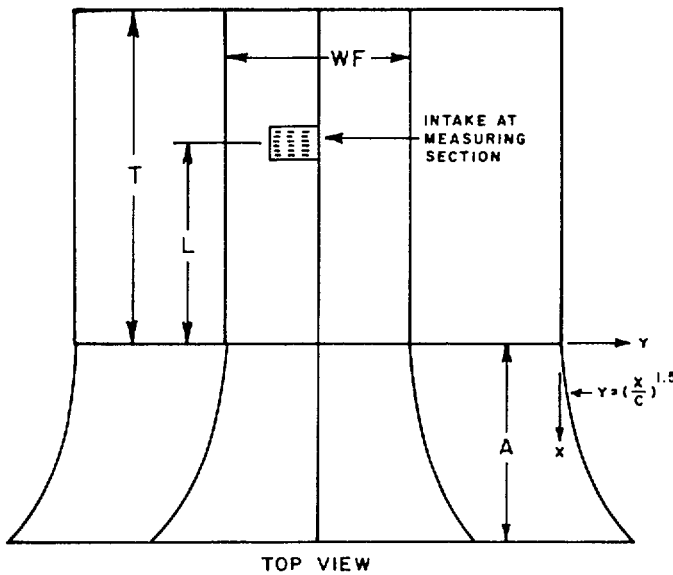
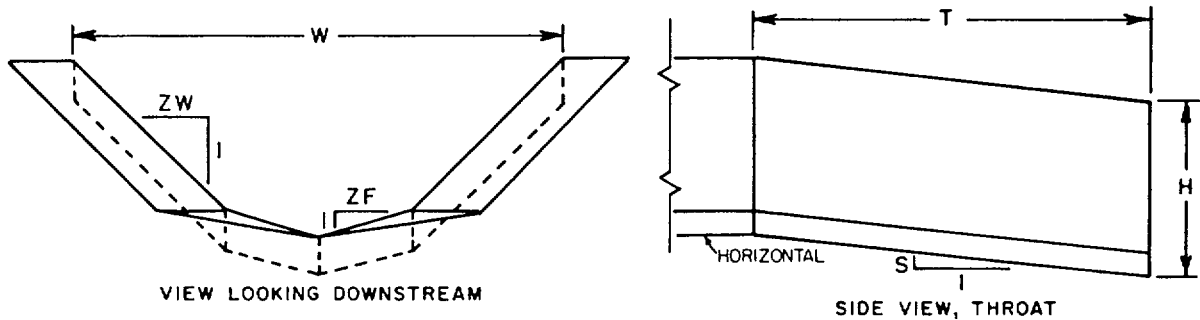
FLUME RATING

Q RANGE MULTIPLIER	HEAD IN METERS AT MEASURING SECTION					
	DISCHARGE, Q, RANGE IN m ³ /s					
	0.01	0.1	1.0	10	100	1000
1.0	0.040	0.113	0.316	1.119		
1.2	0.044	0.122	0.347			
1.4	0.047	0.131	0.376			
1.6	0.050	0.139	0.404			
1.8	0.053	0.147	0.431			
2.0	0.055	0.154	0.457			
3.0	0.066	0.183	0.572			
4.0	0.075	0.206	0.672			
5.0	0.083	0.227	0.761			
6.0	0.090	0.246	0.843			
7.0	0.096	0.265	0.919			
8.0	0.102	0.282	0.990			
9.0	0.108	0.299	1.056			

Design dimensions of Santa Rita flumes for a range of flow capacities—Con.

SANTA RITA FLUME

DESIGN CAPACITY 50 m³/s



FLUME DIMENSIONS, METERS

L	4.0	ZW	1.0
T	7.50	ZF	5.0
H	3.0	S	0.03
W	9.2	A	≥ 2.5
WF	4.0	C	2.0

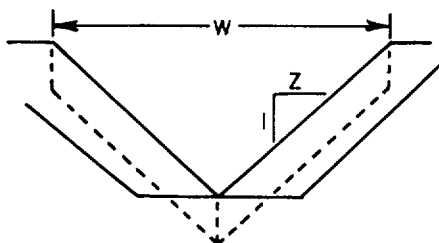
FLUME RATING

Q RANGE MULTIPLIER	HEAD IN METERS AT MEASURING SECTION					
	DISCHARGE, Q, RANGE IN m ³ /s					
	0.01	0.1	1.0	10	100	1000
1.0	0.039	0.107	0.298	0.871		
1.2	0.042	0.116	0.323	0.963		
1.4	0.045	0.124	0.345	1.048		
1.6	0.047	0.132	0.365	1.128		
1.8	0.050	0.139	0.383	1.204		
2.0	0.052	0.146	0.400	1.277		
3.0	0.063	0.175	0.476	1.601		
4.0	0.071	0.198	0.544	1.878		
5.0	0.079	0.219	0.606	2.124		
6.0	0.085	0.238	0.665			
7.0	0.091	0.254	0.720			
8.0	0.097	0.270	0.773			
9.0	0.102	0.284	0.823			

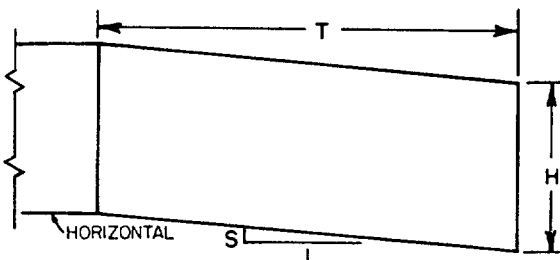
Design dimensions of Santa Rita flumes for a range of flow capacities—Con.

SANTA RITA FLUME - TRIANGULAR SECTION

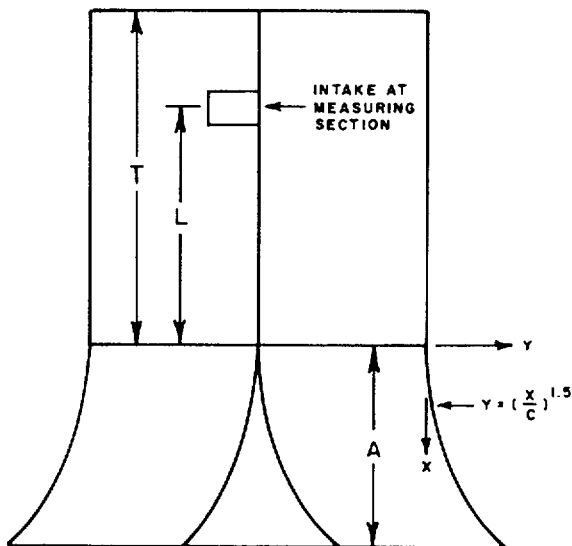
DESIGN CAPACITY 12 ft³/s



VIEW LOOKING DOWNSTREAM



SIDE VIEW, THROAT



TOP VIEW

FLUME DIMENSIONS, FEET

L	6.0
T	8.0
H	1.4
W	5.4
S	0.03
Z	2.0
A	4.0
C	4.0

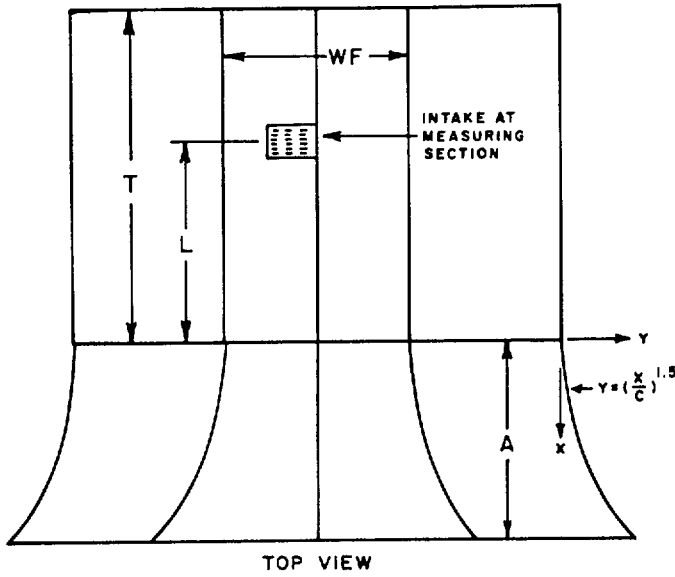
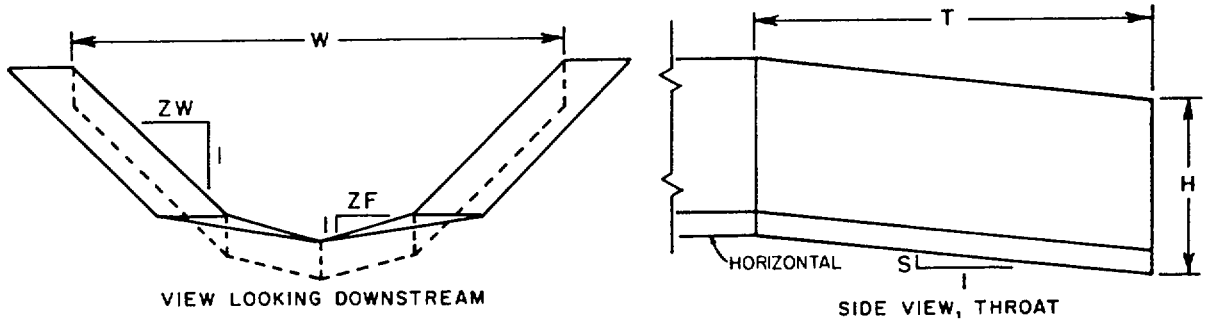
FLUME RATING

Q RANGE MULTIPLIER	HEAD IN FEET AT MEASURING SECTION					
	DISCHARGE, Q, RANGE IN ft ³ /s					
	0.01	0.1	1.0	10	100	1000
1.0	0.044	0.119	0.330	0.906		
1.2		0.129	0.358	0.981		
1.4		0.138	0.383			
1.6		0.146	0.406			
1.8		0.154	0.428			
2.0	0.058	0.161	0.448			
3.0	0.070	0.193	0.536			
4.0	0.079	0.220	0.608			
5.0	0.087	0.243	0.670			
6.0	0.095	0.263	0.726			
7.0	0.101	0.282	0.776			
8.0	0.107	0.299	0.822			
9.0	0.113	0.315	0.866			

Design dimensions of Santa Rita flumes for a range of flow capacities—Con.

SANTA RITA FLUME

DESIGN CAPACITY 20 ft³/s



FLUME DIMENSIONS, FEET

L	6.0	ZW	1.0
T	8.0	ZF	4.0
H	2.0	S	0.03
W	4.75	A	≥ 4.0
WF	1.0	C	4.0

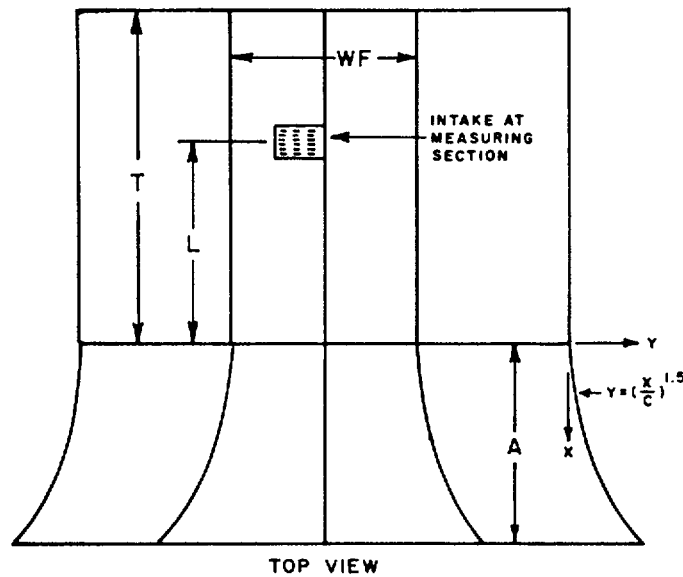
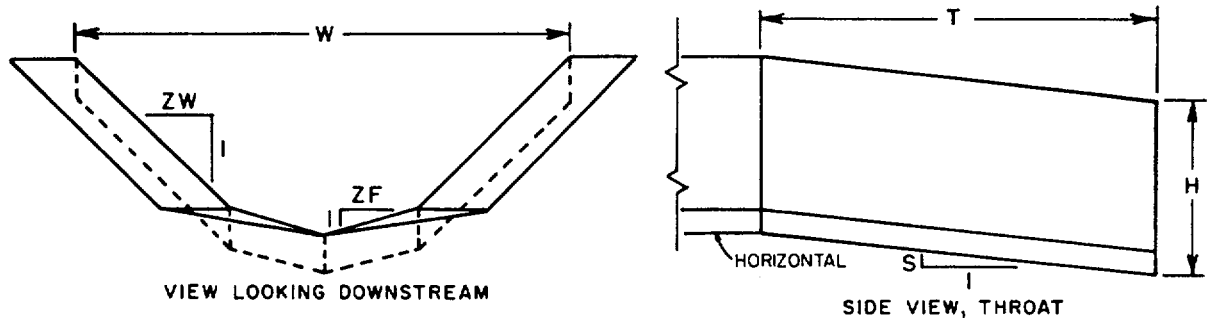
FLUME RATING

Q RANGE MULTIPLIER	HEAD IN METERS AT MEASURING SECTION					
	DISCHARGE, Q, RANGE IN ft ³ /s					
	0.01	0.1	1.0	10	100	1000
1.0	0.031	0.086	0.257	0.930		
1.2		0.093	0.284	1.025		
1.4		0.099	0.310	1.111		
1.6		0.106	0.335	1.191		
1.8		0.111	0.358	1.266		
2.0	0.042	0.116	0.380	1.336		
3.0	0.050	0.139	0.479			
4.0	0.057	0.159	0.563			
5.0	0.063	0.177	0.638			
6.0	0.068	0.195	0.705			
7.0	0.073	0.211	0.767			
8.0	0.078	0.227	0.825			
9.0	0.082	0.242	0.879			

Design dimensions of Santa Rita flumes for a range of flow capacities—Con.

SANTA RITA FLUME

DESIGN CAPACITY 50 ft³/s



FLUME DIMENSIONS, FEET

L	7.0	ZW	1.0
T	9.0	ZF	4.0
H	2.375	S	0.03
W	7.0	A	≥ 5.0
WF	3.0	C	4.0

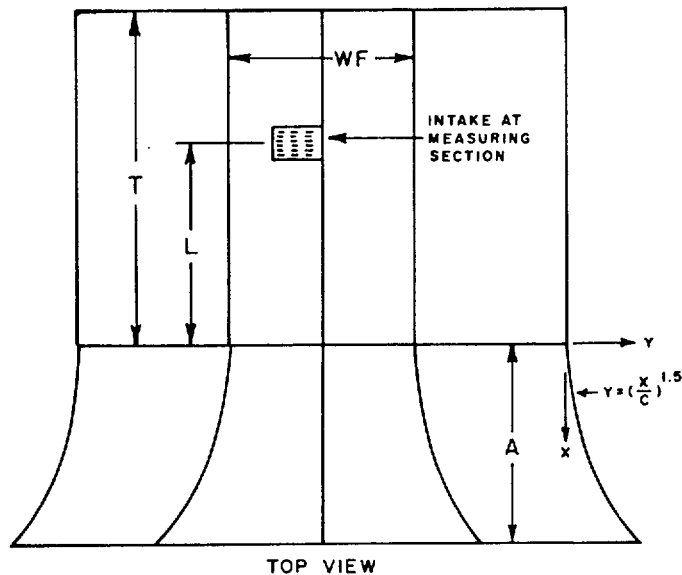
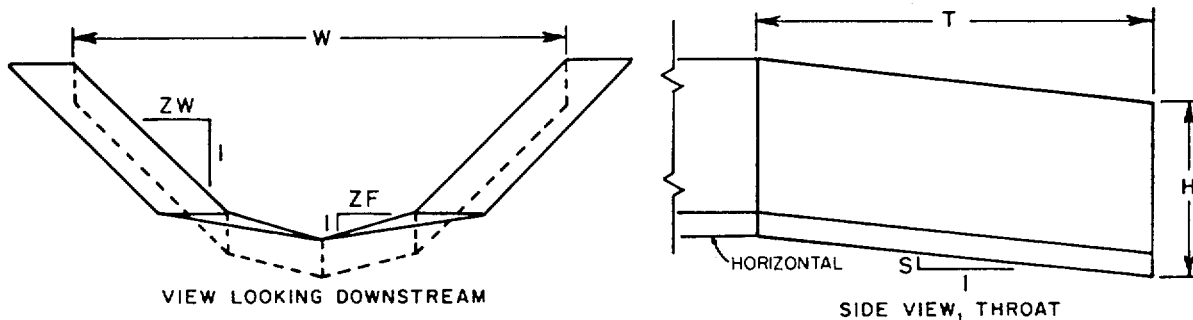
FLUME RATING

Q RANGE MULTIPLIER	HEAD IN METERS AT MEASURING SECTION					
	DISCHARGE, Q, RANGE IN ft ³ /s					
	0.01	0.1	1.0	10	100	1000
1.0	0.031	0.084	0.236	0.682		
1.2		0.091	0.256	0.752		
1.4		0.098	0.274	0.817		
1.6		0.104	0.291	0.879		
1.8		0.110	0.307	0.937		
2.0	0.042	0.115	0.321	0.994		
3.0	0.050	0.138	0.381	1.244		
4.0	0.056	0.157	0.433	1.458		
5.0	0.062	0.173	0.480	1.648		
6.0	0.067	0.188	0.524			
7.0	0.072	0.201	0.566			
8.0	0.076	0.214	0.607			
9.0	0.080	0.225	0.645			

Design dimensions of Santa Rita flumes for a range of flow capacities—Con.

SANTA RITA FLUME

DESIGN CAPACITY 100 ft³/s



FLUME DIMENSIONS, FEET

L	8.0	ZW	1.0
T	12.0	ZF	4.0
H	3.125	S	0.03
W	10.0	A	≥ 6.0
WF	5.0	C	4.0

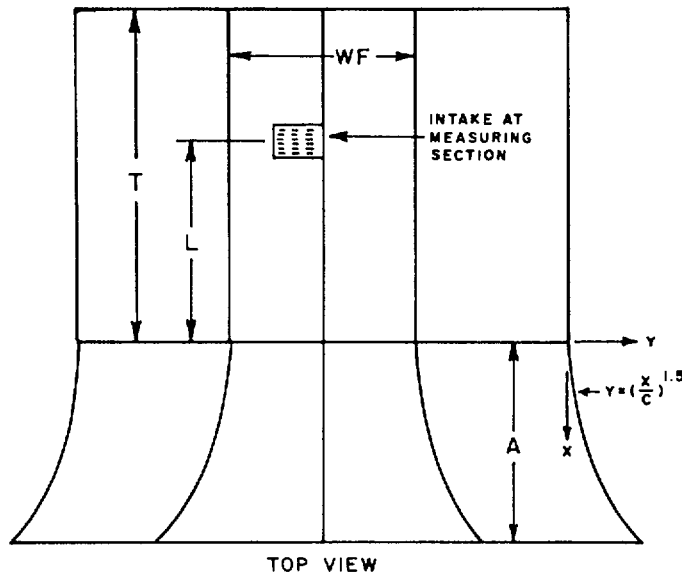
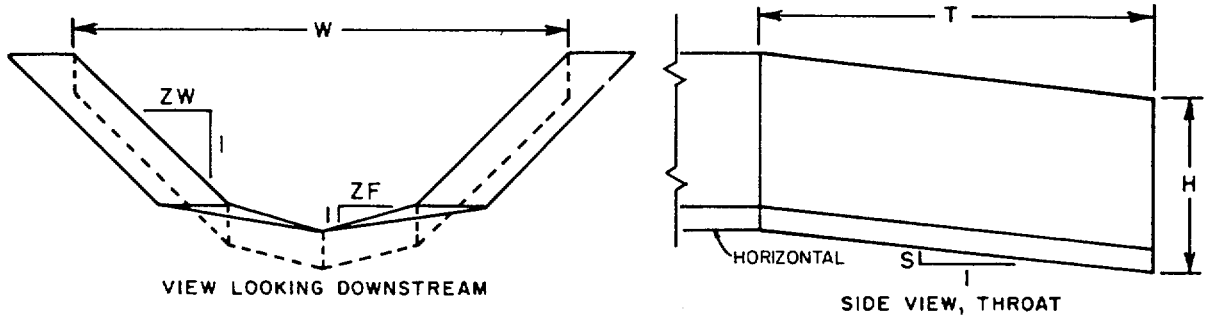
FLUME RATING

Q RANGE MULTIPLIER	HEAD IN METERS AT MEASURING SECTION					
	DISCHARGE, Q, RANGE IN ft ³ /s					
	0.01	0.1	1.0	10	100	1000
1.0	0.032	0.084	0.234	0.643	2.066	
1.2		0.091	0.254	0.695		
1.4		0.098	0.272	0.745		
1.6		0.104	0.289	0.792		
1.8		0.109	0.304	0.837		
2.0	0.042	0.114	0.319	0.881		
3.0	0.050	0.137	0.382	1.081		
4.0	0.057	0.156	0.434	1.257		
5.0	0.062	0.172	0.479	1.416		
6.0	0.067	0.186	0.519	1.563		
7.0	0.072	0.200	0.554	1.700		
8.0	0.076	0.212	0.586	1.829		
9.0	0.081	0.223	0.616	1.950		

Design dimensions of Santa Rita flumes for a range of flow capacities—Con.

SANTA RITA FLUME

DESIGN CAPACITY 500 ft³/s



FLUME DIMENSIONS, FEET

L	10.0	ZW	1.0
T	18.0	ZF	4.0
H	6.0	S	0.03
W	18.0	A	≥ 6.0
WF	8.0	C	4.0

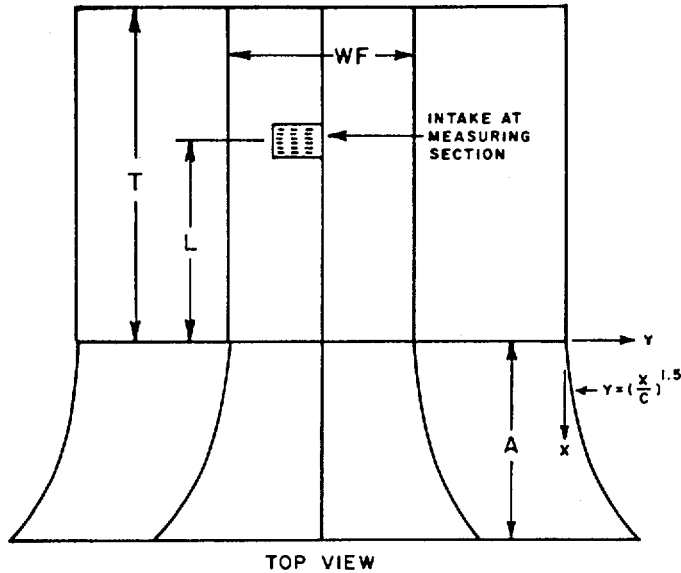
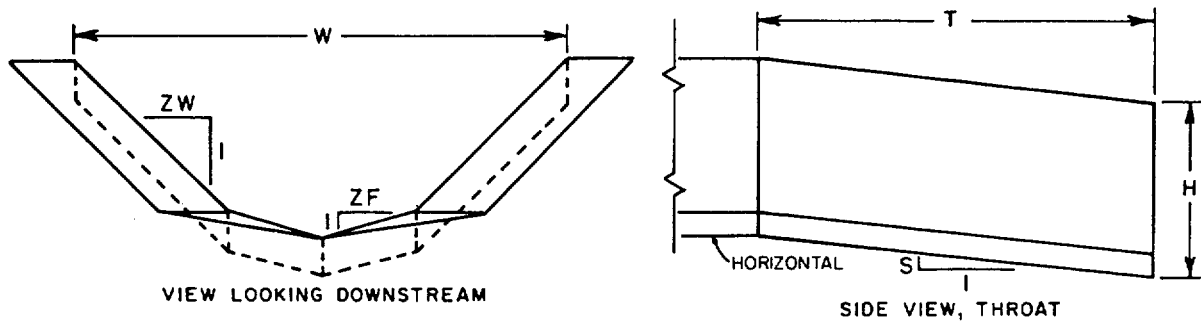
FLUME RATING

Q RANGE MULTIPLIER	HEAD IN METERS AT MEASURING SECTION					
	DISCHARGE, Q, RANGE IN ft ³ /s					
	0.01	0.1	1.0	10	100	1000
1.0	0.031	0.083	0.228	0.635	1.797	
1.2		0.089	0.247	0.689	1.977	
1.4		0.096	0.265	0.737	2.144	
1.6	0.038	0.101	0.281	0.782	2.303	
1.8		0.107	0.296	0.823	2.453	
2.0	0.042	0.112	0.311	0.862	2.597	
3.0	0.049	0.134	0.372	1.020	3.235	
4.0	0.056	0.152	0.423	1.154	3.782	
5.0	0.061	0.168	0.467	1.277	4.267	
6.0	0.066	0.182	0.507	1.392		
7.0	0.071	0.195	0.543	1.501		
8.0	0.075	0.206	0.576	1.604		
9.0	0.079	0.218	0.607	1.703		

Design dimensions of Santa Rita flumes for a range of flow capacities—Con.

SANTA RITA FLUME

DESIGN CAPACITY 1000 ft³/s



FLUME DIMENSIONS, FEET

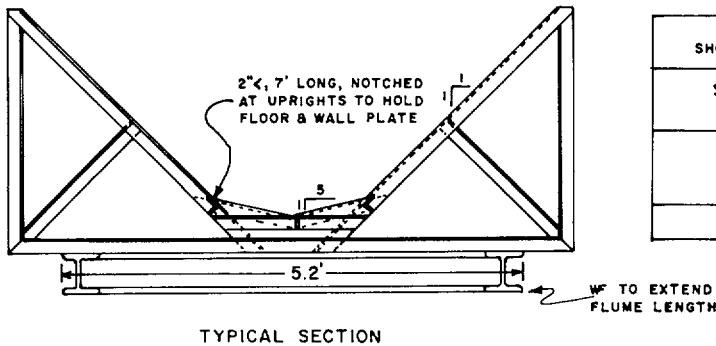
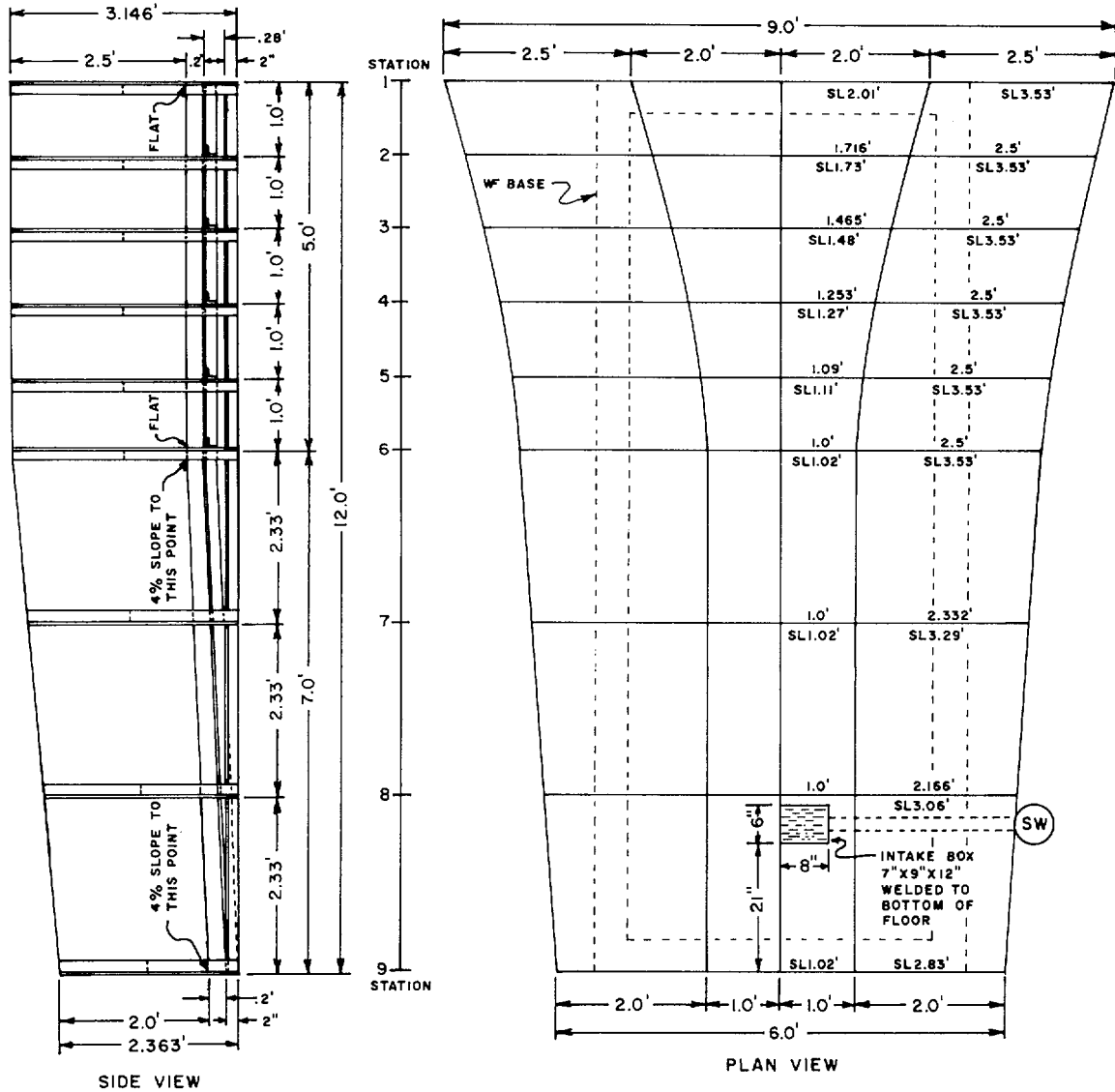
L	15.0	ZW	1.0
T	25.0	ZF	5.0
H	8.0	S	0.03
W	24.0	A	≥ 9.0
WF	10.0	C	4.0

FLUME RATING

Q RANGE MULTIPLIER	HEAD IN METERS AT MEASURING SECTION					
	DISCHARGE, Q, RANGE IN ft ³ /s					
	0.01	0.1	1.0	10	100	1000
1.0	0.029	0.073	0.197	0.55	1.539	5.485
1.2		0.079	0.214	0.597	1.691	
1.4		0.084	0.229	0.639	1.835	
1.6		0.089	0.243	0.678	1.971	
1.8		0.094	0.256	0.715	2.102	
2.0	0.038	0.098	0.268	0.749	2.227	
3.0	0.044	0.117	0.321	0.893	2.791	
4.0	0.050	0.132	0.366	1.007	3.281	
5.0	0.055	0.146	0.404	1.107	3.722	
6.0	0.059	0.158	0.438	1.201	4.124	
7.0	0.063	0.169	0.469	1.291	4.497	
8.0	0.067	0.179	0.498	1.377	4.846	
9.0	0.070	0.188	0.525	1.460	5.174	

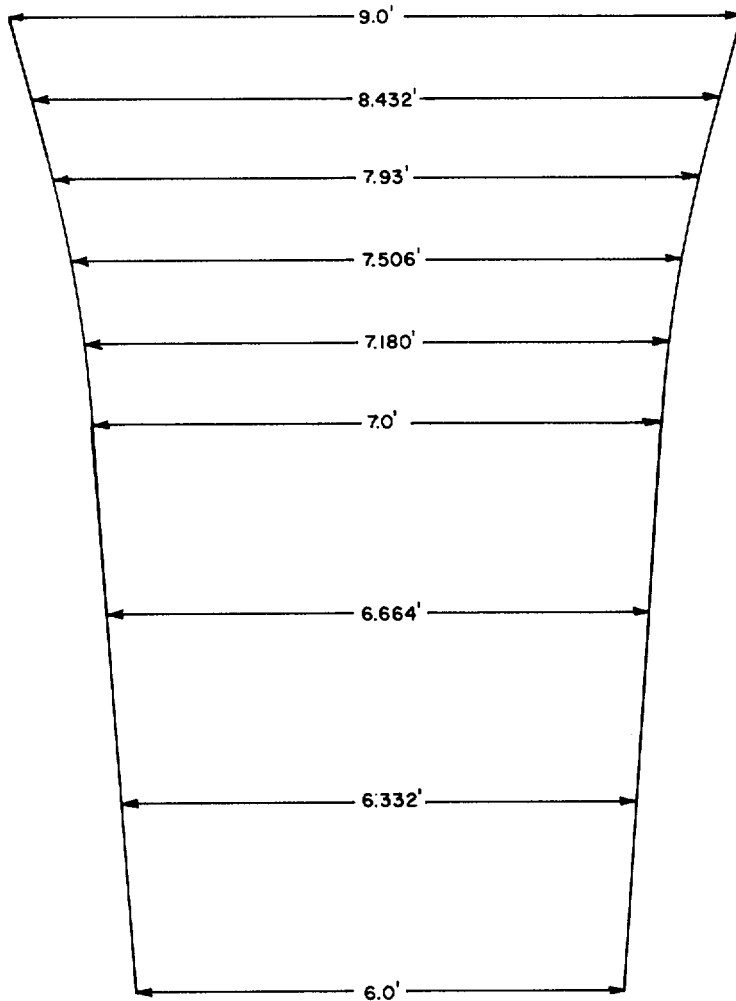
Appendix D

Construction drawings for a 1.5-m³/s metal Santa Rita flume.

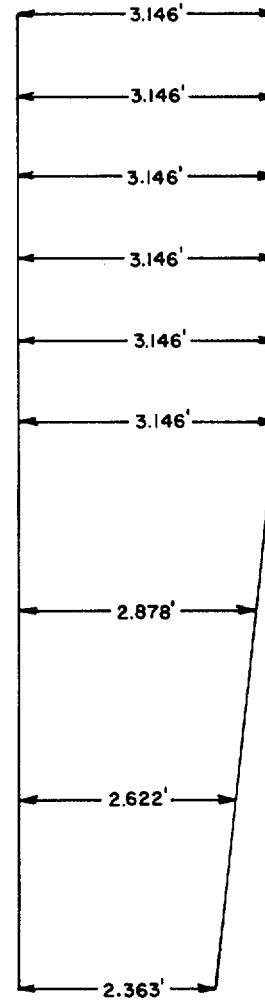


CONSTRUCTION DETAILS 50 CFS FLUME SHOP ASSEMBLED, WELDED STEEL CONSTRUCTION
SOUTHWEST RANGELAND WATERSHED RESEARCH CENTER
U.S.D.A. - S.E.A. - A.R.
442 E. 7th ST. TUCSON, AZ 85705
SCALE : 1/2" = 1'

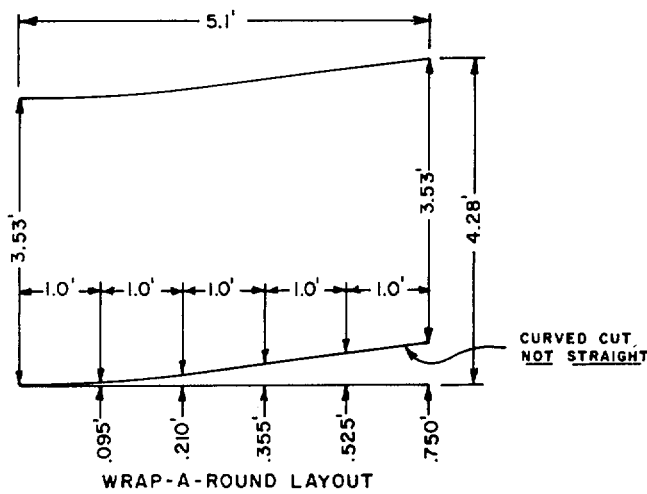
Construction drawings for a 1.5-m³/s metal Santa Rita flume—Con.



STATION WIDTHS FINISHED
AT FLUME TOP



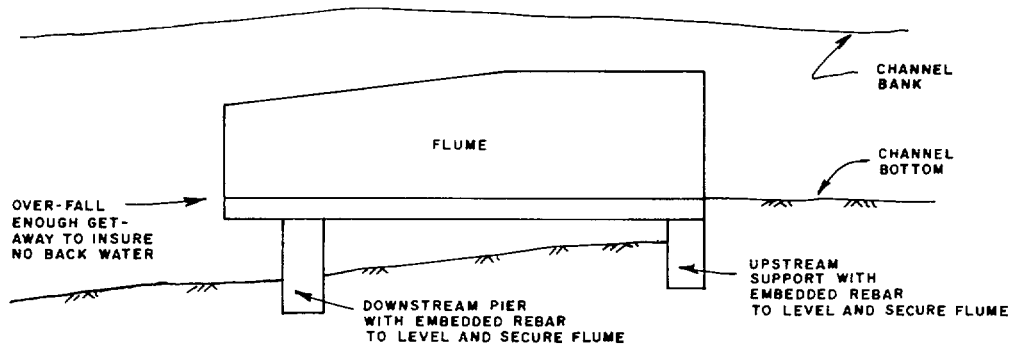
STATION HEIGHTS FINISHED
FROM LEVEL FRAME



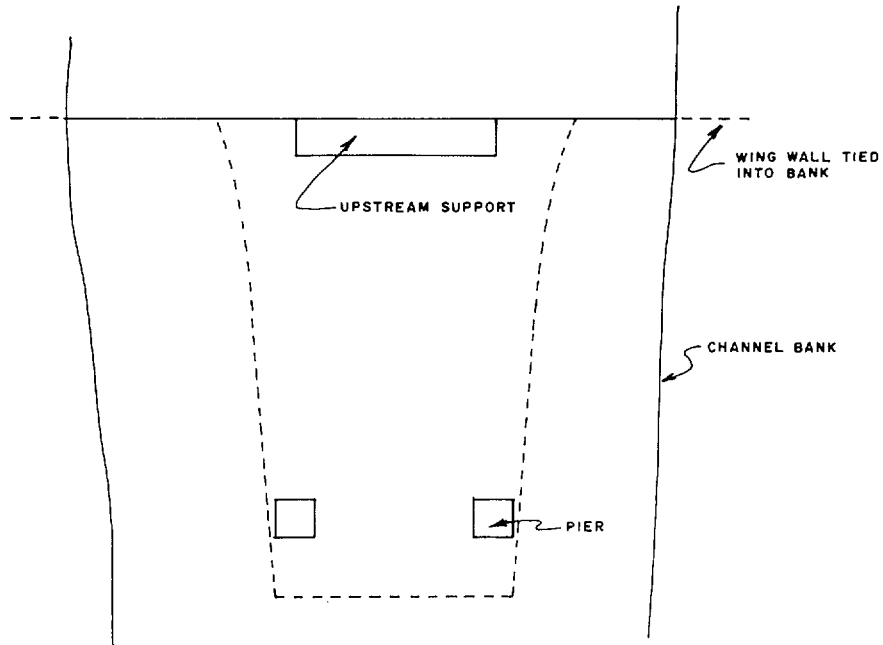
WRAP-A-ROUND LAYOUT

CONSTRUCTION DETAILS 50 CFS FLUME SHOP ASSEMBLED, WELDED STEEL CONSTRUCTION
SOUTHWEST RANGELAND WATERSHED RESEARCH CENTER
U.S.D.A. - S.E.A. - A.R.
442 E. 7th ST. TUCSON, AZ 85705
SCALE : 1/2" = 1'

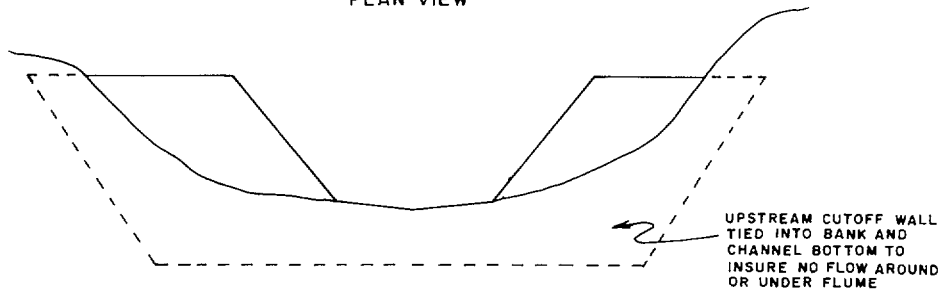
Construction drawings for a 1.5-m³/s metal Santa Rita flume—Con.



PROFILE VIEW



PLAN VIEW



DOWNSTREAM VIEW

SCHEMATIC OF A TYPICAL SITE INSTALLATION
NOT TO SCALE